DEVELOPMENT OF A MODEL OF SPACE STATION SOLAR ARRAY

BY

PAUL A. BOSELA

DEPARTMENT OF ENGINEERING TECHNOLOGY
CLEVELAND STATE UNIVERSITY

(NASA-CR-188911) DEVELOPMENT OF A MODEL OF SPACE STATION SOLAR ARRAY Final Report, 15 Sep. 1989 - 15 Mar. 1990 (Cleveland State Univ.) 228 p CSCL 10B

N92-10220

Unclas
G3/44 0045750

FINAL REPORT
NAG 3-1008
NASA LEWIS RESEARCH CENTER
CLEVELAND. OHIO 44135

PRINCIPAL INVESTIGATOR: PAUL A. BOSELA

INTRODUCTION

This research project represented a cooperative effort between Lewis Research Center (LeRC) and Cleveland State University (CSU). This project has been continued under contract with Analex Corporation.

SUMMARY OF RESEARCH ACCOMPLISHMENTS

Initial investigation by the principal investigator occurred during the summer of 1988 under a NASA/ASEE Summer Faculty Fellowship, and discussed in the Interim Status Report #1. Continued investigation which occurred under NAG3-1008, for the time period February 8, 1989-June 15, 1989, was also reported in the first interim status report.

Additional work was continued during Summer, 1989, under a NASA/ASEE Summer Faculty Fellowship. This was also included in the first interim status report.

NASA LeRC approved the continued funding of this grant for the period September 15, 1989 through September 14, 1990. The following accomplishments occurred during the period September 15, 1989 through March 15, 1990:

1. A rigorous solution for the dynamic analysis of a free/free beam with an axial tension pre-load was developed. Solution of the characteristic equation suggested that the three required rigid body modes were present.

2. A paper entitled,"Dynamic Analysis of Space-related Linear and Non-linear Structures", was co-authored by Professor Bosela, Dr. Francis Shaker (NASA LeRC), and Professor Demeter Fertis (University of Akron, Akron, Ohio). The paper was presented by Professor Bosela at the Southeast Conference of Theoretical and Applied Mechanics XV, Atlanta, Georgia, during March, 1990.

3. A three-node beam element was developed, using Martin's methodology. It was duplicated using a variational formulation. Its performance in various sample problems was tested.

4. The bow-string problem was identified as an idealized model of a solar array which had potential to yield rigid body rotation capability.

5. Numerous papers regarding derivation of higher-order stiffness matrices were reviewed, including work by Argyris, Saunders, Paz, Martin, Marcal, and others. Their matrices were tested for rigid body capabilities.

From March 16, 1990, through the completion of this grant, the following accomplishments were made:

1. Exact solutions of various pre-loaded beam problems were examined, and the Galerkin criterion was used to develop stiffness and mass matrices.

2. The modified matrices developed using the Galerkin criterion were incorporated into a finite element dynamic analysis algorithm, and the resulting finite element solution compared with the rigorous solution.

3. A directed force correction matrix for the pre-loaded 2 dimensional beam element was developed at the global level. This matrix produced a tangential stiffness matrix which does possess all of the required rigid body modes.

4. This global force correction was incorporated into a finite element dynamics algorithm, and was shown to correct the missing zero eigenvalue customary in traditional finite element solutions, without affecting the eigenvalues corresponding to the flexible modes. It also performed very well in the diagonalization/partitioning methodology used in matrix dynamic analysis.

5. The detailed results of this study were published as a doctoral dissertation at the University of Akron, Akron, Ohio, and are attached. The period of performance for this grant expired on April 6, 1991. The final dissertation was submitted for publication during the summer of 1991, and is available at the University of Akron library.

ABSTRACT

Space structures, such as the space station solar arrays, must be extremely light-weight, flexible structures. Accurate prediction of the natural frequencies and mode shapes is essential for determining the structural adequacy of components, and designing a controls system. The tension preload in the "blanket" of photovoltaic solar collectors, and the free/free boundary conditions of a structure in space, causes serious reservations on the use of standard finite element techniques of solution. In particular, a phenomena known as "grounding", or false stiffening, of the stiffness matrix occurs during rigid body rotation.

This dissertation examines the grounding phenomena in detail. Numerous stiffness matrices developed by others are examined for rigid body rotation capability, and found lacking. Various techniques are utilized for developing new stiffness matrices from the rigorous solutions of the differential equations, including the solution of the directed force problem. A new directed force stiffness matrix developed by the author provides all the rigid body capabilities for the beam in space.

Key words (Geometric stiffness matrix, grounding, rigid body modes, Galerkin criterion, finite element dynamic analysis, eigenvalues/eigenvectors)

ACKNOWLEDGEMENT

The author wishes to express his sincere gratitude and appreciation to his advisor, Dr. Demeter Fertis, whose guidance, encouragement, and assistance contributed to the completion of this dissertation.

The author also wishes to thank Dr. Paul Bellini, who has been a friend, colleague, and mentor throughout my Engineering career. He is also indepted to Dr. Frank Shaker and Dr. James McAleese, whose NASA funding supported this project, and whose insights to the grounding problem, as well as doctoral studies in general, were immeasurable.

The author wishes to thank his parents, Paul and Viola, who instilled in him the desire to strive for knowledge. It is with deep regret that my father's recent death prevented us from celebrating together. He has been a loving father, and a constant inspiration for me. As he rests in eternal peace, his memories will be with me forever.

Finally, the author wishes to thank his wife, Angie, and children Denise, Sheila, and Paul Jr., whose support and understanding helped me see this to completion. May you realize that you can reach your own goals if you always do your best, work "hard and smart", and refuse to quit.

TABLE OF CONTENTS

LIST OF FIGURES

LIST OF TABLES

LIST OF APPENDICES

LIST OF SYMBOLS

A	area (in^2)
$[A_1]$	Paz's second order mass-geometrical matrix
B	$\sqrt{(P/EIR)}$
b_1, b_2, b_3, b_4	constants in polynomial expression for Marcal's initial displacement matrices
C	coefficient used in Saunders' development
c	bowstring spring constant
D	coefficient used in Saunders' development
E	Young's modulus (psi)
G	shear modulus
$[G_0]$	Paz's consistent geometric stiffness matrix
$[G_1]$	Paz's second order geometric matrix
H_i	Hermitian polynomials
I	moment of inertia (in^4)
I^*	$I/(1+P/K'AG)$
$K'AG$	beam shear rigidity
K	support spring stiffness
K'	shear factor
K_T	tangential stiffness matrix
K_{bow}	bowstring stiffness matrix
K^{DFC}	directed force correction matrix

$[K]$	stiffness matrix
$[Ke]$	elastic stiffness matrix
$[Ke]_T$	elastic stiffness matrix for a Timoshenko beam
$[Kg]$	geometric stiffness matrix
$[Kg]_{3\text{-node}}$	geometric stiffness matrix for a 3-node beam formulation
$[K_{NC}]$	Argyris load correction matrix for a tangent follower force
$[K_{ROT}]$	shear and rotatory stiffness matrix from Galerkin formulation
L	beam length
$\hat{L}$	L/number of elements
$[M_0]$	Paz's first order mass matrix
$[M_1]$	Paz's second order mass matrix
$[M]$	mass matrix
$M(x)$	moment
m	mass per unit length ($lb\text{-}sec^2/in^2$)
$N(x)$	internal axial force
$\tilde{[N_1]}$	Marcal's first initial displacement matrix
$\tilde{[N_2]}$	Marcal's second initial displacement matrix
P	axial tension load
$\hat{P}$	$PL^2/30EI$
P'	pseudo-force
$\tilde{P}$	directed force component
R	$(1-P/K'AG)$
$\{R_i\}$	forces

$[R_0]$	Paz's rotary inertia and shear matrix
R^{DFC}	directed force correction vector
$[S]$	Paz's dynamic stiffness matrix
S_x	Saunders internal shear
T	kinetic energy
t	time
U_a	strain energy due to axial load
U_b	strain energy due to bending
$\{U_{TX}\}$	rigid body translation vector in axial direction
$\{U_{TY}\}$	rigid body translation vector in transverse direction
$\{U_{RBR}\}$	rigid body rotation vector
u	axial displacement
$\hat{u}$	rigid body displacement in axial direction
$V(x)$	shear
$\tilde{V}$	$V_1 - P \sin \phi$
v	transverse displacement
$\hat{v}$	rigid body displacement in transverse direction
$W(x)$	displacement function
$\tilde{W}(x)$	displacement function approximated using Galerkin
$\{X\}$	displacement vector
y	displacement in y direction
z	sin(BL)(2tanBL/2-BLR)
α	(BL)
β	1/2 the angle of rigid body rotation

Γ_x	rotation due to shear strain
Φ	shear factor = $12\ EI/L^2K'AG$ for Timoshenko beam
ϕ	directed force angle
$\phi(\beta^4)$	a function of β^4
ϕ_i	shape functions
$[\phi]$	matrix of mode shapes
δ	mass per unit volume ($lb\text{-}sec^2/in^4$)
θ	rotation angle
$\hat{\theta}$	rigid body rotation angle
σ	stress
Ω	frequency (radians/sec)
Lambda	Ω^2
EIG.	Eigenvalues

CHAPTER 1

INTRODUCTION

In order to be cost-effective, space structures must be extremely light-weight, and subsequently, very flexible structures. The power system for Space Station Freedom is such a structure. Each array consists of a deployable truss mast and a split "blanket" of photovoltaic solar collectors. The solar arrays are deployed in orbit, and the blanket is stretched into position as the mast is extended during deployment. Geometric stiffness due to the tension preload in the blanket make this an interesting non-linear problem.

The space station will be subjected to various dynamic loads, during shuttle docking, solar tracking, attitude adjustment, etc.. Accurate prediction of the natural frequencies and mode shapes of the space station components, including the solar arrays, is critical for determining the structural adequacy of the components, and for designing a dynamic controls system.

This dissertation has the following objectives:

1. Examine in detail the "grounding" phenomenon associated with rigid body rotation of a pre-loaded beam in space.

2. Examine beam geometric stiffness matrices developed by others with respect to rigid body motion capabilities.

3. Develop higher order stiffness matrices from the rigorous solution utilizing Galerkin's criterion, incorporate these stiffness matrices into a finite element algorithm, and compare the finite element solutions with the rigorous solutions.

4. Examine the directed force (bow-string) problem for its potential as a basis for developing stiffness matrices which possess rigid body rotational capabilities.

5. Check the performance of any new matrix which possesses a complete set of rigid body motion capabilities in the diagonalization/partitioning methodology used in dynamic response.

CHAPTER 2

LIMITATIONS OF CURRENT METHODOLOGY

Most structural systems are rigidly attached to supports at either or both ends. In order for any movement to occur, the structure must deform, and internal strain energy is developed. Space structures, on the other hand, are not rigidly attached to the ground. Instead, they are free to move as rigid bodies as well as to deform.

Complex structures are generally analyzed using finite element computer programs which solve the dynamic equations of motion using matrix analysis techniques. The equations of motion are set up in the form of the generalized eigenvalue problem

$$[[K]-\Omega_i^2[M]]\ \{u_i\} = \{R_i\}$$

where [K] is the global stiffness matrix

[M] is the global mass matrix

Ω_i are the natural frequencies of vibration

$\{u_i\}$ are the displacement or mode shape vectors

$\{R_i\}$ are the forces

Using that basis, rigid body modes are the eigenvectors associated with zero frequencies of vibrations (eigenvalues).

Current methodology utilizes MSC/NASTRAN solution 64 to generate the tangential stiffness matrix for the deployed array, storing this matrix in a database, then using this matrix in solution 63 dynamic analysis, to obtain the frequencies of vibration. As a routine check of the model, the global stiffness matrix is multiplied with a matrix of the rigid body modes to determine whether any pseudo-forces occur. (Whether strain energy has developed.) Since no internal stresses should occur during rigid body motion, the generation of pseudo-forces indicates that an internal "grounding", or false stiffening, of the system occurs, due to errors or deficiencies in the finite element model.

It was found that the global stiffness matrix does not possess rigid body rotation capabilities. In order to predict the dynamic response of the structure, a Craig-Bampton substructuring scheme is used. However, certain erroneous non-zero terms appear in the null set of the partitioned matrices due to the grounding effect. They must be zeroed out, and the missing rigid body modes appended to the matrix, in order to more accurately predict the dynamic response [1].

The author idealized the problem as a free/free beam in tension, and found [2] that the pseudo-forces are developed at the element level due to limitations inherent in the geometric stiffness matrices currently in acceptable use. In particular, the geometric stiffness matrices for the beam element lack the capability for rigid body rotations, especially when the rotations are large.

The geometric (initial stress) stiffness matrices in current use developed from a Bernoulli-Euler formulation have been shown to provide acceptable results for most static displacement and buckling problems, provided a sufficient number of elements are used [3]. However, refinement of the mesh does not produce convergence to the missing zero frequency in the dynamics problem of the pre-loaded beam with free/free boundary conditions. In addition, higher frequencies may be significantly in error. Table 1 compares the finite element solution for a pre-tensioned beam with pinned/roller and free/free boundary conditions.

TABLE 1 Comparison of Finite Element Method Versus Exact Solution for a Beam in Tension

$A = 48\ in^2$

$E = 30 \times 10^6\ psi$

$I = 1000\ in^4$

$m = 0.03525\ lb\text{-}sec^2/in^2$

$P = 10{,}000{,}000\ lb$

$L = 100\ IN$

Pin/Roller

freq	number of elements 1	2	4	8	% error	rigorous sol Fertis[19]
1	1142	1056	1053	1053	3.5	1043
2	3501	3257	3195	3180	axial	
3	4758	4180	3807	3794	4.0	3647
4		10291	8494	8357	9.0	7669

Free/Free Beam

freq	number of elements 1	2	4	8	% error	rigorous sol [16] Bosela/Shaker [17]
1	0	0	0	0	0	0
2	0	0	0	0	0	0
3	580	580	579	579	∞	0
4	2798	2383	2381	2378	15.0	2017
5	7001	6725	5991	5958	4.7	5725

CHAPTER 3

ELASTIC STIFFNESS MATRIX

The elastic stiffness matrix for a 2-node Bernoulli beam is

$$[Ke] = \frac{EI}{L^3} \begin{bmatrix} AL^2/I & 0 & 0 & -AL^2/I & 0 & 0 \\ 0 & 12 & 6L & 0 & -12 & 6L \\ 0 & 6L & 4L^2 & 0 & -6L & 2L^2 \\ -AL^2/I & 0 & 0 & AL^2/I & 0 & 0 \\ 0 & -12 & -6L & 0 & 12 & -6L \\ 0 & 6L & 2L^2 & 0 & -6L & 4L^2 \end{bmatrix}$$

The [Ke] matrix must possess the capacity of a full set of rigid body modes. In other words, the element must be able to both translate and rotate without developing stresses (see Figure 1).

a. Rigid Body Translation in Axial Direction

$$\{U_{TX}\} = [1,0,0,1,0,0]^T$$

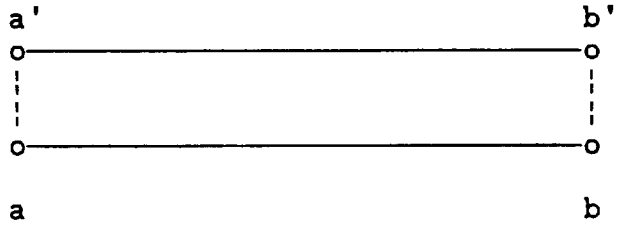

b. Rigid Body Translation in Transverse Direction

$$\{U_{TY}\} = [0,1,0,0,1,0]^T$$

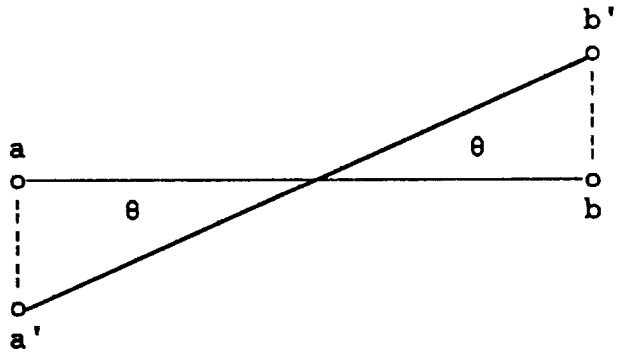

c. Rigid Body Rotation

$$\{U_{RBR}\} = \theta[0,-L/2,1,0,L/2,1]^T$$

Figure 1 Rigid Body Modes

Note that in Fig 1(c) that the rotation is considered to be relatively small, such that the displacement in the axial direction due to the rotation is negligible.

Multiplying [Ke] x [Rigid Body Mode] =

[0,0,0,0,0,0]

holds for all three modes. Hence, [Ke] possesses all the required rigid body mode capabilities.

Another way of determining whether [Ke] possesses all the rigid body mode capabilities is to solve the dynamic analysis of the beam with free/free boundary conditions. This was done [5] using the finite element dynamics algorithm in the computer program NLFINITE.FOR (Appendix C). The results were three zero eigenvalues and corresponding rigid body mode shapes.

Another beam stiffness matrix which incorporates shear effects is referred to as a Timoshenko beam. The elastic stiffness matrix for a Timoshenko beam is

$$[Ke]=\frac{EI(1/(1+\Phi))}{L^3}\begin{bmatrix} AL^2(1+\Phi)/I & 0 & 0 & -AL^2(1+\Phi)/I & 0 & 0 \\ 0 & 12 & 6L & 0 & -12 & 6L \\ 0 & 6L & (4+\Phi)L^2 & 0 & -6L & (2-\Phi)L^2 \\ -AL^2(1+\Phi)/I & 0 & 0 & AL^2(1+\Phi)/I & 0 & 0 \\ 0 & -12 & -6L & 0 & 12 & -6L \\ 0 & 6L & (2-\Phi)L^2 & 0 & -6L & (4+\Phi)L^2 \end{bmatrix}$$

Where $\Phi = 12\ EI/(L^2K'AG)$, which corrects for shear deformation. As K'AG becomes very large, $\Phi \approx 0$, and $[Ke]_T = [Ke]$. The Timoshenko elastic stiffness also possesses a full set of rigid body modes.

A major difference in the Timoshenko approach is that the bending rotation is considered independently in the derivation, not simply the derivative of the displacement equation, as is done in the Bernoulli derivation.

CHAPTER 4

GEOMETRIC STIFFNESS MATRIX DEVELOPMENT

The presence of an axial force introduces additional stiffness terms, resulting in the geometric stiffness, or initial stress stiffness matrix. Various formulations of the geometric stiffness matrix have been developed.

When the Hermitian interpolating polynomials (used to derive the [Ke] matrix) are used in deriving the geometric stiffness coefficients [4], the resulting [Kg] is referred to as the consistent geometric stiffness matrix (Bernoulli beam geometric stiffness).

$$[Kg] = P/(30L)\begin{bmatrix} 0 & 0 & 0 & 0 & 0 & 0 \\ 0 & 36 & 3L & 0 & -36 & 3L \\ 0 & 3L & 4L^2 & 0 & -3L & -L^2 \\ 0 & 0 & 0 & 0 & 0 & 0 \\ 0 & -36 & -3L & 0 & 36 & -3L \\ 0 & 3L & -L^2 & 0 & -3L & 4L^2 \end{bmatrix}$$

Application of the rigid body modes to [Kg] results in

$$[Kg] \times \begin{bmatrix} 1 & 0 & 0 \\ 0 & 1 & -L\theta/2 \\ 0 & 0 & \theta \\ 1 & 0 & 0 \\ 0 & 1 & L\theta/2 \\ 0 & 0 & \theta \end{bmatrix} = \begin{bmatrix} 0 & 0 & 0 \\ 0 & 0 & -P\theta \\ 0 & 0 & 0 \\ 0 & 0 & 0 \\ 0 & 0 & P\theta \\ 0 & 0 & 0 \end{bmatrix}$$

The terms ± Pθ are fictitious forces generated during the rigid body rotation. Similarly, dynamic analysis, using NLFINITE.FOR, yields only two zero eigenvalues for the free/free beam in tension, corresponding to axial and transverse rigid body translations only.

Various formulations have been used for establishing the geometric stiffness matrices from the static displacement problem. Martin [6] used a strain energy formulation with interpolating polynomials. Clough [7] used minimization of the potential function with the Hermitian polynomials. Both approaches yield a consistent geometric stiffness matrix, which lacks rigid body rotation capability, as was previously demonstrated.

The author followed Martin's methodology in developing a 3-node beam geometric stiffness matrix [8]. The following matrix was obtained.

$$P\begin{bmatrix}
\frac{7}{3L} & & & & & & & & & \\
0 & \frac{18272}{105L} & & & & & & & & \\
0 & \frac{3469}{105} & \frac{659L}{105} & & & & & & & \\
\frac{-20}{3L} & 0 & 0 & \frac{64}{3L} & & & & & & \\
0 & \frac{-22096}{105L} & \frac{-4208}{105} & 0 & \frac{27292}{105L} & & & & & \\
0 & \frac{304}{5} & \frac{23L}{2} & 0 & -72 & \frac{109L}{5} & & & & \\
\frac{13}{3L} & 0 & 0 & \frac{-44}{3L} & 0 & 0 & \frac{31}{3L} & & & \\
0 & \frac{3824}{105L} & \frac{739}{105} & 0 & \frac{-5296}{105L} & \frac{56}{5} & 0 & \frac{1472}{105L} & & \\
0 & \frac{-3469}{105} & \frac{-659L}{105} & 0 & \frac{4208}{105} & \frac{-23L}{2} & 0 & \frac{-739}{105} & \frac{659L}{105} &
\end{bmatrix}$$

SYMMETRIC

$$[Kg]_{3\text{-NODE}}$$

By inspection, $[Kg]_{3\text{-node}}$ has two rigid body translational capabilities. The exact rigid body rotation vector is

$[L(1-COS(2\beta))/2, -LSIN(2\beta)/2, 2\beta, 0, 0, 2\beta,$

$-L(1-COS(2\beta))/2, LSIN(2\beta)/2, 2\beta]^T,$

where ß is 1/2 the angle of rotation.

If this vector is expanded in power series form, upon retaining the first two terms, and factoring out ßL, one obtains

$$\{U_{RBR}\}^T = [ß-ß^3/3,-1+2ß^2/3,2/L,0,0,2/L,-ß+ß^3/3,1-2ß^2/3,2/L].$$

Multiplying [Kg] by $\{U_{RBR}\}$ yields

$$[-2ß^2,91.73ß^3-16ß,1(17.3ß^3-3ß),8ß^2,16ß-106.7ß^3,$$
$$L(33.01ß^3-6ß),-6ß^2,14.93ß^3,L(3ß-17.33ß^3)],$$

which contains numerous non-zero terms. Hence, $[Kg]_{3\text{-node}}$ does not possess rigid body rotation capability.

Saunders [9] solves for the exact solution of the differential equations using a Timoshenko approach, then expands his "exact" stiffness matrix in a power series solution, obtaining a series of matrices of increasing order.

Saunders "exact" stiffness matrix is

$$[K]=\frac{P}{Z}\begin{bmatrix} BR\cdot SIN(BL) & & & \text{SYMMETRIC} \\ 1-COS\ BL & \dfrac{SIN(BL)}{BR}-L\cdot COS(BL) & & \\ -BR\cdot SIN(BL) & COS(BL)-1 & BR\cdot SIN(BL) & \\ 1-COS(BL) & L-\dfrac{SIN(BL)}{BR} & COS(BL)-1 & \dfrac{SIN(BL)}{BR}-L\cdot COS(BL) \end{bmatrix}$$

where

$B = \sqrt{(P/EIR)}$

$\alpha = BL$

$R = (1-P/K'AG)$

P = AXIAL LOAD

K'AG = beam shear rigidity

I = moment of inertia

$z = SIN(BL)\cdot(2\cdot TAN(BL/2)-BLR)$

By observation, rigid body translation capability is present in the transverse direction.

$$\text{Upon multiplying } [K]\cdot\{U_{RBR}\} = \frac{P\theta}{z}\begin{bmatrix} -2COS(\alpha)-LR\beta\cdot SIN(\alpha)+2 \\ 0 \\ 2COS(\alpha)+LR\beta\cdot SIN(\alpha)-2 \\ 0 \end{bmatrix}$$

For small α, $COS(\alpha)\approx 1$, $SIN(\alpha)\approx\alpha$.

$$\begin{aligned} -2COS(\alpha)-LR\beta\cdot SIN(\alpha)+2 &= -LR\beta\alpha \\ &= -LRB\cdot BL \\ &= -L^2RB^2 \end{aligned}$$

$$\frac{P\theta}{z} = \frac{P\theta}{\sin(\alpha)\ (2\cdot \mathrm{Tan}\ (\alpha/2) - \alpha R)}$$

$$\approx \frac{P\theta}{\alpha\ (\alpha - \alpha R)}$$

$$= \frac{P\theta}{\alpha^2\ (1 - R)}$$

Thus, $(P/z)(-PL^2/EI) = \dfrac{P\theta(-B^2L^2R)}{\alpha^2\ (1-R)}$

$$= \frac{-\ P\theta R}{(1-R)}$$

$$= \frac{-\ \dfrac{P\theta(K'AG - P)}{K'AG}}{\dfrac{P}{K'AG}}$$

$$= (P - K'AG)\theta.$$

Thus, Saunders' "exact stiffness matrix does not possess the required rigid body rotation mode.

Argyris [10] uses his "natural formulation" to develop [Ke] and [Kg], which are identical with traditional [Ke] and [Kg]. He obtains another matrix $[K_{nc}]$, referred to as his load correction matrix, which compensates for non-conservative forces.

If we consider the axial load to remain tangent to the slope of the beam at the end points, Argyris's total geometric stiffness matrix $[Kg + K_{nc}]$ becomes

$$[Kg]_{TOTAL} = P \begin{bmatrix} 0 & 0 & SIN2\beta & 0 & 0 & 0 \\ 0 & 6/5L & 1/10+COS2\beta & 0 & -6/5L & 1/10 \\ 0 & 1/10 & 2L/15 & 0 & -1/10 & -L/30 \\ 0 & 0 & 0 & 0 & 0 & -SIN2\beta \\ 0 & -6/5L & -1/10 & 0 & 6/5L & -1/10-COS2\beta \\ 0 & 1/10 & -L/30 & 0 & -1/10 & 2L/15 \end{bmatrix}$$

The matrix is nonsymmetric. Multiplying $[Kg]_{TOTAL}$ by the exact rigid body rotation vector, then applying small angle considerations, yields $[4\beta^2,0,0,-4\beta^2,0,0]^T$, which contains non-zero terms. Hence, $[Kg]_{TOTAL}$ does not possess rigid body rotation capability. Note that the pseudo-forces now occur in the axial direction.

Martin [11] summarizes work done by Marcal [12] which introduced higher order terms in his initial

displacement matrices. In addition to the conventional [Ke] and [Kg], his initial displacement matrices are

$$[\tilde{N}_1]=AE/L \begin{bmatrix} 0 & b_4 & 0 & 0 & -b_4 & 0 \\ b_4 & b_2 & 0 & -b_4 & -b_2 & 0 \\ 0 & 0 & 0 & 0 & 0 & 0 \\ 0 & -b_4 & 0 & 0 & b_4 & 0 \\ -b_4 & -b_2 & 0 & b_4 & b_2 & 0 \\ 0 & 0 & 0 & 0 & 0 & 0 \end{bmatrix}$$

and

$$[\tilde{N}_2] = P \begin{bmatrix} 0 & 0 & 0 & 0 & 0 & 0 \\ 0 & 1.5b_4^2 & 0 & 0 & -1.5b_4^2 & 0 \\ 0 & 0 & 0 & 0 & 0 & 0 \\ 0 & 0 & 0 & 0 & 0 & 0 \\ 0 & -1.5b_4^2 & 0 & 0 & 1.5b_4^2 & 0 \\ 0 & 0 & 0 & 0 & 0 & 0 \end{bmatrix}$$

where $u = b_1 + b_2x$

$v = b_3 + b_4x$.

The basic non-linear equation is

$[K + 1/2\ \tilde{N}_1 + 1/3\ \tilde{N}_2]\cdot\{U\} = \{R\}$.

By inspection, $[\tilde{N}_1]$ and $[\tilde{N}_2]$ possess the required rigid body translation capabilities.

Let the rotation angle = 2β (Figure 2).

$u_1 = b_1 \qquad v_1 = b_3$

$u_2 = b_1 + b_2 L \qquad v_2 = b_3 + b_4 L$

$b_4 = (v_2 - v_1)/L$

$b_4 = (L\beta + L\beta)/L$

$b_4 = 2\beta$

$b_4^2/2 = 4\beta^2/2 = 2\beta^2$.

Similarly, $b_2 = -2\beta^2$.

Thus, the rigid body rotation check becomes

$[K + N_1 + N_2]\cdot\{U_{RBR}\}$ must equal 0,

where

$$[N_1] = AE/L \begin{bmatrix} 0 & \beta & 0 & 0 & -\beta & 0 \\ \beta & -\beta^2 & 0 & -\beta & \beta^2 & 0 \\ 0 & 0 & 0 & 0 & 0 & 0 \\ 0 & -\beta & 0 & 0 & \beta & 0 \\ -\beta & \beta^2 & 0 & \beta & -\beta^2 & 0 \\ 0 & 0 & 0 & 0 & 0 & 0 \end{bmatrix}$$

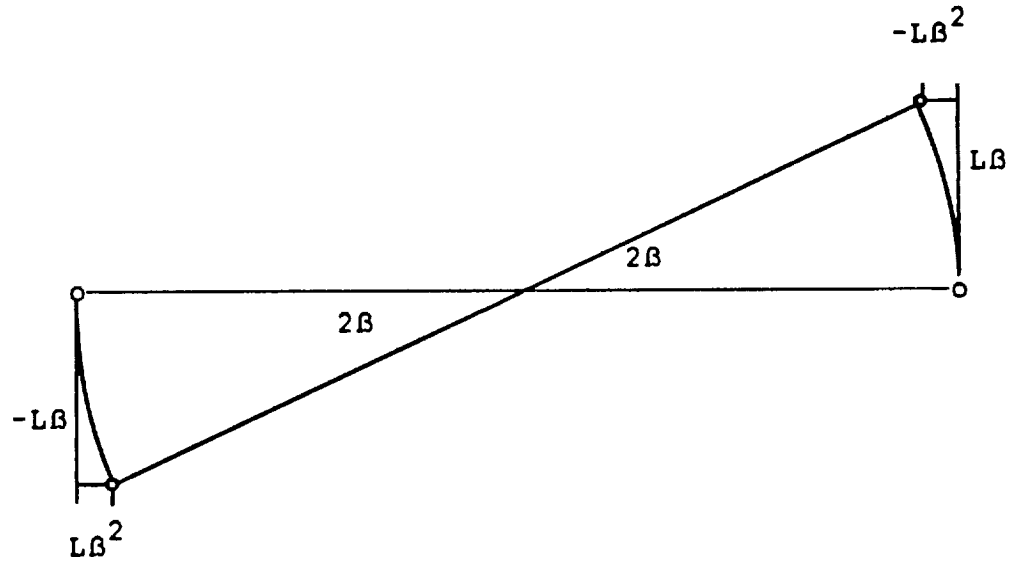

Figure 2 Rigid Body Rotation Angle of 2ß

and

$$[N_2] = P \begin{bmatrix} 0 & 0 & 0 & 0 & 0 & 0 \\ 0 & 2\beta^2 & 0 & 0 & -2\beta^2 & 0 \\ 0 & 0 & 0 & 0 & 0 & 0 \\ 0 & 0 & 0 & 0 & 0 & 0 \\ 0 & -2\beta^2 & 0 & 0 & 2\beta^2 & 0 \\ 0 & 0 & 0 & 0 & 0 & 0 \end{bmatrix}$$

Performing the rigid body rotation check yields

$[0, 4A\beta^3E - 4\beta^3LP - 2\beta P, 0, 0, -4A\beta^3E + 4\beta^3LP + 2\beta P, 0]^T$.

Note that non-zero pseudo-force terms still appear.

Development of the stiffness matrices from the equation of motion has been investigated by Paz, using both a Bernoulli [13] and Timoshenko [14] beam approach. He developed his "exact" stiffness matrix, then expanded it in a power series solution.

His solution, based on the transverse vibration of a beam with an axial compression load, is of the form

$$[S] = [K] - [G_0]P - [M_0]\Omega^2 - [A_1]P\Omega^2 - [G_1]P^2 - [M_1]\Omega^4 \cdots.$$

where

$[K]$ is the traditional elastic stiffness matrix with no axial terms.

$[G_0]$ is the standard geometric stiffness matrix.

$[M_0]$ is the first order mass matrix (consistent mass matrix).

$$[M_0] = mL/420 \begin{bmatrix} 156 & & \text{symmetric} & \\ 22L & 4L^2 & & \\ 54 & 13L & 156 & \\ -13L & -3L^2 & -22L & 4L^2 \end{bmatrix}$$

$[A_1]$ is the second order mass-geometrical matrix.

$$[A_1]=mL^3/EI \begin{bmatrix} 1/3150 & & \text{SYMMETRIC} & \\ L/1260 & L^2/3150 & & \\ -1/3150 & L/1680 & 1/3150 & \\ -L/1680 & L^2/3600 & -L/1260 & L^2/3150 \end{bmatrix}$$

$[G_1]$ is the second order geometrical matrix.

$$[G_1] = 1/EI \begin{bmatrix} L/700 & & \text{SYMMETRIC} & \\ L^2/1400 & 11L^3/6300 & & \\ -L/700 & -L^2/1400 & L/700 & \\ L^2/1400 & -13L^3/12600 & -L^2/1400 & 11L^3/6300 \end{bmatrix}$$

$[M_1]$ is the second order mass matrix.

$$[M_1] = \frac{m^2L^5}{1000\ EI}\begin{bmatrix} \frac{59}{161\cdot 7} & & \text{SYMMETRIC} & \\ \frac{223L}{2910\cdot 6} & \frac{71L^2}{4365\cdot 9} & & \\ \frac{1279}{3880\cdot 8} & \frac{1681L}{23284\cdot 8} & \frac{59}{161\cdot 7} & \\ \frac{-1681L}{2384\cdot 8} & \frac{-1097L^2}{69854\cdot 4} & \frac{-223L}{2910\cdot 6} & \frac{71L^2}{4365\cdot 9} \end{bmatrix}$$

The mass matrices don't possess rigid body modes, but they are not intended to, since they generate the inertial forces. $[G_1]$ possesses all the rigid body modes. Hence, no correction to $[G_0]$, which lacks rigid body rotation capability, is applied. Thus, "grounding" during rigid body rotation still occurs.

Similarly, Paz's Timoshenko formulation (which includes rotary inertia and shear terms), generates the matrix

$$[R_0]=mL/30)(R/L)^2(1+E/K'G)\begin{bmatrix} 36 & \text{SYMMETRIC} & & \\ 3L & 4L^2 & & \\ -36 & -3L & 36 & \\ 3L & -L^2 & -3L & 4L^2 \end{bmatrix}$$

where the terms within the matrix are the same as the consistent geometric stiffness matrix. Thus, $[R_0]$ lacks rigid body rotation capabilities.

CHAPTER 5

FORCE UNBALANCE

Closer examination of the traditional static formulation of [Kg] indicated that there is a load imbalance in the representation, and that pseudo-forces occur to maintain equilibrium (Figure 3).

Recall that $[Kg]\cdot\{U_{RBR}\} = \{-P\theta,0,P\theta,0\}$. Using Figure 3, and letting the sum of the moments at O equal zero, yields

$$PLSIN2\beta - P'LCOS\beta = 0$$

$$P' = P\cdot TAN2\beta$$

$$= P\cdot TAN\theta$$

$$= P\theta + \text{higher order terms}$$

Thus, P' represents pseudo-forces required for equilibrium.

In reference [15], Collar and Simpson acknowledge the lack of rigid body rotation capability of [Kg], but indicate that it is not a problem, because the energy representation is correct.

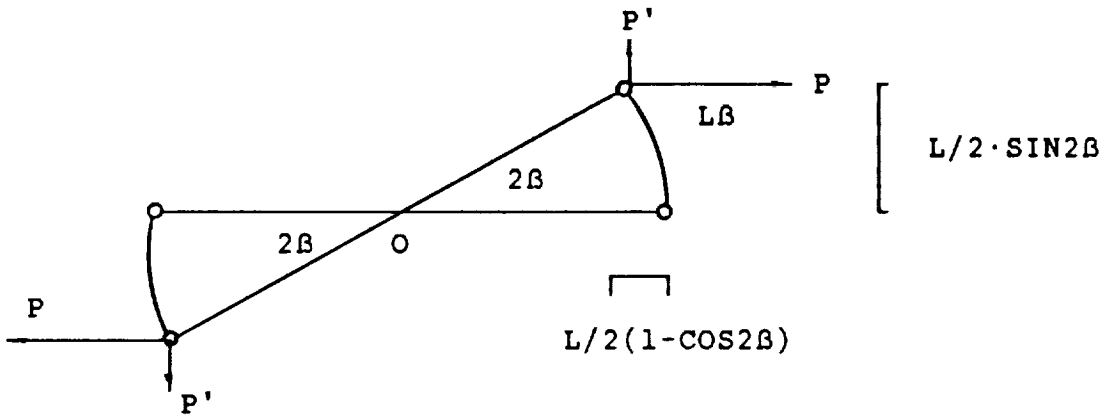

Figure 3 P' Represents Pseudo-forces Required for Equilibrium

Consider the work/energy relationship from Figure 3, without P'.

$$\text{WORK DONE BY P} = PL(1-\cos 2\beta)$$
$$= 2PL(1-\cos 2\beta)/2$$
$$= 2PL\cdot \sin^2\beta$$
$$= 2PL\beta^2 + \phi(\beta^4) + \text{higher order terms}$$

Similarly, using a matrix development

$$\text{ENERGY} = 1/2\{U\}^T\cdot[K]\cdot\{U\}$$
$$= P\beta^2/2[-2,0,2,0]\cdot[-L,2,L,2]^T$$
$$= 2PL\beta^2.$$

Therefore, the energy relationship is correct for the β^2 terms, but the higher order terms are neglected. For large rigid body rotation, this is significant.

It should be noted that as long as the pre-load P is assumed to remain horizontal during rotation, work will be done by the force. Thus, true rigid body rotation cannot occur. In order for the true strain energy to equal zero, the force P must change its orientation as the beam rotates (ie. a follower force, as in Figure 4).

$$\text{WORK DONE} = -L(P+P\cdot\cos 2\beta)(1-\cos 2\beta)/2 + P\cdot\sin 2\beta(L\cdot\sin 2\beta)/2$$
$$= PL[-(1+\cos 2\beta)(1-\cos 2\beta)+\sin^2 2\beta]$$
$$= PL/2(-1+\cos^2 2B+\sin^2 2\beta)$$
$$= PL/2(-1+1)$$
$$= 0.$$

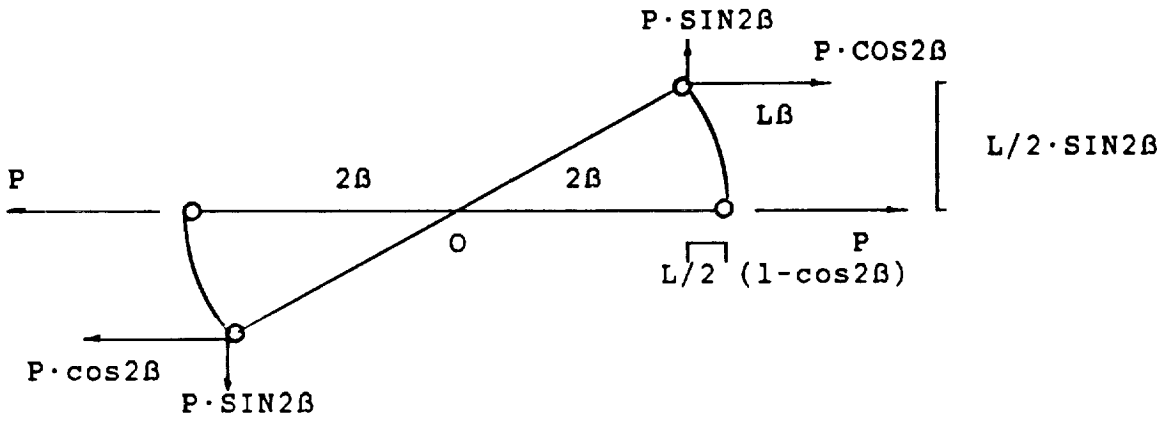

Figure 4 Work Done During Rigid Body Rotation by Follower Force

CHAPTER 6

RIGOROUS SOLUTION OF FREE/FREE BEAM WITH AXIAL TENSION LOAD

The author [16] also developed the rigorous free vibration solution of a free/free beam with an axial tension pre-load. The equation of motion developed agrees with that given by Paz [13] uses to develop his dynamic stiffness matrix. Solution of the differential equation is similar to that given by Shaker [17]. It was also shown that the characteristic equation developed indicated the presence of three zero frequencies, and the corresponding rigid body modes.

CHAPTER 7

DIRECTED FORCE PROBLEM

Since, as was shown in Section 4, traditional formulations did not satisfy equilibrium conditions during rigid body rotation, it was determined that investigation of the directed force problem is necessary.

Consider a beam with axial forces which remain directed at the opposite end points (Figure 5). This force system can be shown to be conservative. Derivation of stiffness matrices for this system was examined, utilizing Clough' methodology [7], Saunders' methodology [9], and Galerkin's criterion. The first two methods are discussed in this section. The last method is discussed in Section 9.

Clough's Methodology for the Directed Force Problem

Consider the beam in the deformed state shown in Figure 6. Summing forces in the X direction and setting them equal to zero yields

$$P \cos \theta = N(x) \cos W'(x) + V(x) \sin W'(x)$$

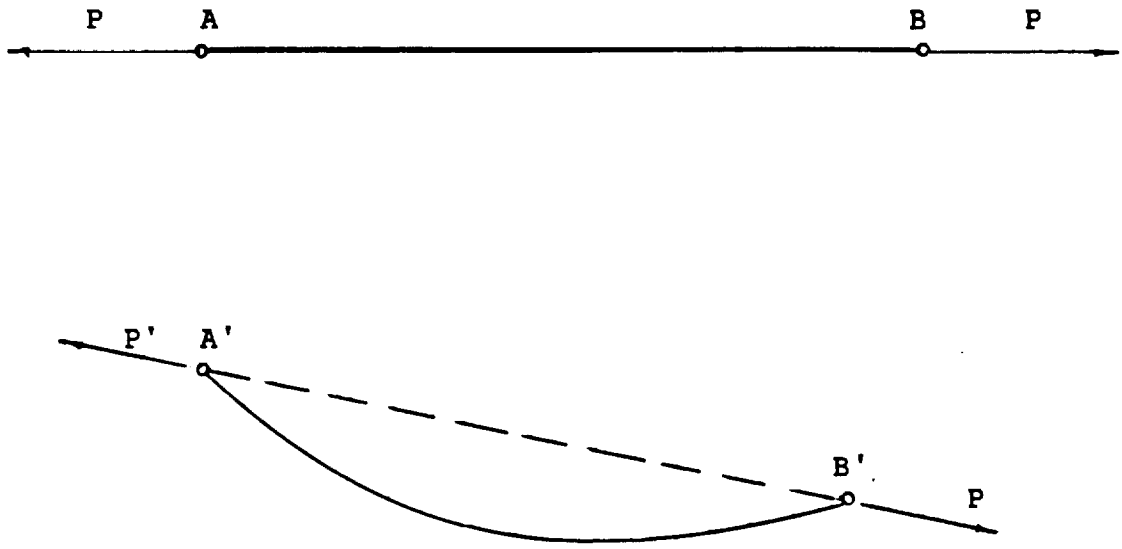

Figure 5 Beam with a Directed Force

$$N(x) = \frac{P \cos \theta}{\cos W'(x)} - \frac{V(x) \sin W'(x)}{\cos W'(x)} \quad \text{----------(7.1)}$$

For small displacements

$$N(x) = P \cos \theta - V(x)\, W'(x)$$

Summing forces in the Y direction and setting them equal to zero yields

$$P \sin \theta = N(x) \sin W' - V(x) \cos W'$$

$$N(x) = \frac{P \sin \theta}{\sin W'} + \frac{V(x) \cos W'}{\sin W'} \quad \text{----------(7.2)}$$

For small rotations, Eq.(7.2) becomes

$$N(x) = \frac{P \sin \theta}{W'} + \frac{V(x)}{W'}$$

Equations (7.1) and (7.2) can be rewritten

$$\frac{N(x) \cos W'}{\sin W'} = \frac{P \cos \theta \cos W'}{\cos W' \sin W'} - V(x) \quad \text{----------(7.3)}$$

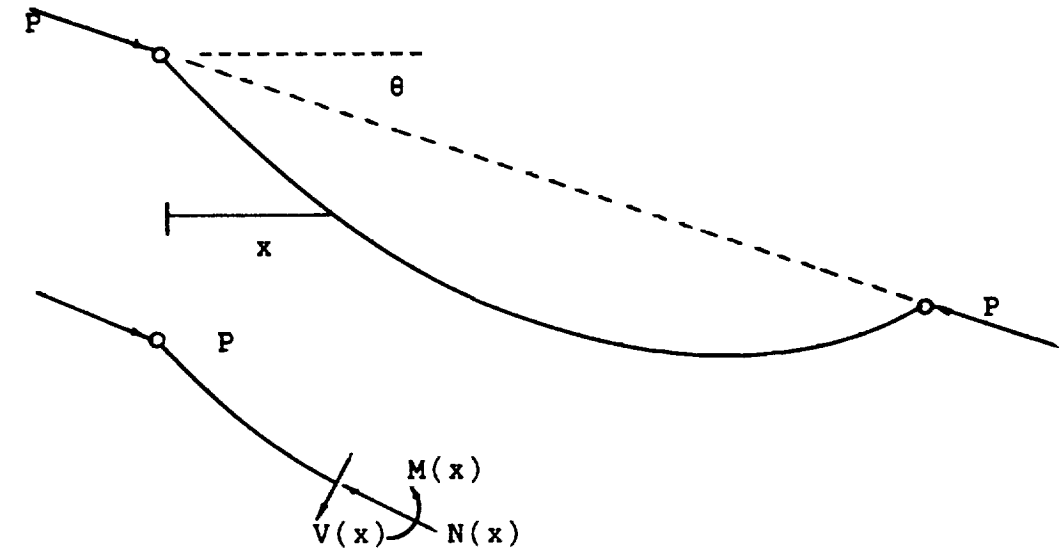

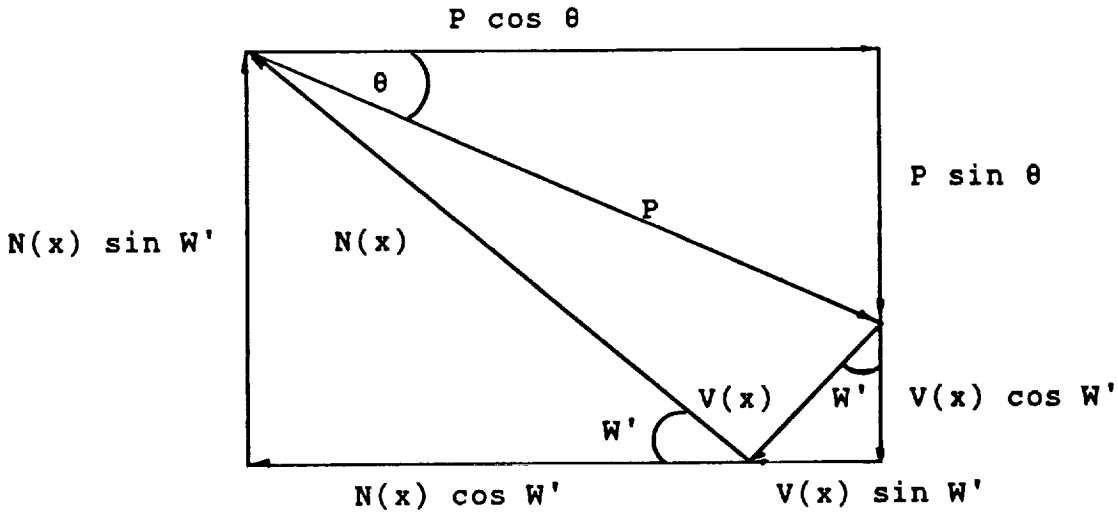

Figure 6 Bowstring in Deformed Position and Resultant Shear, Moment, and Axial Forces

$$\frac{N(x)\ \sin W'}{\cos W'} = \frac{P\ \sin\theta\ \sin W'}{\sin W'\ \cos W'} + V(x) \text{ ----------(7.4)}$$

Adding equations (7.3) and (7.4) yields

$$N(x)\left[\frac{\cos W'}{\sin W'} + \frac{\sin W'}{\cos W'}\right] = P\left[\frac{\cos\theta}{\sin W'} + \frac{\sin\theta}{\cos W'}\right] \text{ ---------(7.5)}$$

or

$$N(x) = \frac{\dfrac{P(\cos\theta\ \cos W' + \sin\theta\ \sin W'}{\sin W'\ \cos W'}}{\dfrac{\cos W'^2 + \sin W'^2}{\sin W'\ \cos W'}}$$

$$N(x) = P(\cos\theta\ \cos W' + \sin\theta\ \sin W') \text{ ----------(7.6)}$$

During rigid body rotation, $W' = \theta$, and equation (7.6) becomes

$$N(x) = P.$$

Clough and Penzien [7] develop the equation for the geometric stiffness matrix as

$$Kg_{ij} = \int_0^L N(x)\, H_i'(x)\, H_j'(x)\, dx \qquad \text{----------(7.7)}$$

The Hermitian interpolating polynomials, and their derivatives, are

$$\begin{aligned} H_2 &= 1 - 3(x/L)^2 + 2(x/L)^3 & H_5 &= 3(x/L)^2 - 2(x/l)^3 \\ H_2' &= -6\, x/L^2 + 6x^2/L^3 & H_5' &= 6x/L^2 - 6x^2/L^3 \\ H_3 &= X - 2x^2/L + x^3/L^2 & H_6' &= -x^2/L + x^3/L^2 \\ H_3' &= 1 - 4x/L + 3x^2/L^2 & H_6' &= -2x/L + 3x^2/L^2 \end{aligned} \qquad \text{----(7.8)}$$

Substituting equation (7.6) into equation (7.7) yields

$$\begin{aligned} Kg_{ij} &= \int_0^L P(\cos\theta \cos W' + \sin\theta \sin W')\, H_i'(x)\, H_j'(x)\, dx \\ &= P\cos\theta \int_0^L \cos W'\, H_i'(x) H_j'(x)\, dx \\ &\quad + P\sin\theta \int_0^L \sin W'\, H_i'(x) H_j'(x)\, dx \qquad \text{-----(7.9)} \end{aligned}$$

For the special case of pure rigid body rotation only ($W'(0) = W'(L) = \theta \neq f(x)$), equation (7.9) reduces to

$$Kg_{ij} = P(\cos^2\theta + \sin^2\theta) \int_0^L H_i'(x) H_j'(x)\, dx$$

$$= P \int_0^L H_i'(x) H_j'(x)\, dx$$

which yields the consistent K_g matrix.

Therefore, K_g using this formulation does not possess rigid body rotation capability. It may be necessary to include separate interpolating functions for the rotation instead of the derivatives of the shape functions.

Consider the appropriateness of the Hermitian polynomials for shape functions.

$$u = \{H_1 \; H_4\} \begin{bmatrix} u_1 \\ u_2 \end{bmatrix} \qquad v = \{H_2 \; H_3 \; H_5 \; H_6\} \begin{bmatrix} u_2 \\ u_3 \\ u_5 \\ u_6 \end{bmatrix}$$

For rigid body translation

$u = u_1 = u_2 = \text{constant} = \hat{u}$

$\hat{u} = H_1 \hat{u} + H_4 \hat{u}$

$= (H_1 + H_4) \hat{u}$

But, $H_1 + H_4 = 1$, so the equality is satisfied.

Similarly, $v = u_2 = u_5 = \text{constant} = \hat{v}$

and $u_3 = u_6 = 0$.

$$\hat{v} = H_2\ \hat{v} + H_5\ \hat{v}$$

$$\hat{v} = (H_2 + H_5)\ \hat{v}$$

Since $H_2 + H_5 = 1$, the equality is satisfied.

$$\theta = dv/dx = \{H_2'\ H_3'\ H_5'\ H_6'\}\begin{bmatrix} u_2 \\ u_3 \\ u_5 \\ u_6 \end{bmatrix}$$

For rigid body rotation

$$\theta = u_3 = u_6 = \text{constant} = \hat{\theta}$$

$$u_2 = -u_5 = -L \sin \hat{\theta}/2$$

$$\hat{\theta} = H_2' (-L \sin \hat{\theta})/2 + H_3'\ \hat{\theta} + H_5' (L \sin \hat{\theta})/2 + H_6'\ \hat{\theta}$$

$$= (H_5' - H_2')\ L \sin \hat{\theta}\ /2 + (H_3' + H_6')\ \hat{\theta}$$

For small angles, $\sin \hat{\theta} \approx \hat{\theta}$. Therefore,

$$\hat{\theta} = [(H_5' - H_2)\ L/2 + H_3' + H_6']\ \hat{\theta}$$

$\hat{\theta} = \hat{\theta}$. Thus, the equality is satisfied during rigid body rotation.

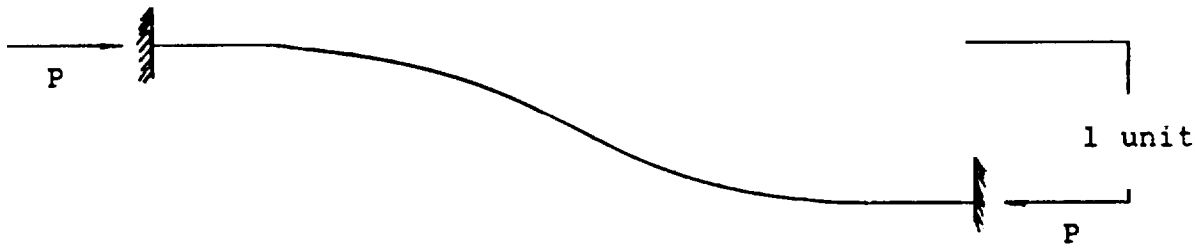

Figure 7 Application of Unit Displacements to a Beam

Saunders' Methodology for the Directed Force Problem

Saunders considers a beam with a horizontal load as shown in Figure 7, and applies various unit displacements to develop the stiffness matrices. This can be changed to a directed force problem by letting

$$P \longrightarrow \tilde{P} = P \cos \phi$$

and

$$V_1 \longrightarrow \tilde{V}_1 = V_1 - P \sin \phi$$

as shown in Figure 8.

$$S(x) = V_1 - P \cos \phi \, dy/dx - P \sin \phi \qquad (7.10)$$

$$= \tilde{V} - P \cos \phi \, y'$$

$$M(x) = V_1 x + P \cos \phi \, (y_1 - y_x) - P \, x \sin \phi - M_1 \qquad (7.11)$$

$$= \tilde{V}_1 x + P \cos \phi \, (y_1 - y_x) - M_1$$

Applying Saunders' methodology using equations(7.10) and (7.11) for the general directed force problem yields

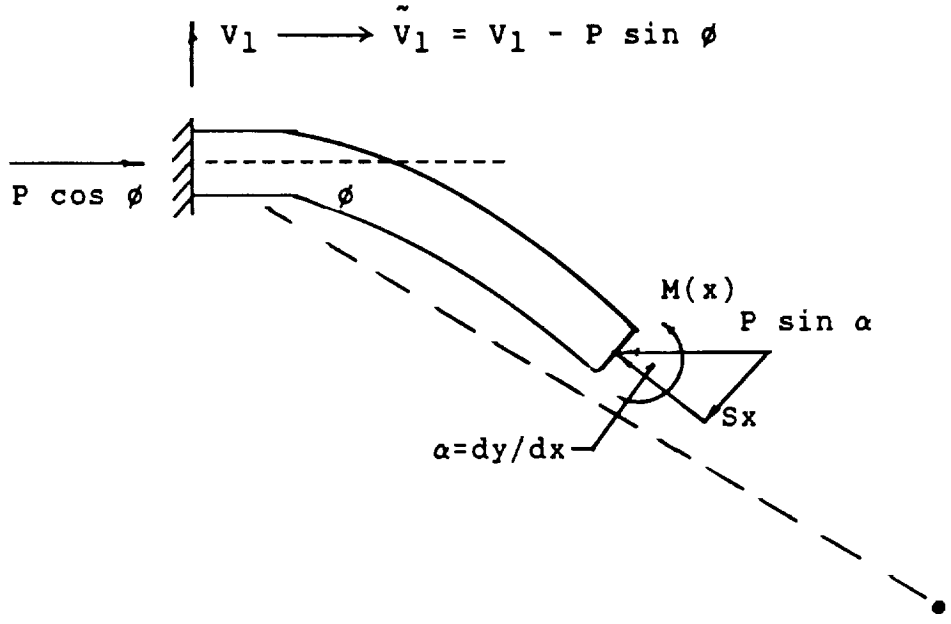

Figure 8 Directed Force Components

$$M_x/EI = \theta'_x \text{ ----------(7.12)}$$

$$y'_x = \theta_x + \Gamma_x \text{ ----------(7.13)}$$

Rotation due to shear strain

$$\Gamma_x = -\delta_x/K'AG \text{ ----------(7.14)}$$

$$S_x = \tilde{V}_1 - P \cos \phi \, y' \text{ ----------(7.15)}$$

Therefore,

$$\Gamma_x = - \frac{\tilde{V}_1}{K'AG} + \frac{P \cos \phi \, y'}{K'AG}$$

$$\Gamma_x = - \frac{\tilde{V}_1}{K'AG} + \frac{P \cos \phi (\theta_x + \Gamma_x)}{K'AG}$$

$$\Gamma_x = - \frac{\tilde{V}_1}{K'AG} + \frac{P \cos \phi \, \theta_x}{K'AG} + \frac{P \cos \phi \, \Gamma_x}{K'AG}$$

$$\Gamma_x \left[1 - \frac{P \cos \phi}{K'AG} \right] = - \frac{\tilde{V}_1}{K'AG} + \frac{P \cos \phi \, \theta_x}{K'AG}$$

Let $R = 1 - P \cos \phi / K'AG$

$$\Gamma_x = - \frac{\tilde{V}_1^2}{K'AGR} + \frac{P \cos \phi \, \theta_x}{K'AGR} \qquad \text{----------(7.16)}$$

Differentiate equation (7.16).

$$\Gamma_x' = \frac{P \cos \phi \, \theta_x'}{K'AGR}$$

But $K'AGR = (K'AG)(1 - P \cos \phi / K'AG)$

$= K'AG - P \cos \phi.$

Thus,

$$\Gamma_x' = \frac{P \cos \phi \, \theta_x'}{K'AG - P \cos \phi}$$

Let $P = \tilde{P} \cos \phi.$

Then,

$$\Gamma_x = \tilde{P} \, \theta_x' / (K'AG - \tilde{P})$$

Differentiate Equation (7.13).

$$y_x'' = \theta_x' + \Gamma_x'$$

$$= \theta_x' + \tilde{P} \, \theta_x' / (K'AG - \tilde{P})$$

$$= \theta_x' (1 + \tilde{P} / (K'AG - \tilde{P})) \qquad \text{----------(7.17)}$$

Substituting Equation (7.11) into Equation (7.12) yields

$$\frac{\tilde{V}_1 x - M_1 + P \cos \phi \, (y_1 - y_x)}{EI} = \theta_x'$$

Substitute into Equation (7.17).

$$y_x'' = \frac{\tilde{V}_1 x - M_1 + \tilde{P}(y_1 - y_x)}{EI}\left[1 + \tilde{P}/(K'AG - \tilde{P}\right]$$

But

$$(1 + \tilde{P}/K'AG - \tilde{P}) = (K'AG - \tilde{P} + \tilde{P})/(K'AG - \tilde{P})$$

$$= 1/(1 - \tilde{P}/K'AG)$$

Therefore,

$$y_x'' = \frac{\tilde{V}_1 x - M_1 + \tilde{P}(y_1 - y_x)}{EI} (1/(1 - \tilde{P}/K'AG))$$

$$y_x'' + \tilde{P} y_x / EIR = (V_1 x - M_1 + \tilde{P} y_1) / EIR$$

Let $B^2 = \tilde{P} / EIR$

$$y_x + B^2 y_x = B^2 y_1 - M_1 B^2/\tilde{P} + \tilde{V}_1 B^2 x/\tilde{P} \text{ ---------(7.18)}$$

The solution for Equation (7.18) is

$$y_x = C \sin Bx + D \cos Bx + y_1 - M_1/\tilde{P} + \tilde{V}_1 x/\tilde{P} \text{ ----(7.19)}$$

Differentiate Equation (7.19).

$$y_x' = CB \cos Bx - DB \sin Bx + \tilde{V}_1/\tilde{P}$$

Employing Equations (7.13), (7.14), and (7.15) yields

$$\begin{aligned} \theta_X &= y_x' - \Gamma_x \\ &= y_x' + S_x / K'AG \\ &= y_x' + (\tilde{V}_1 - \tilde{P}\, y')/K'AG \end{aligned}$$

Substitution yields

$$\theta_x = C\, B \cos Bx - D\, B \sin Bx + \tilde{V}_1/\tilde{P} + \frac{1}{K'AG}\left[\tilde{V}_1 - \tilde{P}\left[C\, B \cos Bx - D\, B \sin Bx + \tilde{V}_1/\tilde{P}\right]\right.$$

$$\theta_x = C\, B(1-\tilde{P}/K'AG) \cos Bx - D\, B(1-\tilde{P}/K'AG) \sin Bx + \tilde{V}_1/\tilde{P}$$

$$\theta_x = C\, B\, R \cos Bx - D\, B\, R \sin Bx + \tilde{V}_1/\tilde{P} \text{ --------(7.20)}$$

Let $y_1 = 1$, and apply boundary conditions. (See Figure 9.)

$y(0) = y_1 = 1$

$\theta(0) = \theta_1 = 0$

$y(L) = y_2 = 0$

$\theta(L) = \theta_2 = 0$

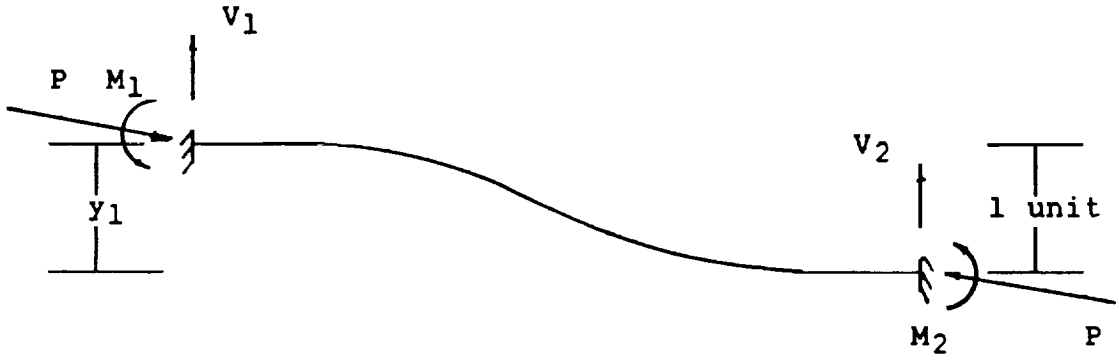

Figure 9 Beam with Unit Displacement of y_1 Only

Substitute $\theta(0) = 0$ into Equation (7.20).

$$0 = C\ B\ R + \tilde{V}_1/\tilde{P}$$

$$C = -\ \tilde{V}_1/(\tilde{P}\ B\ R)$$

Substitute $\theta(L) = 0$ into Equation (7.20).

$$0 = C\ B\ R \cos BL - D\ B\ R \sin BL + \tilde{V}_1/\tilde{P}$$

$$D\ B\ R \sin BL = C\ B\ R \cos BL + \tilde{V}_1/\tilde{P}$$

$$D = \frac{C \cos BL}{\sin BL} + \frac{\tilde{V}_1}{\tilde{P}\ B\ R \sin BL}$$

$$D = -\frac{\tilde{V}_1 \cos BL}{\tilde{P}\ B\ R \sin BL} + \frac{\tilde{V}_1}{\tilde{P}\ B\ R \sin BL}$$

$$D = \frac{\tilde{V}_1}{\tilde{P}B\ R}\left[\frac{1 - \cos BL}{\sin BL}\right] \qquad \text{----------(7.23)}$$

Similarly, solve equation (7.19) at $x = 0$.

$$y_1 = D - M_1 + y_1$$

or

$$D = M_1/\tilde{P} \qquad \text{----------(7.25)}$$

Solve Equation (7.19) when x = L.

$$0 = C \sin BL + D \cos BL + y_1 - M_1/\tilde{P} + \tilde{V}_1 L/\tilde{P}$$

$$y_1 = M_1/\tilde{P} - \tilde{V}_1 L/\tilde{P} - C \sin BL - D \cos BL$$

Substituting Equation (7.25)

$$y_1 = D - D \cos BL - \tilde{V}_1 L/\tilde{P} - C \sin BL$$

$$y_1 = D(1 - \cos BL) - \tilde{V}_1 L/\tilde{P} - C \sin BL \text{ ----------(7.26)}$$

Substituting the values for C and D from Equations (7.23) and (7.22) yields

$$y_1 = \frac{\tilde{V}_1}{\tilde{P}\ B\ R}\left[\frac{1 - \cos BL}{\sin BL}\right]\left[1 - \cos BL\right] - \frac{\tilde{V}_1 L}{\tilde{P}} + \frac{\tilde{V}_1 \sin BL}{\tilde{P} B\ R}$$

$$y_1 = \frac{\tilde{V}_1}{\tilde{P}}\left[\frac{(1 - \cos BL)^2}{B\ R \sin BL} - L + \frac{\sin BL}{B\ R}\right] \text{ ----------(7.27)}$$

$$y_1 = \frac{\tilde{V}_1}{\tilde{P}}\left[\frac{2(1 - \cos BL) - L\ B\ R \sin BL}{B\ R \sin BL}\right]$$

Let $z = 2(1 - \cos BL) - L\ B\ R \sin BL$

$$y_1 = \frac{\tilde{V}_1 \, z}{\tilde{P} \, B \, R \sin BL}$$

$$K_{11} = \frac{\tilde{V}_1}{y_1} = \tilde{V}_1 \, \tilde{P} \, B \, R \sin BL \; / \; \tilde{V}_1 z$$

$$K_{11} = \tilde{P} B \, R \sin BL) \; / \; z$$

$$K_{21} = \frac{M_1}{y_1} = \frac{\tilde{P} \, \tilde{V}_1 \, (1 - \cos BL) \, \tilde{P} B \, R \sin BL}{(\tilde{P} \, B \, R \sin BL \, \tilde{v}_1 \, z)}$$

$$K_{21} = \tilde{P} \, (1 - \cos BL)/z.$$

Let $\theta_1 = 1$ and apply boundary conditions. (See Figure 10).

$$y(0) = y_1 = 0$$

$$\theta(0) = \theta_1 = 1$$

$$y(L) = y_2 = 0$$

$$\theta(L) = \theta_2 = 0$$

$$y_1 = 0 = D - M_1/\tilde{P} \text{ ----------(7.28)}$$

Therefore, $D = M_1/\tilde{P}$ ----------(7.29)

$$y_2 = 0 = C \sin BL + D \cos BL - M_1/\tilde{P} + \tilde{V}_1 x/\tilde{P}$$

$$- C \sin BL + D(1 - \cos BL) = \tilde{Y}L/\tilde{P} \text{ ----------(7.30)}$$

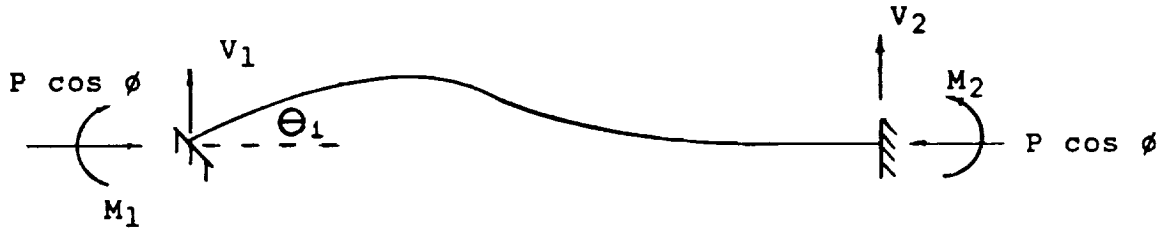

Figure 10 Beam with Unit Rotation θ_1 and Other Degrees of Freedom Fixed

$$\theta_2 = 0 = C\ B\ R \cos BL - D\ B\ R \sin BL + \tilde{V}_1/\tilde{P} \quad \text{----(7.31)}$$

Therefore, $C\ B\ R \cos BL - D\ B\ R \sin BL = -\tilde{V}_1/\tilde{P}$ ----(7.32)

Solve Equations (7.30) and (7.32) simultaneously.

$$\begin{bmatrix} -\sin BL & 1 - \cos BL \\ B\ R \cos BL & -B\ R \sin BL \end{bmatrix} \begin{bmatrix} C \\ D \end{bmatrix} = \begin{bmatrix} \tilde{V}_1\ L/\tilde{P} \\ -\tilde{V}_1\ L/\tilde{P} \end{bmatrix}$$

$$C = -\frac{L\ \tilde{V}_1 \cot BL}{\tilde{P}} - \frac{L\ \tilde{V}_1}{\tilde{P} \sin BL} + \frac{\tilde{V}_1}{\tilde{P}\ B\ R} \quad \text{----------(7.33)}$$

$$= \frac{\tilde{V}_1}{\tilde{P}\ B\ R}\left[\frac{B\ L\ R \sin BL - 1 + \cos BL}{1 - \cos BL}\right] \quad \text{----------(7.34)}$$

$$D = \frac{\tilde{V}_1\ (B\ L\ R \cos BL - \sin BL)}{\tilde{P}\ B\ R\ (\cos BL - 1)}$$

$$D = -\frac{\tilde{V}_1}{\tilde{P}\ B\ R}\left[\frac{B\ L\ R \cos BL - \sin BL}{1 - \cos BL}\right] \quad \text{----------(7.35)}$$

Using Equation (7.20) we get

$$\theta_1 = C\ B\ R + \tilde{V}_1/\tilde{P}$$

$$\theta_1 = -\frac{\tilde{V}_1}{\tilde{P}\ B\ R}\left[\frac{B\ L\ R\ \sin BL - 1 + \cos BL}{1 - \cos BL}\right] + \frac{\tilde{V}_1}{\tilde{P}}$$

$$\theta_1 = \frac{\tilde{V}_1}{\tilde{P}}\left[\frac{1 - \cos BL - B\ L\ R\ \sin BL + 1 - \cos BL}{1 - \cos BL}\right]$$

$$\theta_1 = \frac{\tilde{V}_1}{\tilde{P}}\left[\frac{2 - 2\ \cos BL - B\ L\ R\ \sin BL}{1 - \cos BL}\right]$$

$$\theta_1 = \frac{\tilde{V}_1\ z}{\tilde{P}\ (1 - \cos BL)}$$

$$K_{12} = \tilde{V}_1/\theta_1$$

$$K_{12} = \tilde{P}\ (1 - \cos BL)/z$$

Equations (7.29) and (7.35) yield

$$\frac{M_1}{\tilde{P}} = -\frac{\tilde{V}_1}{\tilde{P}\ B\ R}\left[\frac{B\ L\ R\ \cos BL - \sin BL}{1 - \cos BL}\right]$$

$$M_1 = -\frac{\tilde{V}_1}{B\ R}\left[\frac{B\ L\ R\ \cos BL - \sin BL}{1 - \cos BL}\right]$$

$$K_{22} = \frac{M_1}{\theta_1} = -\frac{\tilde{V}_1}{B\ R}\left[\frac{B\ L\ R\ \cos BL - \sin BL}{1 - \cos BL}\right]\left[\frac{\tilde{P}\ (1 - \cos BL)}{\tilde{V}_1\ z}\right]$$

$$K_{22} = \frac{\tilde{P}}{z}\left[\frac{\sin BL}{B\ R} - L \cos BL\right] = K_{44}$$

The reaction can be obtained using static equilibrium.

$$V_2 = - V_1 \text{ ----------(7.36)}$$

$$- M_1 - M_2 + V_1\ L + \tilde{P}\ y_1 - \tilde{P}\ y_2 = 0 \text{ ----------(7.37)}$$

or

$$M_2 = - M_1 + V_1\ L + \tilde{P}\ y_1 - \tilde{P}\ y_2 \text{ ----------(7.38)}$$

$$K_{31} = V_2/y_1 = - V_1/y_1 = - \tilde{P}(B\ R \sin BL)/z$$

$$K_{31} = - \tilde{P}\ (B\ R \sin BL)/z = K_{13}$$

and

$$K_{41} = \frac{M_2}{y_1} = -\frac{M_1 + V_1\ L + \tilde{P}\ y_1 - \tilde{P}\ y_2}{y_1}$$

$$= -\frac{\tilde{P}(1 - \cos BL)}{z} + \frac{\tilde{P}\ L\ (B\ R \sin BL)}{z} + \frac{\tilde{P}\ z}{z}$$

$$= \tilde{P}(-1 + \cos BL + B\ L\ R \sin BL + 2 - 2 \cos BL$$

$$- B\ L\ R \sin BL)/z$$

$$K_{41} = \tilde{P}\,(1 - \cos BL)/z = K_{14}$$

$$K_{32} = V_2/\theta_2 = -\,V_1/\theta_1$$

$$K_{32} = -\,\tilde{P}\,(1 - \cos BL)/z = K_{23}$$

Using Equation (7.39) yields K_{42}.

$$K_{42} = M_2/\theta_1 = (-\,M_1 + V_1\,L + \tilde{P}\,y_1 - \tilde{P}\,y_2)/\theta_1$$

$$= \frac{\tilde{P}}{z}\left[-\frac{\sin BL}{B\,R} + L\cos BL + L(1 - \cos BL)\right]$$

$$K_{42} = \frac{\tilde{P}}{z}\left[L - \frac{\sin BL}{B\,R}\right] = K_{24}$$

Similarly,

$$K_{33} = \tilde{P}(B\,R\sin BL)/z$$

and

$$K_{34} = -\,\tilde{P}(1 - \cos BL)/z = K_{43}$$

or, the final directed stiffness matrix is

$$\underset{\sim}{K}=\frac{P}{z}\begin{bmatrix} BR\sin BL & 1-\cos BL & -BR\sin BL & 1-\cos BL \\ 1-\cos BL & \frac{\sin BL}{BR}-L\cos BL & \cos BL-1 & L-\frac{\sin BL}{BR} \\ -BR\sin BL & \cos BL-1 & BR\sin BL & \cos BL-1 \\ 1-\cos BL & L-\frac{\sin BL}{BR} & \cos BL-1 & \frac{\sin BL}{BR}-L\cos BL \end{bmatrix}$$

By inspection, K has rigid body translation capability.

For rigid body rotation (Figure 11),

$$U_{RBR} = \left[-\frac{L}{2}\theta,\ \theta,\ \frac{L}{2}\theta,\ \theta\right]$$

or

$$= [-L,\ 2,\ L,\ 2]$$

$$K_{2j} \cdot U_{RBR} = 0$$

$$K_{1j} \cdot U_{RBR} = -2\dot{\theta}\cos BL - B\,L\,R\,\theta\sin BL + 2\theta$$

$$= 2\theta(1-\cos BL)) - B\,L\,R\,\theta\sin BL$$

$$\neq 0, \text{ No good.}$$

This matrix does not possess rigid body rotation capability.

By observation, this [K] is identical with Saunders [K], except P has been replaced with P cos ø, which is the component of P in the horizontal direction. It does not

possess rigid body rotation capability. It should also be noted that the approximation for shear $\tilde{V}_1 \approx V_1$ was used to determine the stiffness coefficients. Without that approximation the stiffness coefficients would be a function of the shear.

ie.

$$\hat{K}_{11} = \frac{V_1 \tilde{P} B R \sin BL}{(V_1 - P \sin \phi) z}$$

$$\lim_{\phi \to 0} \hat{K}_{11} = \frac{\tilde{P} (B R \sin \beta L)}{z} = K_{11}$$

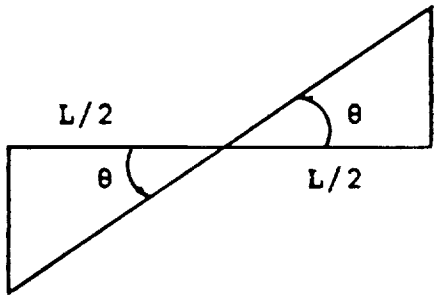

Figure 11 Rigid Body Rotation

CHAPTER 8

MATRIX DEVELOPMENT USING GALERKIN CRITERION

Consider a simply-supported beam with an axial load. The differential equation for static displacement is

$$E\ I\ d^4W/dx^4 = 0.$$

Let $\tilde{W} = \Sigma\ \phi_i(x)\ W_i$

Shape functions — $\phi_i(x)$; Nodal displacements — W_i

Application of Galerkin's criterion yields

$$\int_{x_1}^{x_2} EI\ \phi_j(x)\ \frac{d^4W}{dx^4}\ dx = 0$$

Integrate by parts

Let $U = \phi_j$ $\qquad dV = \dfrac{d^4W}{dx^4}\ dx$

$dU = \dfrac{d\phi_j}{dx}\ dx$ $\qquad V = \dfrac{d^3W}{dx^3}$

$$EI\ \phi_j\ (x)\ \frac{d^3W}{dx^3}\ \Bigg|_{x_1}^{x_2} - \int_{x_1}^{x_2} EI\ \frac{d\phi_j}{dx}\ \frac{d^3W}{dx^3}\ dx = 0$$

Integrate by parts.

Let $U = \phi_j'$ $\qquad$ $dv = W'''$

$dU = \phi_j''\ dx$ $\qquad$ $V = W''$

$$EI\ \phi_j(x)\ \frac{d^3W}{dx^3}\ \Bigg|_{x_1}^{x_2} - EI\ \frac{d\phi_j}{dx}\ \frac{d^2W}{dx^2}\ \Bigg|_{x_1}^{x_2} + \int_{x_1}^{x_2} EI\ \frac{d^2\phi_j}{dx^2}\ \frac{d^2W}{dx^2}\ dx$$

The first two terms are part of the boundary conditions. The last term produces the elastic stiffness matrix.

$$[K_e] = \int_0^L EI\ \phi_i''\ \phi_j''\ dx$$

$$[Ke] = \int_0^L EI \begin{bmatrix} H_2''H_2'' & & & \\ H_3''H_2'' & H_3''H_3'' & \text{symmetric} & \\ H_5''H_2'' & H_5''H_3'' & H_5''H_5'' & \\ H_6''H_2'' & H_6''H_3'' & H_6''H_5'' & H_6''H_6'' \end{bmatrix} dx$$

If the Hermitian polynomials are chosen for the shape functions, the resultant matrix is

$$[Ke] = EI \begin{bmatrix} 0 & & & & & \\ 0 & 12/L^3 & & & & \\ 0 & 6/L^2 & 4/L & & \text{Symmetric} & \\ 0 & 0 & 0 & 0 & & \\ 0 & -12/L^3 & -6/L^2 & 0 & 12/L^3 & \\ 0 & 6/L^2 & 2/L & 0 & -6/L^2 & 4/L \end{bmatrix}$$

This $[K_E]$ has four zero eigenvalues. Note that the K_{11}, K_{14}, K_{41}, and K_{44} terms are zero, since we did not develop the relationship for the axial terms. Development of these terms using a standard Bernoulli formulation yields the appropriate terms. If the AE/L terms are developed via a classic Bernoulli formulation, the resulting matrix has three zero eigenvalues.

For an axially-loaded beam, the static deformation equation becomes

$$EI \frac{d^4W}{dx^4} + P \frac{d^2W}{dx^2} = 0$$

Application of Galerkin's criterion yields

$$\int_0^L \left[EI\, \phi_j \frac{d^4W}{dx^4} + P\, \phi_j \frac{d^2W}{dx^2} \right] dx = 0$$

The first term produces $[K_e]$ as shown previously.

Integrate the second term by parts.

Let $U = \phi_j$ $\quad dV = W''$

$dU = \phi_j' dx$ $\quad V = W'$

$$P \int_0^L \phi_j \frac{d^2W}{dx^2} dx = P\, \phi_j \frac{dW}{dx}\Big|_0^L - P \int_0^L \phi_j' \frac{dW}{dx} dx$$

The second term on the right hand side produces the geometric stiffness matrix.

$$[Kg] = P \int_0^L \phi_i' \, \phi_j' \, dx$$

$$[Kg] = P \int_0^L \begin{bmatrix} H_1'H_1' & & & & & \\ H_2'H_1' & H_2'H_2' & & \text{symmetric} & & \\ H_3'H_1' & H_3'H_2' & H_3'H_3' & & & \\ H_4'H_1' & H_4'H_2' & H_4'H_3' & H_4'H_4' & & \\ H_5'H_1' & H_5'H_2' & H_5'H_3' & H_5'H_4' & H_5'H_5' & \\ H_6'H_1' & H_6'H_2' & H_6'H_3' & H_6'H_4' & H_6'H_5' & H_6'H_6' \end{bmatrix} dx$$

Choosing the Hermitian Polynomials for the shape functions yields

$$[Kg] = P \begin{bmatrix} 1/L & & & & & \\ 1/L & 6/5L & & & \text{symmetric} & \\ 0 & 1/10 & 2L/15 & & & \\ -1/L & -1/L & 0 & 1/L & & \\ -1/L & -6/5L & -1/10 & 1/L & 6/5L & \\ 0 & 1/10 & -L/30 & 0 & -1/10 & 2L/15 \end{bmatrix}$$

Recall that the $K_{1,j}$, $K_{4,J}$,$K_{i,1}$,$K_{i,4}$ were all zero in the consistent geometric stiffness matrix. When 1/2 angle of rotation equals one radian, this $[K_g]$ agrees with the modified [Kg] developed by Bosela in [2]. Hence, it possesses the required three zero eigenvalues. It should also be noted that these new terms are not directly attributable to the differential equation.

It should be noted that the consistent $[K_e]$ matrix, which has three zero eigenvalues, is utilized along with the modified $[K_g]$, which also has three zero eigenvalues, in an equation of the form

$$\left| \left[[K_e] + P\,[K_g] \right] - \Omega^2\,[M] \right| = 0 ,$$

There are only two zero eigenvalues, corresponding to rigid body translations. Apparently, the third zero

eigenvalue, corresponding to rigid body rotation, is lost, due to differences in the rotation eigenvector produced.

For example, consider the free free beam shown in Figure 12. When E= 0 (so that [Ke] is not calculated, and only [K] = [Kg] is assembled) and P= $10x10^6$ LBS, the following results are obtained (using the computer program MODFINITE.FOR:

Lambda (1) = -0.0010

Omega (1) = 0.0000 RAD/S

The associated eigenvector is:

0.1000000000D+01

-0.1000000020D+01

0.2000000039D-01

-0.9999999973D+00

0.9999999829D+00

0.2000000039D-01

Lambda (2) = 0.0000

Omega (2) = 0.0000 RAD/S

The associated eigenvector is:

0.1000000000D+01

0.1166342998D+01

0.6138287495D-09

0.9999999386D+00

0.1166343060D+01

0.6138287603D-09

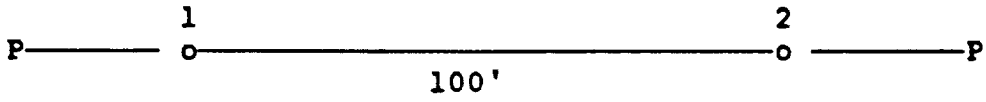

$A = 48\ in^2$

$I = 1000\ in^4$

$m = 0.03525\ lb\text{-}sec^2/in^2$

Figure 12 Free/Free Beam with Axial Compression Load

```
Lambda (3)   =                    0.0000
Omega (3)    =                   0.0000 RAD/S

The associated eigenvector is:

 0.1000000000D+01
-0.8573806678D+00
-0.5222345200D-09
 0.1000000052D+01
-0.8573807200D+00
-0.5222345360D-09

Lambda (4)   =                  552496.2879
Omega (4)    =                    743.3009 RAD/S

The associated eigenvector is:

 0.1000000000D+01
 0.6229578457D+00
 0.2524505863D+01
-0.1000000000D+01
-0.6229578457D+00
 0.2524505863D-01

Lambda (5)   =             1702127.6596
Omega (5)    =                1304.6561 RAD/S

The associated eigenvector is:

-0.1266228240D-15
```

```
 0.1000000000D+01
-0.6000000000D-01
 0.1342393452D-15
 0.1000000000D+01
 0.6000000000D-01
```

Lambda (6) = 4894312.1933

Omega (6) = 2212.3092.RAD/S

The associated eigenvector is:

```
 0.1000000000D+01
 0.1337704207D-02
-0.1505245050D-01
-0.1000000000D+01
-0.1337704207D+02
-0.1505245050D+01
```

It can also be shown that the eigenvectors are linear combinations of the rigid body translations,

$[1\ 0\ 0\ 1\ 0\ 0]^T$

$[0\ 1\ 0\ 0\ 1\ 0]^T$

and $[L\ -L\ 2\ -L\ L\ 2]^T$, which represents rigid body rotation with 1/2 angle or rotation equal to one radian.

Assuming P=0 and E= 30×10^6 psi, the following results (once again using MODFINIT.FOR) are obtained:

$$\left| [K_e] - \Omega^2 [M] \right| = 0 \qquad \text{yields}$$

Lambda (1) = 0.0000

Omega (1) = 0.0000 RAD/S

The associated eigenvector is:

0.1000000000D+01

0.0000000000D+00

0.0000000000D+00

0.1000000000D+01

0.0000000000D+00

0.0000000000D+00

Lambda (2) = 0.0000

Omega (2) = 0.0000 RAD/S

The associated eigenvector is:

0.0000000000D+00

0.9334669755D+00

0.6653302446D-03

0.0000000000D+00

0.1000000000D+01

0.6653302446D-03

```
Lambda (3)   =        0.0000

Omega (3)    =       0.0000 RAD/S

The associated eigenvector is:
 0.0000000000D+00
 0.1000000000D+01
-0.1977319320D-01
 0.0000000000D+00
-0.9773193204D+00
-0.1977319320D-01

Lambda (4)   =      6127659.5745

Omega (4)    =       2475.4110 RAD/S

The associated eigenvector is:
 0.0000000000D+00
 0.1000000000D+01
-0.6000000000D-01
 0.0000000000D+00
 0.1000000000D+01
 0.6000000000D-01

Lambda (5)   =      49021276.5957

Omega (5)    =       7001.5196 RAD/S

The associated eigenvector is:
 0.1000000000D+01
 0.0000000000D+00
 0.0000000000D+00
```

-0.1000000000D+01

0.0000000000D+00

0.0000000000D+00

Lambda (6) = 71489361.7021

Omega (6) = 8455.1382 RAD/S

The associated eigenvector is

0.0000000000D+00

0.1000000000D+01

-0.1200000000D+00

0.0000000000D+00

-0.1000000000D+01

-012000000000D+00

Once again, the first three eigenvectors can be shown to be linear combinations of rigid body translational modes.

$$[\,1\ 0\ 0\ \ 1\ 0\ 0\,]^T$$

$$[\,0\ 1\ 0\ \ 0\ 1\ 0\,]^T$$

and the rigid body rotation vector

$$[\,0\ -L\ 2\ 0\ L\ 2\,]$$

Considering the same beam, with $P=10X10^6$ lbs and $E=30X10^6$, the following results are obtained from MODFINIT.FOR.

$$|[Ke] + P[Kg] - \Omega^2[M]| = 0$$

Lambda (1) = -0.0688

Omega (1) = 0.0000 RAD/S

The associated eigenvector is:

0.1000000000D+01

-0.1000000016D+01

-0.1577675514D-15

0.1000000000D+01

-0.1000000016D+01

-0.3281352645D-15

Lambda (2) = 0.0688

Omega (2) = 0.2622 RAD/S

The associated eigenvector is:

0.1000000000D+01

-0.9999999841D+00

-0.1577674314D-15

0.1000000000D+01

-0.9999999841D+00

-0.3281350580D-15

Lambda (3) = 403295.7555

Omega (3) = 635.0557 RAD/S

The associated eigenvector is:

0.1000000000D+01

-0.1066270395D+01

0.1239429315D-02

0.1000183829D+01

-0.9339134336D+00

0.1239429315D-02

Lambda (4) = 7829787.2340

Omega (4) = 2798.1757 RAD/S

The associated eigenvector is:

0.1000000000D+01

-0.3571250023D+00

-0.3857249986D-01

0.1000000000D+01

-0.3571250023D+00

0.3857249986D-01

Lambda (5) = 76419084.4813

Omega (5) = 8741.8010 RAD/S

The associated eigenvector is:

0.1000000000D+01

-0.7447662297D+01

0.7700947165D+00

0.1017885331D+01

0.5429776966D+01

0.7700947165D+00

Lambda (6) = **********

Omega (6) = 248742850249.1149 RAD/S

The associated eigenvector is:

0.1000000000D+01

-0.1000000000D+01

0.2272727273D-01

-0.1272727273D+01

0.1272727273D+01

0.2272727273D-01

If the $[K_e]$ matrix generated by the Galerkin method (which has 4 zero eigenvalues) is used along with modified [Kg] from Galerkin (which has three zero eigenvalues), the combined stiffness yields three zero eigenvalues.

The results are obtained from BOFINITE.FOR:

$$|[[Ke] + P[Kg] - \Omega^2[M]]| = 0$$

yields

Lambda (1) = -0.0010

Omega (1) = 0.0000 RAD/S

The associated eigenvector is:

0.1000000000D+01

-0.9999995972D+00

0.1999999995D-01

-0.9999999870D+00

```
 0.1000000396D+01
 0.1999999995D-01

Lambda (2)   =            0.0000
Omega (2)    =          0.0000 RAD/S

The associated eigenvector is:
 0.1000000000D+01
 0.1686129333D+02
-0.2021558453D-06
 0.1000000396D+01
 0.1999999995D-01

Lambda (2)   =                0.0000
Omega (2)    =              0.0000   RAD/S

The associated eigenvector is:
 0.1000000000D+01
 0.1686129333D+02
-0.2021558453D-06
 0.1000020216D+01
 0.1686127311D+02
-0.2021558449D-06

Lambda (3)   =                0.0000
Omega (3)    =              0.0000  RAD/S

The associated eigenvector is:
 0.1000000000D+01
```

-0.5930809082D-01

0.5153549492D-09

0.9999999485D+00

-0.5930803928D-01

0.5153549432D-09

Lambda (4) = 673695.6482

Omega (4) = 820.7896 RAD/S

The associated eigenvector is:

0.1000000000D+01

0.9739809665D+00

-0.1747771626D-01

-0.1000000000D+01

-0.9789809665D+00

-0.1747771626D-01

Lambda (5) = 7829787.2340

Omega (5) = 2798.1757 RAD/S

The associated eigenvector is:

0.2801487156D-16

0.1000000000D+01

-0.6000000000D-01

-0.2859899241D-16

0.1000000000D+01

0.6000000000D-01

Lambda (6) = 76262474.5352

Omega (6) = 8732.8389 RAD/S

The associated eigenvector is:

0.1000000000D+01

0.2230210189D+03

-0.2666252228D+02

-0.1000000000D+01

-0.2230210189D+03

-0.2666252228D+02

Next consider the equation of motion

$$EI \frac{d^4W}{dx^4} + N \frac{d^2W}{dx^2} + m \frac{d^2W}{dt^2} = 0 \quad .$$

The first two terms have already been examined. Now consider only the term $m\, d^2W/dt^2$.

Let $W = \Sigma\, \phi_i(x)\, W_i$

and

$$W(x,t) = \phi(x) \sin \Omega t$$

$$(d/dt)\ W(x,t) = \phi(x)\, \Omega \cos \Omega t$$

$$(d^2/dt^2)\ W(x,t) = -\phi(x)\, \Omega^2 \sin \Omega t$$

$$= -\Omega^2\, W(x,t)$$

Apply Galerkin's criterion

$$\int_{x_1}^{x_2} m\,\phi_i\,d^2W/dt^2 = \delta\,A\int_0^L \phi_i\,\phi_j\,dx$$

$$[M] = \delta\,A\int_0^L \begin{bmatrix} H_1H_1 & & & & & \\ H_2H_1 & H_2H_2 & & \text{symmetric} & & \\ H_3H_1 & H_3H_2 & H_3H_3 & & & \\ H_4H_1 & H_4H_2 & H_4H_3 & H_4H_4 & & \\ H_5H_1 & H_5H_2 & H_5H_3 & H_5H_4 & H_5H_5 & \\ H_6H_1 & H_6H_2 & H_6H_3 & H_6H_4 & H_6H_5 & H_6H_6 \end{bmatrix}$$

Once again, selecting the Hermitian polynomials for the shape functions yields

$$[M] = \frac{\delta\,A\,L}{420}\begin{bmatrix} 140 & & & & & \\ 147 & 156 & & \text{symmetric} & & \\ 21L & 22L & 4L^2 & & & \\ 70 & 63 & 14L & 140 & & \\ 63 & 54 & 13L & 147 & 156 & \\ -14L & -13L & -3L^2 & -21L & -22L & 4L^2 \end{bmatrix}$$

Note that the M_{12}, M_{13}, M_{15}, M_{16}, etc. are zero in the consistent mass matrix, and not directly attributable to the differential equation used.

In order for finite element dynamic analysis alorithims to provide solutions, the mass matrix must always

be positive definite. To test whether the mass matrix would be positive definite, consider the following:

$$\text{Let} \quad m = 0.03525 \ \text{LB Sec}^2/\text{IN}^2$$

$$L = 10 \ \text{IN}$$

The mass matrix becomes

$$[M] = \begin{bmatrix} 0.1175 & 0.1234 & 0.1762 & 0.05875 & 0.05287 & -0.1175 \\ 0.1234 & 0.1309 & 0.1846 & 0.05287 & 0.04532 & -0.1091 \\ 0.1762 & 0.1846 & 0.3357 & 0.1175 & 0.1091 & -0.2518 \\ 0.05875 & 0.05287 & 0.1175 & 0.1175 & 0.1234 & -0.1762 \\ 0.05287 & 0.04532 & 0.1091 & 0.1234 & 0.1309 & -0.1846 \\ -0.1175 & -0.1091 & -0.2518 & -0.1762 & -0.1846 & 0.3357 \end{bmatrix}$$

A positive definite matrix has all positive eigenvalues. Solving the algebraic eigenvalue problem,

$$|[M] - [I]| = 0 \quad \text{yields}$$

$$\text{Eig.}_1 = -3.50 \times 10^{-5}$$

$$\text{Eig.}_2 = 1.41 \times 10^{-2}$$

$$\text{Eig.}_3 = 9.02 \times 10^{-1}$$

$$\text{Eig.}_4 = -4.61 \times 10^{-5}$$

$$\text{Eig.}_5 = 2.14 \times 10^{-1}$$

$$\text{Eig.}_6 = 3.83 \times 10^{-2}$$

The negative eigenvalues indicate that this particular mass matrix is not positive definite.

CHAPTER 9

SAMPLE PROBLEMS

Fertis and Lee [19] developed the equations of motion and obtained rigorous solutions for beams with various loading and end conditions. The Galerkin method can be used to generate stiffness and mass matrices for a finite element application, and the results compared with Fertis and Lee's rigorous solution.

The following beams were considered:

a. Axially-loaded beam on simple supports.

b. Axially-loaded beam with vertical spring supports.

c. Axially-loaded beam with horizontal and vertical support springs.

d. Bow-string

It should be noted that Fertis and Lee's analysis indicate regions of dynamic "flutter" instability, which has not previously been identified. Kounadis [20] has identified similar areas in the stability analysis of beams with follower forces.

Case a. Axially-loaded Beam on Simple Supports

Fertis and Lee [19] develop the general equation of motion in the form

$$\frac{d}{dx^2}\left[EI(x)\frac{d^2y}{dx^2}\right] + \delta A(x)\frac{d^2y}{dt^2} - P\frac{d^2y}{dx^2} - \delta\frac{d}{dx}\left[I_x\frac{d^3y}{dt^2dx}\right] = 0 \quad \text{----------(9.1)}$$

If a beam with a constant cross-section is considered, EQ (9.1) reduces to

$$EI\frac{d^4y}{dx^4} + \delta A\frac{d^2y}{dt^2} - P\frac{d^2y}{dx^2} - \delta I\frac{d^4y}{dt^2dx^2} = 0 \quad \text{----------(9.2)}$$

It can easily be seen that the first three terms of EQ (9.2) yield K_E, M, and K_g matrices previously developed using Galerkin criterion, (with the negative sign on the third term indicative of an axial compression load).

Consider the fourth term.

$$\frac{\delta^2 I}{K'G}\frac{d^4y}{dt^2dx^2}$$

Let $\hat{W} = \Sigma\ \phi_i(x)\ W_i$

and

$$W(x,t)=\phi(x)\ \text{Sin}\ \Omega t$$

$$\frac{d}{dt} W = \phi(x)\ \Omega\ \text{Cos}\ \Omega t$$

$$\frac{d^2}{dt^2} W = -\phi(x)\Omega^2\ \text{Sin}\ \Omega t$$

$$\frac{d^2}{dt^2} W = -\Omega^2\ W(x,t)$$

$$\frac{d^4}{dx^2dt^2} W = -\Omega^2\ \frac{d^2}{dx^2} W\ (x,t)$$

Comparison with term #3 indicates that the following higher order matrix is produced:

$$-\ \Omega^2 \begin{bmatrix} 1/L & & & & & \\ 1/L & 6/5L & & \text{SYMMETRIC} & & \\ 0 & 1/10 & 2L/15 & & & \\ -1/L & -1/L & 0 & 1/L & & \\ -1/L & -6/5L & -1/10 & 1/L & 6/5L & \\ 0 & 1/10 & -L/30 & 0 & -1/10 & 2L/15 \end{bmatrix}$$

The K_{ij}, K_{4j}, K_{il}, and K_{i4} terms could be set equal to zero, (corresponding to more traditional development) since they are not explicitly developed using the differential equation.

Case b. Axially-loaded Beam with Vertical Spring Supports

Fertis and Lee [19] have utilized Hamilton's principle and the dynamic equilibrium method to formulate the characteristic equations for a beam with an axial compression load and vertical spring supports. They have solved for the frequencies of vibration for various parameters utilizing a bisection method, and tabulated the results.

Using Galerkin's criterion, stiffness and mass matrices can be generated, formulated into a finite element algorithm, and the finite element solution compared with Fertis and Lee's rigorous solution.

Fertis and Lee's analysis indicates that regions of dynamic ("flutter") instabilities occur for an axially-loaded beam with spring supports. The modified finite element approach provides correlation with the trial and error procedure.

The differential equation developed by Fertis and Lee [19] is

$$EI^{*}\frac{d^4y}{dx^4} - \frac{EI^{*}\,\delta}{K'G}\frac{d^4y}{dx^2dt^2} - \frac{\delta\, I^{*}}{K'G}\left[\frac{K'G\, d^4y}{dx^2dt^2} - \delta\frac{d^4y}{dt^4}\right] + m\frac{d^2}{dt^2} + \frac{P\, d^2y}{dx^2}$$

(1) (2) (3) (4) (5) (6)

----------(9.3)

C-2

with $I^* = 1/(1+P/K'AG)$

Term (1) yields

$$[K_e] = EI^* \begin{bmatrix} 12/L^3 & & \text{symmetric} & \\ 6/L^2 & 4/L & & \\ -12/L^3 & -6/L^2 & 12/L^3 & \\ 6/L^2 & 2/L & -6/L^2 & 4/L \end{bmatrix}$$

Terms (2) and (3) yield

$$[K_{ROT}] = \left[\frac{\delta EI^*}{K'G} + \delta I^*\right] \begin{bmatrix} 6/5L & & \text{symmetric} & \\ 1/10 & 2L/15 & & \\ -6/5L & -1/10 & 12/L^3 & \\ 1/10 & -L/30 & -6/L^2 & 4/L \end{bmatrix}$$

Term (4) yields

$$[M_1] = \frac{\delta^2 I^*}{420\ K'\ G} \begin{bmatrix} 156 & & & \\ 22L & 4L^2 & & \\ 54 & 13L & 156 & \\ -13L & -3L2 & -22L & 4L^2 \end{bmatrix}$$

Term (5) yields

$$[M_o] = \frac{\delta\ A\ L}{420}\begin{bmatrix} 156 & & \text{symmetric} & \\ 22L & 4L^2 & & \\ 54 & 13L & 156 & \\ -13L & -3L^2 & -22L & 4L^2 \end{bmatrix}$$

Term (6) yields

$$[K_g] = P\begin{bmatrix} 6/5L & & \text{symmetric} & \\ 1/10 & 2L/15 & & \\ -6/5L & -1/10 & 6/5L & \\ 1/10 & -L/30 & -1/10 & 2L/15 \end{bmatrix}$$

In matrix form, EQ (9.3) yields

$$\left[[K_E] + P[K_G]\right] - \Omega^2\left[[M_o] - [K_{ROT}]\right] + \Omega^4\,[M_1] = 0 \qquad \text{----(9.4)}$$

The above matrices were included in a finite element dynamic analysis program (NLFIN.FOR), neglecting the W^4 term. Tables 2-6 compare the finite element output with Fertis and Lee's rigorous solution of the dynamic instability loads.

Table 2 Free/Free Beam with Pre-Load

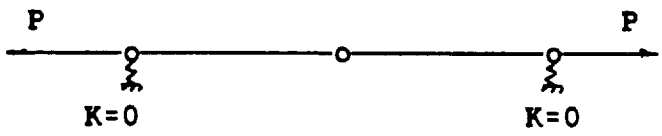

$A = 48\ IN^2$ $m = 0.4224\ LB\text{-}SEC^2/IN^2$

$E = 30 \times 10^6$ $L = 100\ IN$

$I = 256\ IN^4$ $K' = 0.186$

AXIAL LOAD	$\sqrt{K/M}$	NLFIN3 1ST FREQ	ERROR	RIGOROUS 2ND FREQ
-400	0	0	0	1.0670 i
-200	0	0	0	0.7545 i
0	0	0	0	0
200	0	0	0	0.7545
400	0	0	0	1.0670

Table 3 Rigorous Solution Versus NLFIN3.FOR

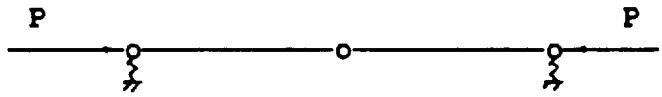

$A = 48\ IN^2$ $\quad m = 0.4224\ LB\text{-}SEC^2/IN^2$

$E = 30 \times 10^6$ $\quad L = 100\ IN$

$I = 256\ IN^4$ $\quad K' = 0.186$

AXIAL COMP LOAD	$\sqrt{K/M}$	RIGOROUS 1ST FREQ RAD/SEC	NLFIN3 1ST FREQ.	% DIFF.	RIGOROUS 2ND FREQ	NLFIN3 2ND FREQ	% DIFF
0	0.688	0.689	0.6881	0.01	1.189	1.1930	0.34
100	0.688	0.689	0.6881	0.01	1.063	1.0670	0.38
200	0.688	0.689	0.6881	0.01	0.921	0.9241	0.34
300	0.688	0.689	0.6881	0.01	0.752	0.7545	0.33
355	0.688*	0.689*	0.6881	0.0	0.689*	0.6881	0.13

*Flutter (dymanic instability) occurs.

Table 4 Rigorous Solution Versus NLFIN3.FOR

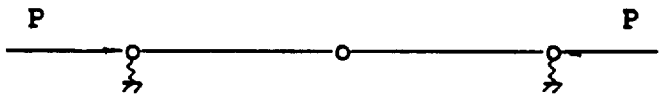

$A = 48\ IN^2$ $m = 0.4224\ LB\text{-}SEC^2/IN^2$

$E = 30 \times 10^6$ $L = 100\ IN$

$I = 256\ IN^4$ $K' = 0.186$

AXIAL COMP LOAD	$\sqrt{K/M}$	RIGOROUS 1ST FREQ RAD/SEC	NLFIN3 1ST FREQ	% DIFF	RIGOROUS 2ND FREQ	NLFIN3 2ND FREQ	% DIFF
0	2.176	2.177	2.176	0	3.758	3.7725	0.39
500	2.176	2.177	2.176	0	3.565	3.5789	0.39
1000	2.176	2.177	2.176	0	3.362	3.3742	0.36
1500	2.176	2.177	2.176	0	3.144	3.1563	0.37
2000	2.176	2.177	2.176	0	2.911	2.2922	0.38
2500	2.176	2.177	2.176	0	2.658	2.6676	0.36
3000	2.176	2.177	2.176	0	2.377	2.3859	0.37
3350	2.176	2.177*	2.176	0	2.177*	2.1671	-0.45

* Flutter (dynamic instability) occurs.

Table 5 Rigorous Solution Versus NLFIN3.FOR

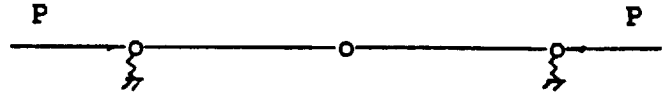

$A = 48\ IN^2$ $I = 256\ IN^4$ $m = 0.4224\ LB\text{-}SEC^2/IN^2$

$E = 30 \times 10^6$ $K' = 0.186$ $L = 100\ IN$

AXIAL COMP LOAD	$\sqrt{K/M}$	RIGOROUS 1ST FREQ RAD/SEC	NLFIN3 1ST FREQ	% DIFF	RIGOROUS 2ND FREQ	NLFIN3 2ND FREQ	% DIFF
0	4.866	4.877	4.863	0.06	8.402	8.4350	0.39
1000	4.866	4.877	4.863	0.06	8.232	8.2646	0.40
2000	4.866	4.877	4.863	0.06	8.057	8.0907	0.42
3000	4.866	4.877	4.863	0.06	7.882	7.9128	0.39
4000	4.866	4.877	4.863	0.06	7.701	7.7309	0.39
5000	4.866	4.877	4.863	0.06	7.510	7.5446	0.46
6000	4.866	4.877	4.863	0.06	7.325	7.3536	0.39
7000	4.866	4.877	4.863	0.06	7.130	7.1575	0.39
8000	4.866	4.877	4.863	0.06	6.929	6.9559	0.39
9000	4.866	4.877	4.863	0.06	6.722	6.7482	0.39
10000	4.866	4.877	4.863	0.06	6.509	6.5339	0.38
11000	4.866	4.877	4.863	0.06	6.288	6.3124	0.39
12000	4.866	4.877	4.863	0.06	6.059	6.0828	0.39
13000	4.866	4.877	4.863	0.06	5.822	5.8422	0.38
14000	4.866	4.877	4.863	0.06	5.315	5.3350	0.38
15000	4.866	4.877	4.863	0.06	5.315	5.3350	0.38
16000	4.866	4.877	4.863	0.06	5.024	5.0612	0.74
16550	4.866	4.877*	4.863	0.06	4.877*	4.9042	0.56

Table 6 Rigorous Solution Versus NLFIN3.FOR

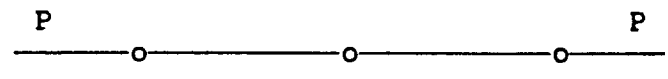

K=1000 LB/IN K=1000 LB/IN

A = 48 IN^2 m = 0.4224 $LB\text{-}SEC^2/IN^2$

E = 30 x 10^6 L = 100 IN

I = 256 IN^4 K'= 0.186

AXIAL COMP LOAD	$\sqrt{K/M}$	1ST FREQ RAD/SEC	1ST FREQ	DIFF	2ND FREQ	2ND FREQ	DIFF
0	6.881	6.876	6.874	0.10	11.882	11.9282	0.39
5000	6.881	6.876	6.874	0.10	11.272	11.3162	0.39
10000	6.881	6.876	6.874	0.10	10.628	11.6692	0.39
15000	6.881	6.876	6.874	0.10	9.941	9.9802	0.39
20000	6.881	6.876	6.874	0.10	9.294	9.2400	-0.58
25000	6.881	6.876	6.874	0.10	8.402	8.4350	0.39
30000	6.881	6.876	6.874	0.10	7.516	7.5446	0.38
31000	6.881	6.876	6.874	0.10	7.325	7.3536	0.39
33501	6.881*	6.876*	6.874	0.10	6.876*	6.8526	-0.34

* Flutter (dynamic instability) occurs.

NLFIN3 has excellent correlation with rigorous solution (See Tables 3-6). However, the rigorous solution has the 2nd frequency varying with axial load, even when K=0. Thus, it does not model rigid body rotation. NLFIN3 was developed from the differential equation in the rigorous solution, using Galerkin's criterion. Thus, it also has the 2nd frequency varying with the axial load, and does not have rigid body rotation capability. Table 7 compares the critical load obtained using the finite element method versus the rigorous solution for varying spring stiffness. Tables 8-10 compare the frequencies for constant spring stiffness but varying lengths.

The critical loads correspond to a coalescing of the first and second flexural eigenfrequencies (dynamic instability) and were located by varying the load. Correlation between the finite element and rigorous solution is evident. The difference is affected by the judgment as to when the first two frequencies have sufficiently coalesced, the excluding of the Ω^4 contribution in the finite element algorithm, the number of elements used, and errors due to the iterative nature of the eigensolver routine.

It should also be noted that in general, as the axial compression load is increased, the second eigenvalue decreases. The first eigenvalue does not change

Table 7 Critical Load Rigorous Solution Versus NLFIN3

$A = 48\ IN^2$ $I = 256\ IN^4$ $m = 0.4224\ LB\text{-}SEC^2/IN^2$

$E = 30 \times 10^6$ $K' = 0.186$ $L = 100\ IN$

SPRING	CRITICAL LOAD (LB)		
CONSTANT	RIGOROUS	NFLIN3	DIFF
10	3.35×10^2	3.335×10^2	-0.4
100	3.35×10^3	3.335×10^3	-0.4
500	1.655×10^4	1.6675×10^4	0.8
1000	3.100×10^4*	3.335×10^4	7.6
2000	6.600×10^4	6.670×10^4	1.1
3000	9.550×10^4	1.0025×10^5	5.0
5000	1.605×10^5	1.6708×10^5	4.1
10000	3.345×10^5	3.3722×10^5	0.8
20000	6.75×10^5	6.8141×10^5	0.9
60000	2.105×10^6	2.1523×10^6	2.2
80000	2.98×10^6	2.9649×10^6	-0.5
100000	3.899×10^6	3.8548×10^6	-1.1
120000	4.858×10^6	4.8700×10^6	0.2
140000	6.250×10^6	6.1600×10^6	-1.4
147000	7.000×10^6	6.7850×10^6	-3.1
150000	7.450×10^6	7.1400×10^6	-4.2
200000	7.450×10^6	7.6400×10^6	2.6
300000	7.450×10^6	7.6400×10^6	2.6
400000	7.450×10^6	7.6400×10^6	2.6
500000	7.450×10^6	7.6400×10^6	2.6

Table 8 Natural Frequency Versus Length

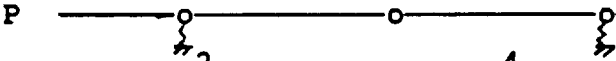

A = 48 IN^2 I = 256 IN^4 m = 0.4224 $LB\text{-}SEC^2/IN^2$

E = 30 x 10^6 K'= 0.666 P = 1,000,000 lb

Spring constant K = 100,000 LB/IN

LENGTH	RIGOROUS 1ST FREQ	NLFIN3 1ST FREQ	% DIFF	RIGOROUS 2ND FREQ	NLFIN3 2ND FREQ	% DIFF
31	123.18	123.188	0.0	123.18	128.860	4.6
32	121.140	121.208	0.1	125.57	130.254	3.7
34	117.439	117.505	0.1	127.653	132.193	3.6
40	107.961	108.040	0.1	130.602	134.802	3.2
42	105.235	105.320	0.1	130.671	134.148	2.7
44	102.683	102.772	0.1	130.470	133.347	2.2
46	100.284	100.377	0.1	130.042	132.445	1.8
48	98.022	98.119	0.1	129.461	132.437	2.3
50	95.880	95.982	0.1	128.757	131.449	2.1
60	86.602	86.726	0.1	124.222	125.956	1.4
70	78.990	79.138	0.2	119.115	120.344	1.0
80	72.424	72.596	0.2	114.079	115.032	0.8
100	61.110	61.328	0.4	104.831	105.574	0.7
110	56.009	56.247	0.4	100.641	101.376	0.7
160	34.069	34.340	0.8	82.686	83.882	1.4
200	20.903	21.147	1.2	70.114	72.098	2.8
210	18.182	18.420	1.3	67.070	69.288	3.3
260	6.329	6.632	4.8	52.364	55.738	6.4
270	3.430	3.892	13.5	49.577	53.140	7.2
275	0	1.742	--	48.211	51.860	7.6

Table 9 Natural Frequency Versus Length

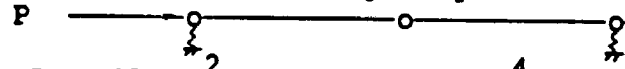

$A = 48\ IN^2$ $I = 256\ IN^4$ $m = 0.4224\ LB\text{-}SEC^2/IN^2$

$E = 30 \times 10^6$ $K' = 0.666$ $P = 1{,}000{,}000$ lb

Spring constant K = 50,000 LB/IN

LENGTH	RIGOROUS 1ST FREQ	NLFIN3 1ST FREQ	% DIFF	RIGOROUS 2ND FREQ	NLFIN3 2ND FREQ	% DIFF
60.5	62.023	61.784	0.4	62.023	63.316	2.1
62	60.977	60.972	0.0	63.197	63.808	1.0
64	59.889	59.930	0.1	63.969	64.546	0.9
66	58.885	58.928	0.1	64.585	65.132	0.8
68	57.919	57.964	0.1	65.070	65.590	0.8
70	56.987	57.034	0.1	65.445	65.939	0.8
72	56.087	56.136	0.1	65.726	66.197	0.7
74	55.217	55.268	0.1	65.928	66.376	0.7
76	54.374	54.427	0.1	66.061	66.490	0.6
78	53.555	53.610	0.1	66.137	66.546	0.6
80	52.760	52.817	0.1	66.161	66.554	0.6
82	51.986	52.046	0.1	66.143	66.520	0.6
84	51.232	51.294	0.1	66.086	66.449	0.5
88	49.777	49.843	0.1	65.880	66.218	0.5
90	49.074	49.143	0.1	65.737	66.064	0.5
100	45.756	45.838	0.2	64.752	65.082	0.5
140	34.326	34.462	0.4	59.105	59.418	0.5
180	24.118	24.296	0.7	53.160	53.651	0.9
240	10.687	10.910	2.1	44.393	45.492	2.5
275	0	1.741	--	39.143	40.768	4.2

Table 10 Natural Frequency Versus Length

A = 48 IN^2 I = 256 IN^4 m = 0.4224 $LB\text{-}SEC^2/IN^2$

E = 30 x 10^6 K'= 0.666 P = 1,000,000 lb

Spring constant K = 25,000 LB/IN

LENGTH	RIGOROUS 1ST FREQ	NLFIN3 1ST FREQ	% DIFF	RIGOROUS 2ND FREQ	NLFIN3 2ND FREQ	% DIFF
115.45	30.529	30.4991	0.1	30.529	30.6904	0.5
120	29.676	29.7156	0.1	31.269	31.3525	0.3
125	28.835	28.8787	0.2	31.827	31.9097	0.3
130	28.015	28.0628	0.2	32.243	32.3257	0.3
135	27.212	27.2636	0.2	32.547	32.6295	0.3
140	26.421	26.4774	0.2	32.759	32.8430	0.3
145	25.640	25.7010	0.2	32.897	32.9829	0.3
150	24.886	24.9315	0.2	32.974	33.0624	0.3
155	24.095	24.1661	0.3	33.000	33.0919	0.3
160	23.326	23.4026	0.3	32.983	33.0797	0.3
165	22.557	22.6390	0.4	32.931	33.0326	0.3
170	21.786	21.8734	0.4	32.848	32.9560	0.3
180	20.231	20.3305	0.5	32.608	32.7313	0.4
190	18.652	18.7644	0.6	32.291	32.4328	0.4
200	17.043	17.1689	0.7	31.915	32.0793	0.7
220	13.718	13.8721	1.1	31.032	31.2548	0.7
230	11.988	12.1592	1.4	30.539	30.7994	0.9
240	10.192	10.3844	1.9	30.019	30.3215	1.0
260	6.164	6.4413	4.5	28.610	29.3091	2.4
275	0	1.7385	--	28.211	28.5057	1.0

considerably. When the first two frequencies coalesce, dynamic (flutter) instability occurs.

NFLIN3 has excellent correlation with the rigorous solution. However, the rigorous solution has the 2nd frequency varying with axial load, even when K=0. Thus, it does not model rigid body rotation. NLFIN3 was developed from the differential equation in the rigorous solution, using Galerkin's criterion. Thus, it also has the 2nd frequency varying with the axial load, and does not have rigid body rotation capability.

Case c. Axially-loaded Beam with Horizontal and Vertical Support Springs

This beam was analyzed using a two-element formulation, and the results tabulated in Table 11. There is excellent correlation between the critical load obtained using finite element model and the rigorous solution.

A four-element model was also used, and the results tabulated in Table 12. Once again, there is excellent correlation between the frequencies of vibration obtained using the finite element model with the rigorous solution.

It should be noted that for this particular problem, flutter does not occur. Instead, instability occurs when the natural frequency drops to zero.

Table 11 Vibration of an Axially-loaded Beam with Horizontal and Vertical Springs

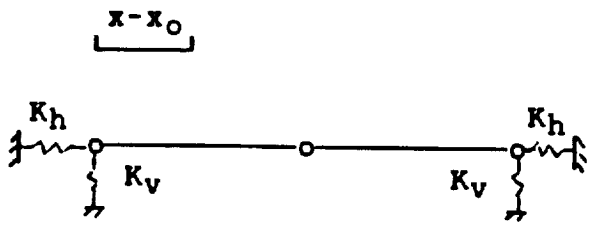

$K_h = 10 \times 10^6$ LB/IN

$K_v = 400 \times 10^3$ LB/IN

L = 100 IN

A = 48 IN^2

I = 256 IN^4

E = 30×10^6 PSI

m = 0.4224 $LB\text{-}SEC^2/IN^2$

LOAD (LB)	1ST FREQUENCY USING NLFIN5 (RAD/S)	1ST FREQUENCY RIGOROUS SOL (RAD/S)
0	93.38	
7,600,000	9.27	
7,610,000	7.92	
7,630,000	4.01	
7,640,000	2.71 i	
7,635,000	2.09	
7,560,000		0

$$\% \text{ DIFF.} = \frac{7{,}637{,}000 - 7{,}560{,}000}{7{,}560{,}000} = 1.0\ \%$$

Table 12 Vibration of Axially-loaded Beam with Horizontal and Vertical Springs

Using 4 elements

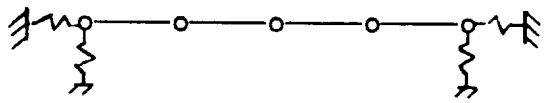

X_o = 0.0

P = 0.0

Freq.	Rig (RAD/SEC)	Modfin 3	% Diff.
1	97.8920	98.1914	0.3
2	221.4823	224.4996	1.4
3	385.4009	419.3890	6.0

X_o = 0.225 IN

P = 2,250,000 LB

Freq	Rig (RAD/SEC)	Modfin 3	% Diff.
1	82.1998	88.8739	8.1
2	214.0995	212.0427	1.0
3	387.5971	389.7464	0.6

Case d. Bowstring

Finally, consider a beam which has a spring connected between the end nodes, such that the force in the spring is always directed between the end nodes. (See Figure 13).

The differential equation for the bowstring developed by Fertis, is

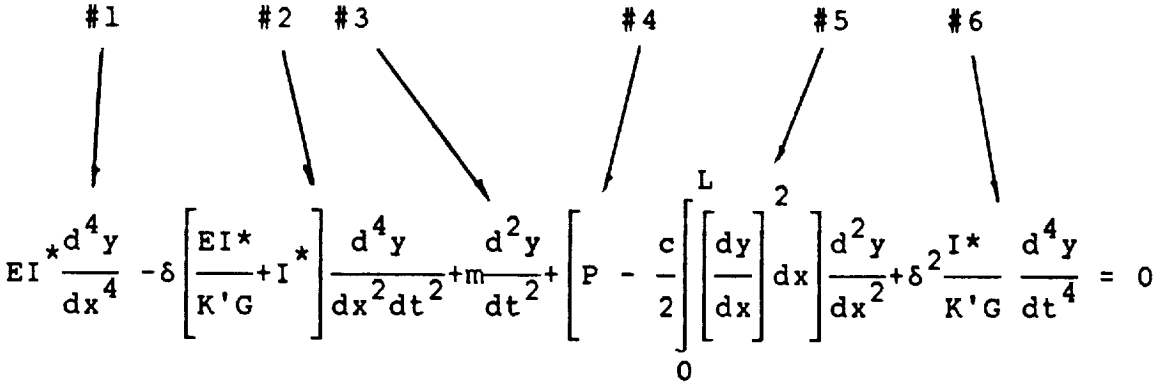

----(9.5)

Where

$I^{*} = I/(1+P/K'AG)$

K' = Shear Coefficient (shape factor)

c = Spring Constant

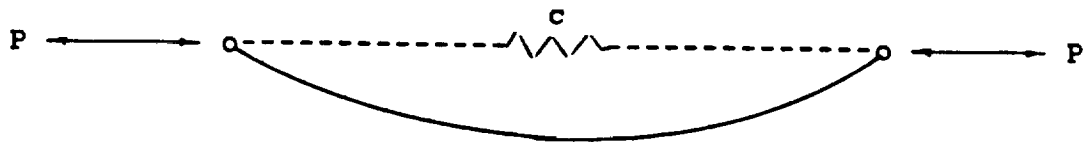

Figure 13 Bowstring Problem

Consider term #1.

$$EI^* \frac{d^4y}{dx^4}$$

As done previously, applying the Galerkin criterion yields

$$[Ke]=EI^* \begin{bmatrix} 12/L^3 & 6/L^2 & -12/L^3 & 6/L^2 \\ 6/L^2 & 4/L & -6/L^2 & 2/L \\ -12/L^3 & -6/L^2 & 12/L^3 & -6/L^2 \\ 6/L^2 & 2/L & -6/L^2 & 4/L \end{bmatrix}$$

Now consider the shear and rotatory inertia effects.

Consider the term

$$\frac{d^4\ y}{dx^2dt^2}$$

Let $W(x,t) = \Sigma\phi(x) \sin \Omega t$

$$\frac{d^4w}{dx^2dt^2} = -\Omega^2\ \phi(x)\ \frac{d^2W}{dx^2}$$

Apply Galerkin's criterion

$$-\phi^2 \int_{x_1}^{x_2} \phi_j \frac{d^2W}{dx^2}\, dx = 0 \qquad \text{Let } u=\phi j \qquad dv = \frac{d^2W}{dx^2}\, dx$$

$$du = \frac{d\phi j}{dx}\, dx \qquad v = \frac{dW}{dx}$$

$$\int_{x1}^{x2} \phi_j \frac{d^2W}{dx^2}\, dx = \phi_j \frac{dW}{dx}\Bigg|_{x=0}^{L} - \int_0^L \phi_j' \frac{dW}{dx}\, dx$$

which yields

$$[K_{Rot}] = \int_0^L \phi' i \;\; \phi' j \; dx$$

Hence, recall term #2.

$$\delta \left[\frac{EI^*}{K'G} + I^* \right] \frac{d^4y}{dt^2\, dx^2}$$

As done previously, applying the Galerkin criterion yields

$$[K_{ROT}] = \delta \left[\frac{EI^*}{K'G} + I^* \right] \begin{bmatrix} \frac{6}{5L} & \frac{1}{10} & \frac{-6}{5L} & \frac{1}{10} \\ \frac{1}{10} & \frac{2L}{15} & \frac{-1}{10} & \frac{-L}{30} \\ \frac{-6}{5L} & \frac{-1}{10} & \frac{6}{5L} & \frac{-1}{10} \\ \frac{1}{10} & \frac{-L}{30} & \frac{-1}{10} & \frac{2L}{15} \end{bmatrix}$$

Where δ = Mass Density

E = Young's Modulus

I = Moment of Inertia

K' = Shear Coefficient (Shape Factor)

G = Modulus of Rigidity

$I^* = I/(1+ P/K'AG)$

P = Axial Load

Consider term #3,

$$m \frac{d^2y}{dt^2} \quad .$$

As done previously, applying the Galerkin criterion yields

$$[M_o] = \frac{\delta AL}{420} \begin{bmatrix} 156 & & \text{SYMMETRIC} & \\ 22L & 4L^2 & & \\ 54 & 13L & 156 & \\ -13L & -3L^2 & -22L & 4L^2 \end{bmatrix}$$

Consider term #4,

$$P \frac{d^2y}{dx^2} \quad .$$

As done previously, applying the Galerkin criterion yields

$$[Kg] = P \begin{bmatrix} 6/5L & & \text{SYMMETRIC} & \\ 1/10 & 2L/15 & & \\ -6/5L & -1/10 & 6/5L & \\ 1/10 & -L/30 & -1/10 & 2L/15 \end{bmatrix}$$

Consider term #6,

$$\frac{\delta^2 I^*}{K'G} \frac{d^4y}{dt^4} \quad .$$

$$W(x,t) = \Sigma \phi(x) \sin \Omega t$$

$$\frac{d^4W}{dt^4} = \Omega^4 \phi(x) \text{ Sin } \Omega t$$

$$\frac{d^4W}{dt^4} = \Omega^4 W$$

Application of Galerkin's Criterion yields

$$\int_{x_1}^{x_2} \phi_i \, W \, dx = \int_{x_1}^{x_2} \phi_i \phi_j \, dx$$

$$[M_1] = \frac{\delta^2 I^* L}{(420)K' G} \begin{bmatrix} 156 & & \text{SYMMETRIC} & \\ 22L & 4L^2 & & \\ 54 & 13L & 156 & \\ -13L & -3L^2 & -22L & 4L^2 \end{bmatrix}$$

Finally, consider the term

$$\frac{c}{2} \int_0^L \left[\frac{dy}{dx} \right]^2 \frac{d^2y}{dx^2} \, dx \quad .$$

Integrate by parts.

Let $U = y'^2$ $\qquad dv = y'' \, dx$

$du = 2 y' y'' \, dx$ $\qquad v = y'$

$$\int_0^L y'^2 y'' \, dx = y'^3 \Big|_0^L - \int_0^L 2 y'^2 y'' \, dx$$

$$3 \int_0^L y'^2 y'' \, dx = y'^3 \Big|_0^L$$

Therefore

$$\frac{1}{3} y'^{3} \Big|_0^L = \int_0^L y'^{2} y'' \, dx$$

Let $y = \Sigma \phi_i y_i$

Apply Galerkin's Criterion

$$\frac{c}{6} \int_0^L \phi_i(x) \left[y'^{3} \right]_0^L dx = 0$$

or

$$K_{Bow} = \frac{c}{6} \int_0^L H \left[(H'^{3} \Big|_0^L \right] dx$$

Evaluate the term $H_i'^{3} \Big|_0^L$

$$H_2 = 1 - 3(X/L)^2 + 2(X/L)^3$$

$$H_2' = - \frac{6x}{L^2} + \frac{6x^2}{L^3}$$

$$H_2'^{3} \Big|_0^L = \left[- \frac{6x}{L^2} + \frac{6x^2}{L^3} \right]^3 \Big|_0^L$$

$$= \left[-\frac{6}{L} + \frac{6}{L} \right]^3 - 0$$

$$= 0 \quad .$$

$$H_3 = x - \frac{2x^2}{L} + \frac{x^3}{L^2}$$

$$H_3' = 1 - \frac{4x}{L} + \frac{3x^2}{L^2}$$

$$H_3'^3 \Big|_0^L = \left[1 - \frac{4x}{L} + \frac{3x^2}{L^2} \right]^3 \Big|_0^L$$

$$= [1 - 4 + 3]^3 - 1$$

$$= -1 \quad .$$

$$H_5 = 3(x/L)^2 - 2(x/L)^3$$

$$H_5' = \frac{6x}{L^2} - \frac{6x^2}{L^3}$$

$$H_5'^3 \Big|_0^L = \left[\frac{6x}{L^2} - \frac{6x^2}{L^3} \right]^3 \Big|_0^L$$

$$= \left[\frac{6}{L} - \frac{6}{L}\right]^3 - 0$$

$$= 0 \quad .$$

$$H_6 = -\frac{x^2}{L} + \frac{x^3}{L^2}$$

$$H_6' = -\frac{2x}{L} + \frac{3x^2}{L^2}$$

$$H_6'^3 \Big|_0^L = \left[-\frac{2x}{L} + \frac{3x^2}{L^2}\right]^3 \Big|_0^L$$

$$= \left[-2 + 3\right]^3 - 0$$

$$= 1 \quad .$$

Thus,

$$[K_{bow}] = \frac{C}{6}\int_0^L \begin{bmatrix} 0 & 0 & 0 & 0 \\ 0 & -H_3 & 0 & H_3 \\ 0 & 0 & 0 & 0 \\ 0 & -H_6 & 0 & H_6 \end{bmatrix} dx$$

Which yields

$$[K_{bow}] = \frac{C}{6}\begin{bmatrix} 0 & 0 & 0 & 0 \\ 0 & -L^2/12 & 0 & L^2/12 \\ 0 & 0 & 0 & 0 \\ 0 & L^2/12 & 0 & -L^2/12 \end{bmatrix}$$

By observation, K_{Bow} possesses both rigid body translation and rotation capability.

For the pre-loaded beam in space, one must consider the bow string without the horizontally applied P force, and replace the spring force with a constant P force in the direction of the spring (Figure 14).

From Galerkin, the matrix equation included the terms

$$P[K_g] - \frac{C}{6}[K_{bow}] = 0$$

or

$$C[K_{bow}] = 6\ P\ [K_g]$$

One can approximate the condition in Figure 14 by replacing C with 6P/L.

Figure 14 Pre-loaded Beam in Space

Thus, one obtains

$$[K_{bow}] = \frac{PL}{12}\begin{bmatrix} 0 & 0 & 0 & 0 \\ 0 & -1 & 0 & 1 \\ 0 & 0 & 0 & 0 \\ 0 & 1 & 0 & -1 \end{bmatrix}$$

Consider the performance of K_{bow} in a buckling problem.

Case 1 Simply-supported Beam (Figure 15).

This problem is traditionally solved using $[K_E]$ and $[K_g]$. However, due to the nodal restraints in the vertical direction, the P forces remain directed at the opposite nodes. Thus, $[K_E$ and $[K_{bow}]$ should provide a similar solution. The well-known rigorous solution is

$$P = \frac{\pi^2 EI}{L^2}$$

a. Solution using K_E and K_g

$$[Ke] = \frac{EI}{L^3}\begin{bmatrix} 12 & 6L & -12 & 6L \\ 6L & 4L^2 & -6L & 2L^2 \\ -12 & -6L & 12 & -6L \\ 6L & 2L^2 & -6L & 4L^2 \end{bmatrix}$$

Figure 15 Simply-Supported Beam Buckling Problem

$$[Kg] = \frac{P}{30L}\begin{bmatrix} 36 & 3L & -36 & 3L \\ 3L & 4L^2 & -3L & -L^2 \\ -36 & -3L & 36 & -3L \\ 3L & -L^2 & -3L & 4L^2 \end{bmatrix}$$

The active degrees of freedom provide the following matrix equation

$$\left[\frac{EI}{L^3}\begin{bmatrix} 4 & 2 \\ 2 & 4 \end{bmatrix} - \frac{P}{30L}\begin{bmatrix} 4 & -1 \\ -1 & 4 \end{bmatrix}\right]\begin{bmatrix} \phi_1 L \\ \phi_2 L \end{bmatrix} = \begin{bmatrix} 0 \\ 0 \end{bmatrix}$$

Let $\hat{P} = \frac{PL^2}{30EI}$

Then

$$\left|\begin{bmatrix} (4 - 4\hat{P}) & (2 + \hat{P}) \\ (2 + \hat{P}) & (4 - 4\hat{P}) \end{bmatrix}\right| = 0.$$

$$(4 - 4\hat{P})(4 - 4\hat{P}) - (2 + \hat{P})^2 = 0$$

$$16 - 32\hat{P} + 16\hat{P}^2 - 4 - 4\hat{P} - \hat{P}^2 = 0$$

$$15\hat{P}^2 - 36\hat{P} + 12 = 0$$

$$5\hat{P}^2 - 12\hat{P} + 4 = 0$$

$$\hat{P} = 0.4,\ 2$$

Therefore,

$$P = \frac{(0.4)(30)EI}{L^2}$$

$$= \frac{12\ EI}{L^2} \quad .$$

$$\text{Error} = \frac{12 - \pi^2}{\pi^2} = 21.6\ \%$$

Consider a two-element model of the beam in Figure 15.

$$[Ke] = \frac{EI}{L^3}\begin{bmatrix} 4L^2 & -6L & 2L^2 & 0 \\ -6L & 24 & 0 & 6L \\ 2L^2 & 0 & 8L^2 & 2L^2 \\ 0 & 6L & 2L^2 & 4L^2 \end{bmatrix}$$

$$[Kg] = \frac{P}{30L}\begin{bmatrix} 4L^2 & -3L & -L^2 & 0 \\ -3L & 72 & 0 & 3L \\ -L^2 & 0 & 8L^2 & -L^2 \\ 0 & 3L & -L^2 & 4L^2 \end{bmatrix}$$

Active DOF: 2, 3, 4, 6

The active degrees of freedom provide the following matrix equation:

$$\left[\frac{EI}{\hat{L}^3}\begin{bmatrix} 4 & -6 & 2 & 0 \\ -6 & 24 & 0 & 6 \\ 2 & 0 & 8 & 2 \\ 0 & 6 & 2 & 4 \end{bmatrix} - \frac{P}{30\hat{L}}\begin{bmatrix} 4 & -3 & -1 & 0 \\ -3 & 72 & 0 & 3 \\ -1 & 0 & 8 & -1 \\ 0 & 3 & -1 & 4 \end{bmatrix}\right]\begin{bmatrix} \phi_1\hat{L} \\ V_2 \\ \phi_2\hat{L} \\ \phi_3\hat{L} \end{bmatrix} = \begin{bmatrix} 0 \\ 0 \\ 0 \\ 0 \end{bmatrix}$$

Letting $\hat{P} = \frac{PL^2}{30EI}$ Yields

$$\left|\begin{bmatrix} 4 - 4\hat{P} & -6 + 3\hat{P} & 2 + \hat{P} & 0 \\ -6 + 3\hat{P} & 24 - 72\hat{P} & 0 & 6 - 3\hat{P} \\ 2 + \hat{P} & 0 & 8 - 8\hat{P} & 2 + \hat{P} \\ 0 & 6 - 3\hat{P} & 2 + \hat{P} & 4 - 4\hat{P} \end{bmatrix}\right| = 0$$

$$8{,}100\,\hat{P}^4 - 28{,}800\,\hat{P}^3 + 29{,}664\,\hat{P}^2 - 9{,}216\,\hat{P} + 576 = 0$$

$$\hat{P} = 0.0828653,\ 0.4,\ 1.07269,\ 2$$

$$\hat{P} = \frac{PL^2}{30\ EI}$$

$$P = \frac{30EI}{\hat{L}^2}\hat{P}$$

But $\hat{L} = L/2$

Thus

$$P = \frac{(30)\ EI\ (0.0828653)\ (4)}{L^2}$$

$$P = 9.9438$$

$$\text{Error} = \frac{\pi^2 - 9.9438}{\pi^2}$$

$$= 0.75\% \quad .$$

Now consider 1 element with Ke and K_{bow}.

$$\left[\frac{EI}{L^3}\left[\begin{matrix}4 & 2\\ 2 & 4\end{matrix}\right] - \frac{P}{12L}\left[\begin{matrix}1 & -1\\ -1 & 1\end{matrix}\right]\right]\left[\begin{matrix}\phi_1 L\\ \phi_2 L\end{matrix}\right] = \left[\begin{matrix}0\\ 0\end{matrix}\right]$$

Let

$$\hat{P} = \frac{PL^2}{12EI}$$

$$\left|\left[\begin{matrix}4-\hat{P} & 2+\hat{P}\\ 2+\hat{P} & 4-\hat{P}\end{matrix}\right]\right| = 0$$

$$(4-\hat{P})^2 - (2+\hat{P})^2 = 0$$

$$16-8\hat{P}+\hat{P}^2-4-4\hat{P}-\hat{P}^2 = 0$$

$$12-12\hat{P} = 0$$

$$\hat{P} = 1 \quad .$$

Therefore,

$P = 12\,\frac{EI}{L^2}$. Which is identical with the one element solution using Ke and Kg.

Now consider the two-element model.

$$[Ke] = \frac{EI}{\hat{L}^3}\begin{bmatrix} 12 & 6\hat{L} & -12 & 6\hat{L} & 0 & 0 \\ 6\hat{L} & 4\hat{L}^2 & -6\hat{L} & 2\hat{L}^2 & 0 & 0 \\ -12 & -6\hat{L} & 24 & 0 & -12 & 6\hat{L} \\ 6\hat{L} & 2\hat{L}^2 & 0 & 8\hat{L}^2 & -6\hat{L} & 2\hat{L}^2 \\ 0 & 0 & -12 & -6\hat{L} & 12 & -6\hat{L} \\ 0 & 0 & 6\hat{L} & 2\hat{L}^2 & -6\hat{L} & 4\hat{L}^2 \end{bmatrix}$$

$$[K_{bow}] = \frac{P}{12\hat{L}}\begin{bmatrix} 0 & 0 & 0 & 0 & 0 & 0 \\ 0 & \hat{L}^2 & 0 & -\hat{L}^2 & 0 & 0 \\ 0 & 0 & 0 & 0 & 0 & 0 \\ 0 & -\hat{L}^2 & 0 & 2\hat{L}^2 & 0 & -\hat{L}^2 \\ 0 & 0 & 0 & 0 & 0 & 0 \\ 0 & 0 & 0 & -\hat{L}^2 & 0 & \hat{L}^2 \end{bmatrix}$$

Active DOF: 2, 3, 4, 6

The active degrees of freedom provide the following matrix equation:

$$\left[\frac{EI}{\hat{L}^3}\begin{bmatrix} 4 & -6 & 2 & 0 \\ -6 & 24 & 0 & 6 \\ 2 & 0 & 8 & 2 \\ 0 & 6 & 2 & 4 \end{bmatrix} - \frac{P}{12\hat{L}}\begin{bmatrix} 1 & 0 & -1 & 0 \\ 0 & 0 & 0 & 0 \\ -1 & 0 & 2 & -1 \\ 0 & 0 & -1 & 1 \end{bmatrix}\right]\begin{bmatrix} \theta_1 L \\ V_2 \\ \theta_2 L \\ \theta_3 L \end{bmatrix} = \begin{bmatrix} 0 \\ 0 \\ 0 \\ 0 \end{bmatrix}$$

Letting $\hat{P} = \dfrac{P\hat{L}^2}{12\ EI}$ yields

$$\left|\begin{bmatrix} 4-\hat{P} & -6 & 2+\hat{P} & 0 \\ -6 & 24 & 0 & 6 \\ 2+\hat{P} & 0 & 8-2\hat{P} & 2+\hat{P} \\ 0 & 6 & 2+\hat{P} & 4-\hat{P} \end{bmatrix}\right| = 0$$

$$576\ \hat{P}^2 - 1{,}152\ \hat{P} + 576 = 0$$

$$\hat{P} = 1$$

$$\hat{P} = \frac{P\ \hat{L}^2}{12\ EI}$$

$$P = \frac{12\ EI\ \hat{P}}{\hat{L}^2}$$

But $\hat{L} = L/2$

Thus

$$P = \frac{(12)\ EI\ (1)\ (4)}{L^2}$$

$$= \frac{48\ EI}{L^2} \quad , \quad \text{no good.}$$

It should be noted that the problem actually modeled by this 2 element formulation is as shown in Figure 16, which does not correctly model a directed force between the support nodes 1 and 3.

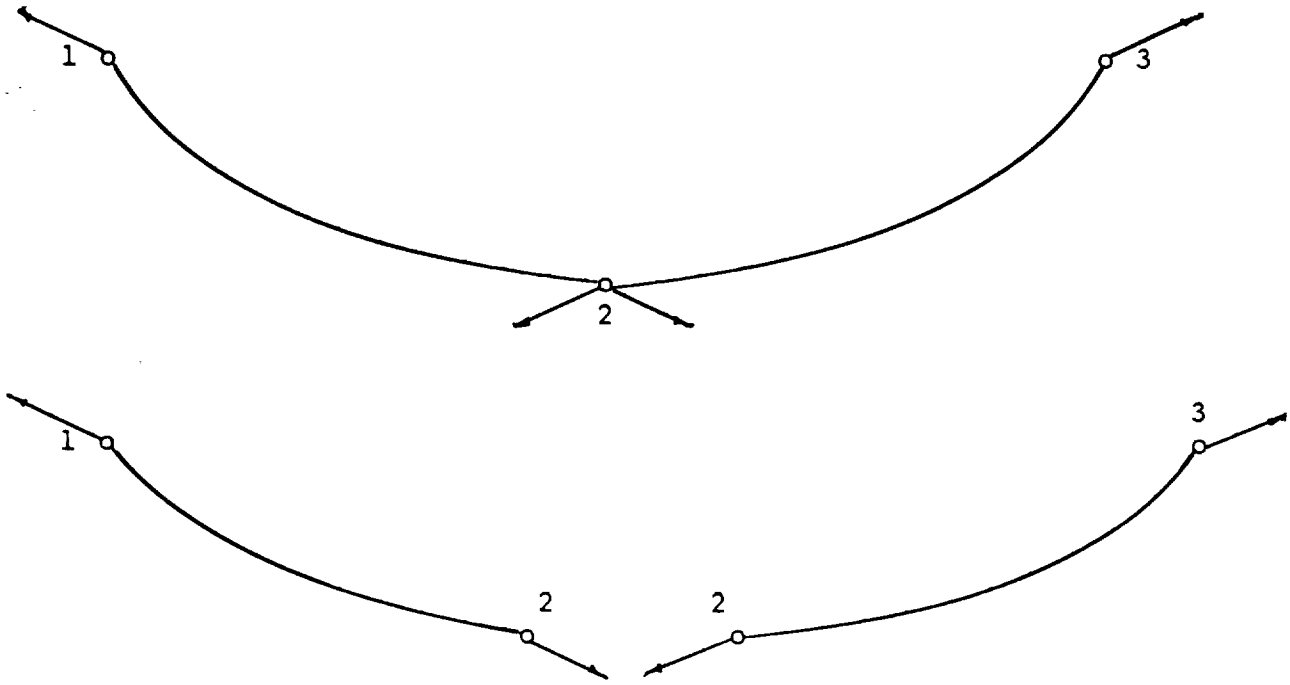

Figure 16 3 Node $[K_E]$ and $[K_{BOW}]$

CHAPTER 10

GLOBAL FORMULATION OF BOW-STRING

Examination of $[K_{bow}]$ indicates that rigid body rotation capabilities occur due to the corresponding rows in the matrix relating to the end shears having all zero coefficients. Hence, any combination of $[K_{bow}]$ and [Kg] will not have rigid body rotation capability. It has also been shown that assemblage of $[K_{bow}]$ elements did not model a force directed between the end nodes.

Examination of a 2-element model (Appendix A) showed that the only fictitious forces that occurred during rigid body rotation were the end shears required for equilibrium. The shear at the center node was zero. The corresponding row in the geometric stiffness matrix is full, indicating that there is a relationship between the stiffness terms at each degree of freedom, and the shear at the center node.

Examination of the first and fifth rows, however, would indicate that there is not any relationship between the end nodes. This is inherent in the assembly process, and is contrary to the basic supposition that we are considering a problem where the applied forces remain directed between the end nodes.

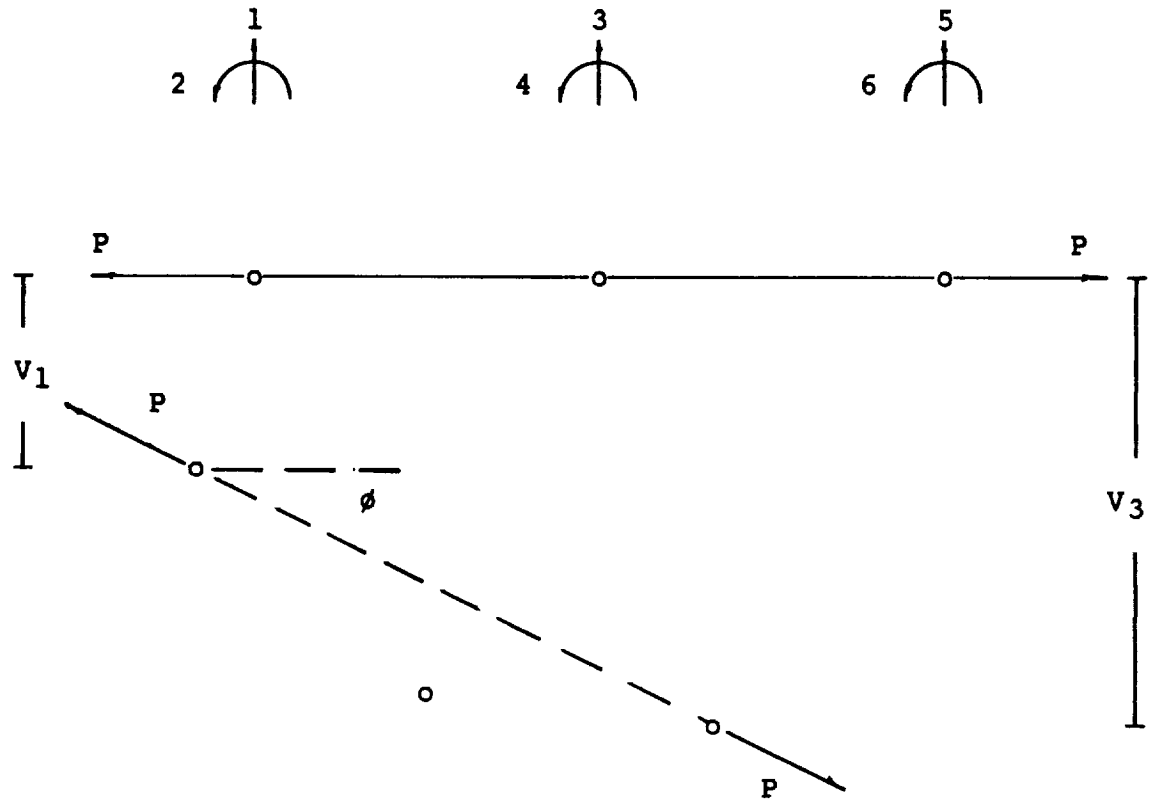

Figure 17 Directed Force 2-element Representation

Consider again Argyris's methodology for the directed force problem (Figure 17).

Let $\phi \approx \dfrac{V_3 - V_1}{L}$.

If one neglects the change in the axial component of P that occurs during rotation, as is customarily done (P cos $\phi \approx$ P), we obtain the consistent geometric stiffness matrix.

Suppose we retain the vertical component, P sin ϕ, and use Argyris's approach to develop a load correction matrix. The load vector for this force becomes

$$R^{DFC} = \left[P \sin (V_3-V_1)/L,\ 0,\ 0,\ 0,\ -P \sin (V_3-V_1)/L,\ 0\right]$$

The load correction matrix is generated using the equation

$$[K^{DFC}] = \left[\frac{dR_i{}^{DF}}{du_i}\right] \quad , \quad \text{which yields}$$

$$[K^{DFC}] = \begin{bmatrix} -\frac{P}{L}\cos\left[\frac{V_1-V_3}{L}\right] & 0 & 0 & 0 & \frac{P}{L}\cos\left[\frac{V_1-V_3}{L}\right] & 0 \\ 0 & 0 & 0 & 0 & 0 & 0 \\ 0 & 0 & 0 & 0 & 0 & 0 \\ 0 & 0 & 0 & 0 & 0 & 0 \\ \frac{P}{L}\cos\left[\frac{V_1-V_3}{L}\right] & 0 & 0 & 0 & -\frac{P}{L}\cos\left[\frac{V_1-V_3}{L}\right] & 0 \\ 0 & 0 & 0 & 0 & 0 & 0 \end{bmatrix}$$

For small rotation, $\cos (V_1-V_3)/L \approx 1$, and $[K^{DFC}]$ becomes

$$[K^{DFC}] = \begin{bmatrix} -\frac{P}{L} & 0 & 0 & 0 & \frac{P}{L} & 0 \\ 0 & 0 & 0 & 0 & 0 & 0 \\ 0 & 0 & 0 & 0 & 0 & 0 \\ 0 & 0 & 0 & 0 & 0 & 0 \\ \frac{P}{L} & 0 & 0 & 0 & -\frac{P}{L} & 0 \\ 0 & 0 & 0 & 0 & 0 & 0 \end{bmatrix}$$

At this point, combine [Kg] + $[K^{DFC}]$ and check rigid body rotation. Since $[K^{DFC}]$ contains non-zero terms in rows 1 and 5, and [Kg] pseudo-forces occur only in the same two rows, only these two rows must be checked for rigid body rotation capability.

Row 1

$$P\left[12/5L - 1/L,\ 1/10,\ -12/5L,\ 1/10,\ 1/L,\ 0\right] \begin{bmatrix} -L\theta/2 \\ \theta \\ 0 \\ \theta \\ L\theta/2 \\ \theta \end{bmatrix}$$

$$= P\left[\ -1.2\theta + 0.5\theta + 0.1\theta + 0.1\theta + 0.5\theta\ \right]$$

$$= 0.$$

Row 5

$$P\left[1/L,\ 0,\ -12/5L,\ -1/10,\ 12/5L\ -1/L,\ -1/10\right] \begin{bmatrix} -L\theta/2 \\ \theta \\ 0 \\ \theta \\ L\theta/2 \\ \theta \end{bmatrix}$$

$$= P\left[\ -0.5L - 0.1L + 1.2L - 0.5L - 0.1L\ \right]$$

$$= 0.$$

Therefore, [Kg] + [K^{DFC}] does possess rigid body rotation capability. By inspection, it also possesses rigid body translation capabilities.

CHAPTER 11

PERFORMANCE OF $[K_T] + [K]^{DFC}$

Consider a two-element model using $[K_T] + [K]^{DFC}$, utilizing the computer program NLBO.FOR. Table 13 compares the results from NLBO.FOR with the finite element solution using $[K^T]$ only (consistent [Ke] and [Kg] matrices). Note that the stiffness matrix generated by NLBO.FOR does possess the additional zero eigenvalue, required for a complete set of rigid body modes. The other frequencies have extremely close correlation with the traditional finite element solution obtained using NLFINITE.FOR. Most of them were identical. The largest difference was 2.8 % for frequency #6.

When one considers the stiffness matrix $[K_T]$ generated by NLFINITE.FOR for this problem, the following is obtained:

Table 13 Frequency Comparison using NLFINITE.FOR and NLBO.FOR

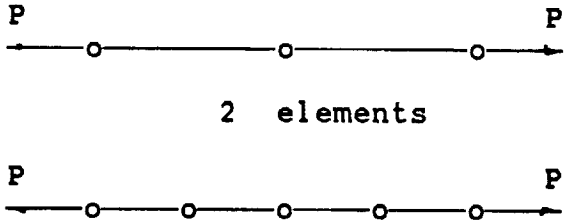

$A = 48\ IN^2$

$E = 30 \times 10^6\ PSI$

$I = 1000\ IN^4$

$m = 0.03525\ LB\text{-}SEC^2/IN^2$

$L = 100\ IN$

$P = 60{,}000{,}000\ LBS$

Freq	NLFINITE.FOR		NLBO.FOR		% Diff	%Diff
#	2 Elem.	4 Elem.	2 Elem.	4 Elem.	2 Elem	4Elem
1	0	0	0	0	0	0
2	0	0	0	0	0	0
3	1390	1385	0	0	0	0
4	3532	3524	3532	3524	0	0
5	7002	6514	7002	6524	0	0
6	7847	7163	7657	6969	2.4	2.7
7	14003	12565	14003	12565	0	0
8	17683	14003	17683	14003	0	0
9	27189	21782	27090	21715	0.4	0.3
10		22755		22755		0
11		28006		28006		0
12		33395		33395		0
13		51048		51083		0.07
14		84645		84645		0
15		93157		93200		0.05

$$[K_T] \times [\text{Rigid Body Modes}] = \begin{bmatrix} 0 & 0 & 0 \\ 0 & 0 & -6 \times 10^7 \\ 0 & 0 & 0 \\ 0 & 0 & 0 \\ 0 & 0 & 0 \\ 0 & 0 & 0 \\ 0 & 0 & 0 \\ 0 & 0 & 6 \times 10^7 \\ 0 & 0 & 0 \end{bmatrix}$$

As expected, large pseudo-forces occurred during rigid body rotation.

The eigenvalues and eigenvectors generated by NLFINITE were:

Lambda (1) = 0.0000

Omega (1) = 0.0000 RAD/SEC

The associated eigenvector is:

0.1000000000D+01

0.0000000000D+00

0.0000000000D+00

0.1000000000D+01

0.0000000000D+00

0.0000000000D+00

```
 0.1000000000D+01
 0.0000000000D+00
 0.0000000000D+00

Lambda (2) = 0.0000
Omega (2) = 0.0001 RAD/S

The associated eigenvector is

 0.0000000000D+00
 0.1000000000D+01
-0.1022543458D-17
 0.0000000000D+00
 0.1000000000D+01
-0.1102256093D-15
 0.0000000000D+00
 0.1000000000D+01
-0.5808321841D-16

Lambda (3) = 1930958.5265
Omega (3) = 1389.5893 RAD/S

The associated eigenvector is:

 0.0000000000D+00
-0.1000000000D+01
 0.1508421072D-01
 0.0000000000D+00
 0.1746464363D-14
```

```
 0.2418478835D-01
 0.0000000000D+00
 0.1000000000D+01
 0.1508421072D-01

Lambda (4) = 12477499.9590
Omega (4) = 3532.3505 RAD/S

The associated eigenvector is:

 0.0000000000D+00
 0.1000000000D+01
-0.4125765357D-01
 0.0000000000D+00
-0.6561862202D+00
-0.6954552347D-17
 0.0000000000D+00
 0.1000000000D+01
 0.4125765357D-01

Lambda (5) = 49021276.5957
Omega (5) = 7001.5196 RAD/S

The associated eigenvector is:

 0.1000000000D+01
 0.0000000000D+00
 0.0000000000D+00
```

```
 0.2041110487D-15
 0.0000000000D+00
 0.0000000000D+00
-0.1000000000D+01
 0.0000000000D+00
 0.0000000000D+00

Lambda (6) = 61570298.8787
Omega (6) = 7847.6744 RAD/S

The associated eigenvector is:

 0.0000000000D+00
 0.1000000000D+01
-0.8622993042D-01
 0.0000000000D+00
 0.1067276729D-15
 0.7402023912D-01
 0.0000000000D+00
-0.1000000000D+01
-0.8622993042D-01

Lambda (7) = 196085106.3830
Omega (7) = 14003.0392 RAD/S

The associated eigenvector is:

 0.1000000000D+01
 0.0000000000D+00
```

```
 0.0000000000D+00
-0.1000000000D+01
 0.0000000000D+00
 0.0000000000D+00
 0.1000000000D+01
 0.0000000000D+00
 0.0000000000D+00
```

Lambda (8) = 312696968.0165

Omega (8) = 17683.2397

The associated eigenvector is:

```
 0.0000000000D+00
 0.1000000000D+01
-0.1694400209D+00
 0.0000000000D+00
 0.4120001744D+00
-0.3619443243D-18
 0.0000000000D+00
 0.1000000000D+01
 0.1694400209D+00
```

Lambda (9) = 739222146.5762

Omega (9) = 27188.6400

The associated eigenvector is:

0.0000000000D+00

0.1000000000D+01

-0.2124292332D+00

0.0000000000D+00

0.3363477755D-15

-0.1091964722D+00

0.0000000000D+00

-0.1000000000D+01

-0.2124292332D+00

Let $[\phi]$ be the matrix of mode shapes (eigenvectors). Then $[\phi]^T [K] [\phi]$ would yield a diagonalized stiffness matrix if all of the rigid body modes were present. Performing that matrix multiplication yields

$$\begin{bmatrix}
0 & 0 & 0 & 0 & 0 & 0 & 0 & 0 & 0 \\
0 & 1 & 1.92 & -0.66 & 0 & -1.98 & 0 & 0.41 & -1.36 \\
0 & 1 & 2.54\text{x}10^{6} & 0 & 0 & 109 & 0 & -1 & 41 \\
0 & -2 & 1 & 1.19\text{x}10^{7} & 0 & -3 & 0 & 220 & -2 \\
0 & 0 & 0 & 0 & 5.76\text{x}10^{7} & 0 & -2 & 0 & 0 \\
0 & -1 & 113 & -1 & 0 & 4.91\text{x}10^{7} & 0 & -1 & -909 \\
0 & 0 & 0 & 0 & -1 & 0 & 2.30\text{x}10^{8} & 0 & 0 \\
0 & 2 & 1 & 219 & 0 & -1 & 0 & 1.33\text{x}10^{8} & -1 \\
0 & 1 & 43 & -1 & 0 & -908 & 0 & 0 & 3.30\text{x}10^{8}
\end{bmatrix}$$

It should be noted that small errors occur during the computations (initial data errors, roundoff errors, truncation errors, relative errors, etc.). The 2.54×10^{6} term in the 3,3 position is due to the lack of rigid body rotation capability. The other non-diagonal terms should also be zero, but may be attributed to the above mentioned errors. The largest of these, ± 909, is still relatively insignificant compared to the magnitude of the diagonal terms.

If one neglects the relatively small terms due to arithmetic errors, the following diagonal matrix is obtained:

$$\begin{bmatrix} 0 & 0 & 0 & 0 & 0 & 0 & 0 & 0 & 0 \\ 0 & 0 & 0 & 0 & 0 & 0 & 0 & 0 & 0 \\ 0 & 0 & 2.54\times10^{6} & 0 & 0 & 0 & 0 & 0 & 0 \\ 0 & 0 & 0 & 1.19\times10^{7} & 0 & 0 & 0 & 0 & 0 \\ 0 & 0 & 0 & 0 & 5.76\times10^{7} & 0 & 0 & 0 & 0 \\ 0 & 0 & 0 & 0 & 0 & 4.91\times10^{7} & 0 & 0 & 0 \\ 0 & 0 & 0 & 0 & 0 & 0 & 2.30\times10^{8} & 0 & 0 \\ 0 & 0 & 0 & 0 & 0 & 0 & 0 & 1.33\times10^{8} & 0 \\ 0 & 0 & 0 & 0 & 0 & 0 & 0 & 0 & 3.30\times10^{8} \end{bmatrix}$$

Now consider the modified finite element solution from NLBO.FOR, which utilized the directed force correction matrix. The two-element stiffness matrix generated is:

$$\begin{bmatrix}
.288E8 & 0 & 0 & -.288E8 & 0 & 0 & 0 & 0 & 0 \\
0 & .372E7 & .78E8 & 0 & -.432E7 & .78E8 & 0 & 0 & 0 \\
0 & .78E8 & .28E10 & 0 & -.78E8 & .11E10 & 0 & 0 & 0 \\
-.288E8 & 0 & 0 & .576E8 & 0 & 0 & -.288E8 & 0 & 0 \\
0 & -.432E7 & -.78E8 & 0 & .864E7 & 0 & 0 & -.432E7 & .78E8 \\
0 & .78E8 & .11E10 & 0 & 0 & .56E10 & 0 & -.78E8 & .11E10 \\
0 & 0 & 0 & -.288E8 & 0 & 0 & .288E8 & 0 & 0 \\
0 & .6E6 & 0 & 0 & -.432E7 & -.78E8 & 0 & .372E7 & -.78E8 \\
0 & 0 & 0 & 0 & .78E8 & .11E10 & 0 & -.78E8 & .28E1
\end{bmatrix}$$

The rigid body rotation matrix is

$$\begin{bmatrix}
1 & 0 & 0 & 1 & 0 & 0 & 1 & 0 & 0 \\
0 & 1 & 0 & 0 & 1 & 0 & 0 & 1 & 0 \\
0 & -50 & 1 & 0 & 0 & 1 & 0 & 50 & 1
\end{bmatrix}^T$$

$$[K_T] \times [\text{Rigid Body Modes}] = \begin{bmatrix}
0 & 0 & 0 \\
0 & 0 & 0 \\
0 & 0 & 0 \\
0 & 0 & 0 \\
0 & 0 & 0 \\
0 & 0 & 0 \\
0 & 0 & 0 \\
0 & 0 & 0 \\
0 & 0 & 0
\end{bmatrix}$$

The large, erroneous term ($\pm$ 6 x 10^7) due to lack of rigid body rotation capability has been eliminated.

The eigenvalues and eigenvectors generated by NLBO, corresponding to all rigid body and elastic modes and frequencies, were:

Lambda (1) = -0.0122

Omega (1) = 0.0000 RAD/S

The associated eigenvector is:

 0.0000000000D+00

-0.9999999660D-01

 0.0000000000D+00

 0.1701762335D-07

 0.1999999966D-01

 0.0000000000D+00

 0.1000000000D+01

 0.1999999971D-01

Lambda (2) = 0.0000

Omega (2) = 0.0000 RAD/S

The associated eigenvector is:

 0.0000000000D+00

 0.1000000000D+01

-0.1021057361D-08

 0.0000000000D+00

```
 0.9999999489D+00
-0.1021057341D-08
 0.0000000000D+00
 0.9999998979D+00
-0.1021057345D-08

Lambda (3) = 0.0000
Omega (3) = 0.0001 RAD/S

The associated eigenvector is:

 0.1000000000D+01
 0.0000000000D+00
 0.0000000000D+00
 0.1000000000D+01
 0.0000000000D+00
 0.0000000000D+00
 0.1000000000D+01
 0.0000000000D+00
 0.0000000000D+00

Lambda (4) = 12477499.9590
Omega (4) = 3532.3505 RAD/S

The associated eigenvector is:

 0.0000000000D+00
 0.1000000000D+01
```

-0.4125765357D-01

 0.0000000000D+00

-0.6561862202D+00

-0.1373447533D-16

 0.0000000000D+00

 0.1000000000D+01

 0.4125765357D-01

Lambda (5) = 49021276.5957

Omega (5) = 7001.5196 RAD/S

The associated eigenvector is:

 0.1000000000D+01

 0.0000000000D+00

 0.0000000000D+00

 0.8376574057D-16

 0.0000000000D+00

 0.0000000000D+00

-0.1000000000D+01

 0.0000000000D+00

 0.0000000000D+00

Lambda (6) = 58630070.5158

Omega (6) = 7657.0275

The associated eigenvector is:

 0.0000000000D+00

```
 0.1000000000D+01
-0.8951411454D-01
 0.0000000000D+00
 0.1259126794D-15
 0.7572882821D-01
 0.0000000000D+00
-0.1000000000D+01
-0.8951411454D-01
```

Lambda (7) = 196085106.3830

Omega (7) = 14003.0392 RAD/S

The associated eigenvector is:

```
 0.1000000000D+01
 0.0000000000D+00
 0.0000000000D+00
-0.1000000000D+01
 0.0000000000D+00
 0.0000000000D+00
 0.1000000000D+01
 0.0000000000D+00
 0.0000000000D+00
```

Lambda (8) = 312696968.0165

Omega (8) = 17683.2397 RAD/S

The associated eigenvector is:

```
 0.0000000000D+00
 0.1000000000D+01
-0.1694400209D+00
 0.0000000000D+00
 0.4120001744D+00
 0.3280451486D-16
 0.0000000000D+00
 0.1000000000D+01
 0.1694400209D+00
```

Lambda (9) = 733880567.5204

Omega (9) = 27090.2301 RAD/S

The associated eigenvector is:

```
 0.0000000000D+00
 0.1000000000D+01
-0.2134858855D+00
 0.0000000000D+00
 0.6206811895D-15
-0.1102288283D+00
 0.0000000000D+00
-0.1000000000D+01
-0.2134858855D+00
```

Let $[\phi]$ be the matrix of mode shapes (eigenvectors). Then $[\phi]^T$ $[K]$ $[\phi]$ should yield a

diagonalized stiffness matrix if all of the rigid body modes were present. Performing that matrix multiplication yields

$$\begin{bmatrix}
0 & 0 & 0 & 0 & 0 & 0 & 0 & 0 & 0 \\
0 & 0 & 0 & 0.08 & 0 & 0 & 0 & 0.34 & 0 \\
0 & 1.71 & 1 & -0.55 & 0 & -1.97 & 0 & 0.33 & 0.84 \\
0 & 1 & -1.99 & 1.19E7 & 0 & -3 & 0 & -39 & -1 \\
0 & 0 & 0 & 0 & 5.76E7 & 0 & -2 & 0 & 0 \\
0 & -1 & -1.91 & -2 & 0 & 4.91E7 & 0 & -1 & -81 \\
0 & 0 & 0 & 0 & -1 & 0 & 2.31E8 & 0 & 0 \\
0 & 0 & 0.56 & -39 & 0 & 1 & 0 & 1.33E8 & -1 \\
0 & 0 & 1.65 & -1 & 0 & -81 & 0 & -2 & 3.32E8
\end{bmatrix}$$

It should be noted that minor errors still occur during the computations (initial data errors, roundoff errors, truncation errors, relative errors, etc.). The examination of these errors is beyond the scope of this dissertation. It can be readily seen, however, that the largest of these error has been reduced an order of magnitude (from ± 909 to 81).

Neglecting the relatively small terms due to arithmetic errors, the following diagonal matrix is obtained:

$$\begin{bmatrix} 0 & 0 & 0 & 0 & 0 & 0 & 0 & 0 & 0 \\ 0 & 0 & 0 & 0 & 0 & 0 & 0 & 0 & 0 \\ 0 & 0 & 0 & 0 & 0 & 0 & 0 & 0 & 0 \\ 0 & 0 & 0 & 1.19E7 & 0 & 0 & 0 & 0 & 0 \\ 0 & 0 & 0 & 0 & 5.76E7 & 0 & 0 & 0 & 0 \\ 0 & 0 & 0 & 0 & 0 & 4.91E7 & 0 & 0 & 0 \\ 0 & 0 & 0 & 0 & 0 & 0 & 2.31E8 & 0 & 0 \\ 0 & 0 & 0 & 0 & 0 & 0 & 0 & 1.33E8 & 0 \\ 0 & 0 & 0 & 0 & 0 & 0 & 0 & 0 & 3.32E8 \end{bmatrix}$$

Most importantly, the large erroneous term in the 3,3 position of the matrix obtained using the conventional finite element formulation is now identically zero, and the matrix has been properly diagonalized. Thus, adding $[K]^{DFC}$, as developed in this dissertation, corrected the lack of rigid body rotation capability of the pre-loaded beam element, as well as provided the correct diagonalized stiffness matrix in the diagonalization/partitioning methodology used in finite element dynamic analysis.

CHAPTER 12

SUMMARY

Based upon this investigation, the following conclusions have been developed:

1. Grounding is due to the development of pseudo-forces at the element level required to counteract a force-imbalance inherent in the development. This causes a lack of rigid body rotational capability of the geometric stiffness matrix.

2. Although the consistent geometric stiffness matrix provides acceptable results for most static displacement and buckling problems, provided a sufficient mesh is used, modifications of the global stiffness matrix (zeroing out of erroneous terms, and appending the missing rigid body modes) must be done to more accurately predict the dynamic response.

3. Although the rigid body mode test is routinely used to detect the presence of modeling errors in finite element models, it is not sufficient reason to invalidate a model subjected to pre-loads.

4. Various higher order stiffness matrices developed by others, which include shear and rotatory inertia effects, were examined. As expected, the inclusion of these higher order effects does not compensate for the inaccuracy (lack of rigid body rotation capability) of the geometric stiffness matrix.

5. Rigorous solutions of the pre-loaded beam with various end conditions were developed.

6. The Galerkin criterion was used to develop stiffness and mass matrices from the rigorous solutions, which were incorporated into a modified finite element algorithm.

7. Sample problems involving pre-loaded beams with various spring support conditions were solved using the modified finite element algorithms, and the results compared with the rigorous solutions.

8. The occurrence of dynamic "flutter" instabilities was determined by the rigorous solutions. There was good correlation obtained using the modified finite element algorithms.

9. The tangential stiffness matrices developed did not possess the three zero eigenvalues required for all the rigid body modes.

10. The directed force (ie., bow-string) problem was examined, since the force unbalance inherent in the other developments does not occur in this situation.

11. Development of the bow-string stiffness using Clough and Penzien's technique provided a modified matrix, but it was shown to lack rigid body rotational capability.

12. Development of the bow-string stiffness using Saunders methodology provided a modified matrix, but it also was shown to lack rigid body rotational capability.

13. A bow-string stiffness matrix developed from the rigorous solution using Galerkin's criterion possessed all the required rigid body modes. $[K_{BOW}]$ was shown to provide an acceptable first approximation to the directed force buckling problem solved by Timoshenko and Gere, and it performs properly in the diagonalization/partitioning methodology used in dynamic response. However, it does not properly model a pre-loaded beam where the force is directed between the end nodes only of an assembled mesh.

14. By considering the directed force problem at the global level, using traditional development of [Kg] from the horizontal component of the directed force, and Argyris's load correction method for the vertical component, a load correction matrix $[K^{DFC}]$ was

developed, which, when combined with [Kg], provided a complete set of rigid body modes. This combined matrix performs properly in the diagonalization/partitioning methodology used in dynamic response.

There is the potential for a great deal of future work with the directed force beam element and the technique used in its development. The use of [Kg] + $[K^{DFC}]$ should be compared with the results using Craig-Bampton's substructuring scheme for various beams. In addition, physical testing of a pre-loaded directed force beam with free/free boundary conditions should be undertaken for comparison. The incorporation of these techniques in the development of a directed force correction matrix for pre-loaded membrane elements would be a logical extension.

REFERENCES

[1] Carney, K., Chien, J., Ludwiczak, D., Bosela, P., and Nekoogar, F., Photovoltaic Array Modeling and Normal Modes Analysis,, NASA Lewis Research Center, Structural Systems Dynamics Branch, Space Station Freedom WP04, Response Simulation and Structural Analysis, September, 1989.

[2] Bosela, Paul., "Limitations of Current Nonlinear Finite Element Methods in Dynamic Analysis of Solar Arrays", MSC World Users Conference, Los Angeles, California, March, 1989. (Appendix A)

[3] Przemieniecki, J., Theory of Matrix Structural Analysis, McGraw-Hill Book Company, 1968.

[4] Bellini, P., CVE 511, Matrix Methods Course Notes, 1988. (Appendix B)

[5] Bosela, P., NLFINITE.FOR computer program and output.(Appendix C)

[6] Martin, H., "On the Derivation of Stiffness Matrices for the Analysis of Large Deflection and Stability Problems", AFFDL-TR-66-80.

[7] Clough, R., and Penzien, J., Dynamics of Structures, McGraw Hill Inc., 1975.

[8] Bosela, P., "Development of a 3-node Beam Element with Tension Pre-load", not published. (Appendix D)

[9] Saunders, H., "Stiffness Matrix of a Beam-Column Including Shear Deformation", Shock and Vibration Bulletin, Bulletin 40, Part 4, December, 1969, pages 187-196.

[10] Argyris, J., and Symeonidis, Sp., "Nonlinear Finite Element Analysis of Elastic Systems Under Non-conservative Loading-Natural Formulation. Part 1. Quasistatic Problems", Computer Methods in Applied Mechanics and Engineering 26, 1981, pages 75-123.

[11] Martin, H., "Finite Elements and the Analysis of Geometrically Non-linear Problems", Recent Advances in Matrix Methods of Structural Analysis and Design , Gallagher, Yamada, and Den, 1971.

[12] Marcal, P., "The Effect of Initial Displacements on Problems of Large Deflection and Stability", Brown University, ARPA E54, November, 1967.

[13] Paz, M., and Dung, L., "Power Series Expansion of the General Stiffness Matrix for Beam Elements",

International Journal for Numerical Methods in Engineering, Volume 9, 1975, pages 449-459.

[14] Paz, M., and Dung, L., "Power Series Expansion of the General Stiffness Matrix Including Rotary Inertia and Shear Deformation", Shock and Vibration Bulletin, Bulletin 46, Part 2, August 1976, pages 181-184.

[15] Collar, A., and Simpson, A., Matrices and Engineering Dynamics, Halsted Press, New York, 1987.

[16] Bosela, P., Shaker, F., and Fertis, D., "Dynamic Analysis of Space-related Linear and Non-linear Structures", Southeast Conference of Theoretical and Applied Mechanics XV, Atlanta, Georgia, March, 1990. (Appendix E)

[17] Shaker, F., "Effect of Axial Load on Mode Shapes and Frequencies of Beams". NASA TN D-8109, 1975.

[18] Ghali, A., and Neville, A., Structural Analysis A Unified Classical and Matrix Approach, Third Edition, Chapman and Hall, 1989.

[19] Fertis, Demeter, and Lee, Chin, "Nonlinear Vibration and Instabilities of Elastically Supported Beams with Axial Restraints", submitted for publication in the ASCE Journal of Engineering Mechanics.

[20] Kounadis, A. N., "The Existing of Regions of Divergence Instability for Non-Conservative Systems under Follower Forces", Journal of Solids and Structures, Volume 19, Number 8, pages 725-733, 1983.

[21] James, M. L., Smith, G. M., Wolford, J. C., and Whaley, P. W., Vibration of Mechanical and Structural Systems with Microcomputer Applications, Harper and Row, Publishers, Inc., 1989.

APPENDICES

APPENDIX A

Limitations of Current Nonlinear Finite Element Methods in Dynamic Analysis of Solar Arrays

PAUL A. BOSELA, MS., P.E.
Cleveland State University

Fenn College of Engineering
Engineering Technology Department
Cleveland, Ohio 44115

Presented at the MSC/NASTRAN World User's Conference
Los Angeles, California
March, 1989

This project was funded by a research grant NAG 3-1008
NASA Lewis Research Center
Cleveland, Ohio 44135

ABSTRACT

Deployable solar arrays consist of a "blanket" of solar collectors, and a mast. The blanket is stretched into position when the array is deployed. The stiffness of the array is a function of the rigidity of the mast as well as the tension in the blanket.

Current finite element frequency analysis consists of using MSC Nastran solution 64 (non-linear analysis) to obtain the tangential stiffness matrix of the array. This matrix is then input, using DMAP alters, into MSC/Nastran Solution 63 (dynamic analysis) to obtain the natural frequencies of the array.

The author has found that pseudo-forces are developed, however, at the element level due to limitations inherent in the geometric stiffness matrices currently in accepted use. In particular, the geometric stiffness matrices lack the capability for rigid body rotation, especially when the rotations are large.

The author demonstrates the limitations of the analysis, shows where the errors are introduced in the derivation of the geometric stiffness matrix, and examines various techniques either to eliminate the pseudo-force

generation and/or improve upon the convergence of the current algorithms.

This paper is the product of an NASA/ASEE* Summer Faculty Fellowship and an on-going joint research effort between Cleveland State University and the NASA Lewis Research Center.

* National Aeronautics and Space Administration/American Society of Engineering Educators

SPACE STATION SOLAR ARRAY

NASA's space station is powered utilizing photovoltaic arrays, consisting of a deployable truss "mast" and blanket substrates (Figure 18). The stiffness of the split-blanket array is a function of the rigidity of the mast as well as the tension maintained in the blankets. The "blankets" themself possess negligible stiffness.

The free vibration characteristics of the split-blanket solar arrays was studied using two methods. Mode shapes and frequencies were calculated using equations of continuum mechanics, as well as a finite element solution using MSC Nastran [1] and [2].

The finite element modeling consisted of generating a tangential stiffness matrix by applying the pre-tensioning load in MSC/Nastran geometric non-linear solution (solution 64). The stiffness matrix generated was then input into MSC/Nastran dynamic analysis (solution 63) to obtain the natural frequencies and mode shapes [3].

The finite element analysis indicated that large internal "pseudo-forces" developed when rigid body motion was applied. An investigation was subsequently made to determine whether the large pseudo-forces which developed

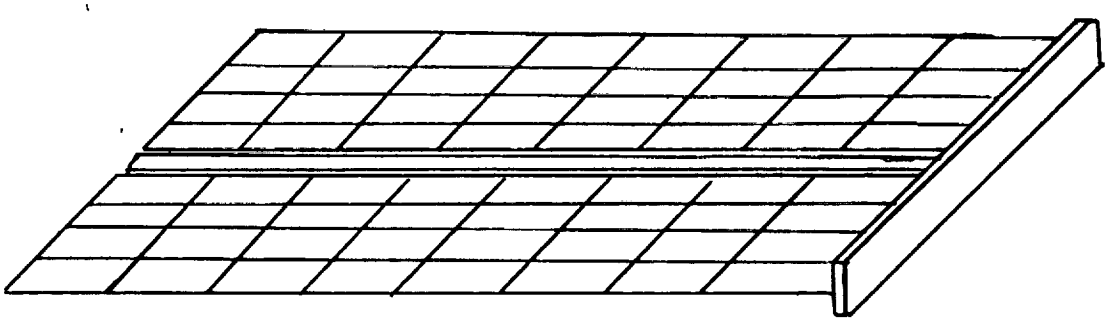

Figure 18 Space Station Split-Blanket Solar Array

were due to user modeling errors or limitations of the finite element process.

The geometric stiffness matrix utilized in MSC/Nastran solution 64 was found to be identical to the stiffness matrix formulated by Martin [4]. For simplicity, a 2-dimensional beam-column element was investigated.

LIMITATIONS OF CURRENT [Kg]

Typically, finite element static analysis is used to solve linear elastic problems of the form

$$[Ke]\{u\} = \{R\} \quad \text{---------- (1)}$$

where [Ke] is the elastic stiffness matrix

{u} is the nodal displacement vector

{R} is the force vector

The [Ke] matrix must possess the capacity for rigid body displacement. In other words, the element must be able to translate or rotate without developing stresses (Figure 19).

The rigid body translation vector is {v, 0, v, 0}. Similarly, the rigid body rotation vector is approximated by {-Lθ/2,θ,Lθ/2,θ}, which can be written as θ{-L/2,1,L/2,1}, where θ is the angle of rotation. Combination yields

a. 2-Node Bernoulli Beam Element with Degrees of Freedom Shown

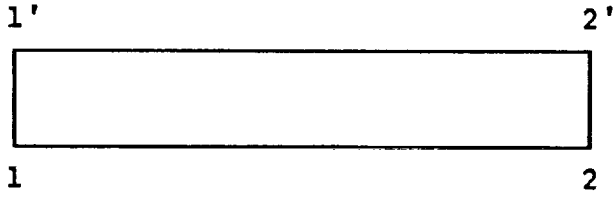

b. Rigid Body Translation in Y-Direction

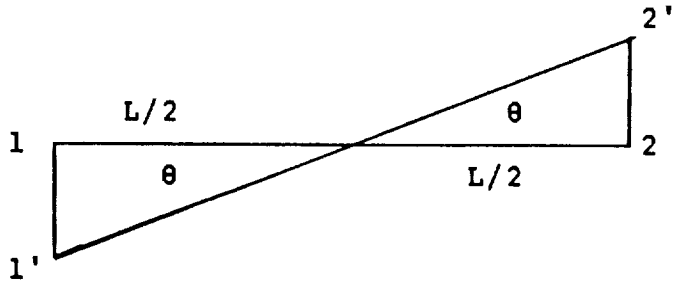

c. Rigid Body Rotation about Z-Axis

Figure 19 Rigid Body Modes

$$\begin{bmatrix} \text{rigid} \\ \text{body} \\ \text{modes} \end{bmatrix} = \begin{bmatrix} v & -L\theta/2 \\ 0 & \theta \\ v & L\theta/2 \\ 0 & \theta \end{bmatrix}$$

The elastic stiffness matrix for a 2-node Bernoulli beam is

$$[Ke] = \frac{EI}{L^3} \begin{bmatrix} 12 & 6L & -12 & 6L \\ 6L & 4L^2 & -6L & 2L^2 \\ -12 & -6L & 12 & -6L \\ 6L & 2L^2 & -6L & 4L^2 \end{bmatrix} \qquad \text{----------(2)}$$

where E = modulus of elasticity

I = moment of inertia

L = length of element

By definition of rigid body motion,

[Ke] {rigid body modes} must equal {0}. ----------(3)

Substituting (1) and (2) into (3) yields

$$[Ke] = \frac{EI}{L^3} \begin{bmatrix} 12 & 6L & -12 & 6L \\ 6L & 4L^2 & -6L & 2L^2 \\ -12 & -6L & 12 & -6L \\ 6L & 2L^2 & -6L & 4L^2 \end{bmatrix} \begin{bmatrix} 1 & -L/2 \\ 0 & 1 \\ 1 & L/2 \\ 0 & 1 \end{bmatrix} = \begin{bmatrix} 0 & 0 \\ 0 & 0 \\ 0 & 0 \\ 0 & 0 \end{bmatrix}$$

Therefore, [Ke] has the capacity for rigid body motion.

NASA LeRC routinely uses a DMAP alter which calculates

[K] {rigid body modes} = {RFORCES (pseudo-forces)}.

For an elastic problem, the presence of large RFORCES would indicate that stresses are being produced during rigid body movement. These pseudo-forces are an indication that "grounding" has occurred, and that the model is not reliable.

Many problems, such as the solar array, are non-linear problems. Finite element solves non-linear problems of the form

$$[[Ke] + [Kg]] \{u\} = \{R\} - \{F\}$$

where [Ke] is the elastic stiffness matrix.

[Kg] is the geometric stiffness matrix.

{R} is the output force vector at the end of a step.

{F} is the input force vector at the beginning of a step.

{u} is the change in the displacement vector during a step.

Graphically, this is shown by Figure 20.

The traditional [Kg] matrix, developed by Martin [4], is

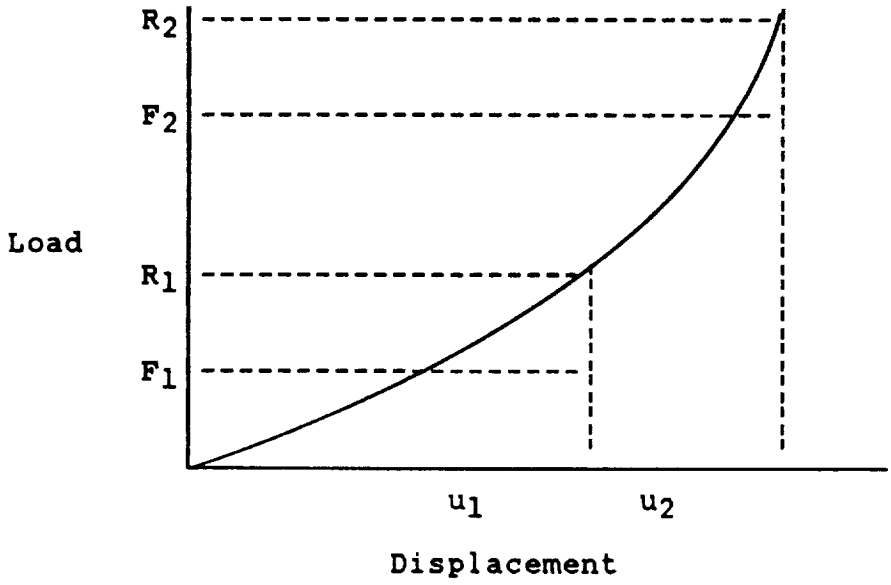

Figure 20 Non-Linear Stiffening Curve

$$[Kg] = P_o \begin{bmatrix} 6/5L & 1/10 & -6/5L & 1/10 \\ 1/10 & 2L/15 & -1/10 & -L/30 \\ -6/5L & -1/10 & 6/5L & -1/10 \\ 1/10 & -L/30 & -1/10 & 2L/15 \end{bmatrix}$$

If I apply rigid body displacement during an incremental load step, I obtain

$$P_o \begin{bmatrix} 6/5L & 1/10 & -6/5L & 1/10 \\ 1/10 & 2L/15 & -1/10 & -L/30 \\ -6/5L & -1/10 & 6/5L & -1/10 \\ 1/10 & -L/30 & -1/10 & 2L/15 \end{bmatrix} \begin{bmatrix} 1 & -L\theta/2 \\ 0 & \theta \\ 1 & L\theta/2 \\ 0 & \theta \end{bmatrix} = \begin{bmatrix} 0 & -P_o\theta \\ 0 & 0 \\ 0 & P_o\theta \\ 0 & 0 \end{bmatrix}$$

It can be seen that [Kg] possesses the capacity for rigid body translation, but not rigid body rotation. Thus, Martin's [Kg] is not exact. It can also be shown that MSC/Nastran non-linear analysis (based on Martin's development) similarly does not have an exact geometric stiffness matrix and will produce pseudo-forces. Therefore, the RFORCE check DMAP alter for MSC/Nastran solution 64 (non-linear) analysis) is not sufficient criteria for determining the validity of a model.

In spite of its deficiencies, Martin's [Kg] provides acceptable results for solving statics problems due to the iteration process. (Although [Kg] is not exact, the process converges to the exact solution.)

In dynamic analysis, however, finite element is used to solve equations of the form

$$[M]\{\ddot{u}\} + [K]\{u\} = \{R\}$$

where [M] is the mass matrix.

{u} is the displacement (mode shape) vector.

$\{\ddot{u}\}$ is the second derivative with respect to time of the displacement vector.

[K] is the stiffness matrix (Ke or Ke + Kg, when applicable).

{R} is the excitation forces

There is no apparent guarantee that the natural frequencies of vibration from (4) are accurate, when [Kg] is known to be inexact.

LARGE ROTATION EFFECTS

The rigid body rotation vector previously used is $C\{-L\theta/2, \theta, L\theta/2, \theta\}$. Figure 21 illustrates rigid body rotation of a beam with an axial load [5]. If we let the angle of rotation equal 2β, then $\hat{u} = \beta\{-L, 2, L, 2\}^T$.

Consider the work/energy relationship of Figure 21

$$\text{work done by } P_o = P_oL(1-\cos 2\beta)$$

$$= 2P_oL(1-\cos 2\beta)/2$$

But, $(1-\cos 2\beta)/2 = \sin^2 \beta \approx \beta^2 + \phi(\beta^4) + \cdots$.

Therefore, the work done $= 2P_o\beta^2 + \phi(\beta^4) = -V = \hat{u}^T K \hat{u}/2$, where -V is the loss of potential energy.

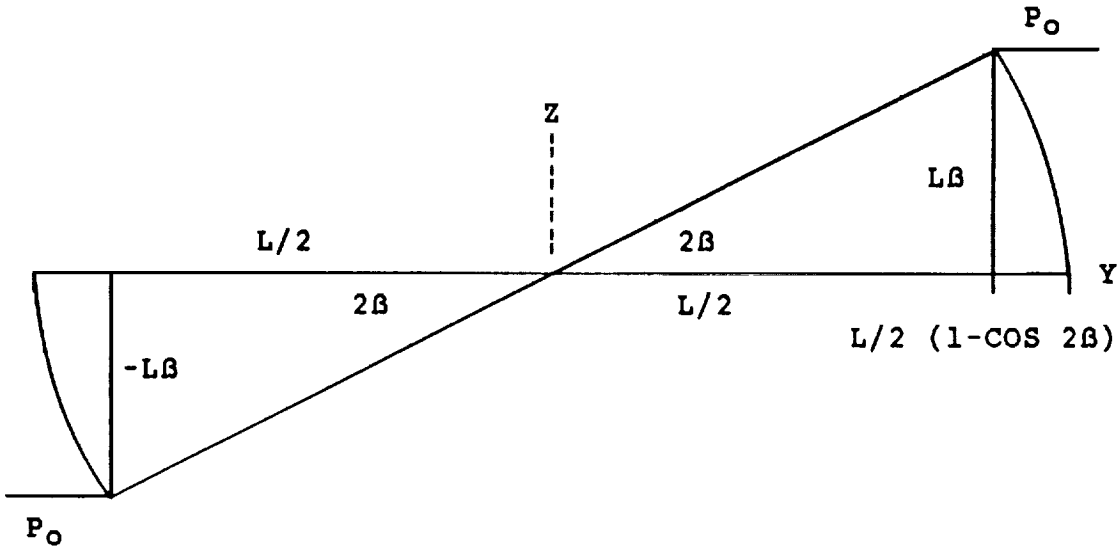

Figure 21 Rigid Body Rotation Angle of 2ß

Similarly

$$\hat{u}^T K \hat{u}/2 = P_o\beta^2/2[-2\ 0\ 2\ 0]\begin{bmatrix} -L \\ 2 \\ L \\ 2 \end{bmatrix} \frac{P_o\beta^2\ (4L)}{2} = 2P_oL\beta^2$$

Therefore, Martin's [Kg] provides a correct energy relationship for the representation shown.

It should be noted, however, that the displacement in the Y direction (axial direction in the original geometry) has been neglected when we let

$$u = \begin{bmatrix} -L \\ 2 \\ L \\ 2 \end{bmatrix} \quad , \text{ which is really } \quad \begin{bmatrix} 0 \\ -L \\ 2 \\ 0 \\ L \\ 2 \end{bmatrix} \qquad \text{----------(5)}$$

The zero terms in (5) negate any contribution to the equation from axial terms in the stiffness matrix. (If there were any axial terms.) Since significant axial loading occurs in the solar array (as well as other beam/column problems), and these axial loads significantly affect the stiffness, it intuitively seems unreasonable to

loading occurs in the solar array (as well as other beam/column problems), and these axial loads significantly affect the stiffness, it intuitively seems unreasonable to arbitrarily neglect the contribution of axial stiffness terms and axial displacements.

The exact rigid body rotation vector is

$$u_{exact} = \begin{bmatrix} L/2\ (1-\cos 2\beta) \\ -L/2\ \sin 2\beta \\ 2\beta \\ -L/2\ (1-\cos 2\beta) \\ L/2\ \sin 2\beta \\ 2\beta \end{bmatrix} \qquad \text{----------(6)}$$

Series expansion, and truncation of higher order terms yields

$$\hat{u} = \begin{bmatrix} L\beta^2 \\ -L\beta \\ 2\beta \\ -L\beta^2 \\ L\beta \\ 2\beta \end{bmatrix} \qquad \text{----------(7)}$$

$$P_o \begin{bmatrix} 0 & 0 & 0 & 0 & 0 & 0 \\ 0 & 6/5L & 1/10 & 0 & -6/5L & 1/10 \\ 0 & 1/10 & 2L/15 & 0 & -1/10 & -L/30 \\ 0 & 0 & 0 & 0 & 0 & 0 \\ 0 & -6/5L & -1/10 & 0 & 6/5L & -1/10 \\ 0 & 1/10 & -L/30 & 0 & -1/10 & 2L/15 \end{bmatrix} \begin{bmatrix} L\beta^2 \\ -P_o \\ 2\beta \\ -L\beta^2 \\ \beta L \\ 2\beta \end{bmatrix} = \begin{bmatrix} 0 \\ -P_o(2\beta) \\ 0 \\ 0 \\ P_o(2\beta) \\ 0 \end{bmatrix} \quad (8)$$

and

$$\frac{EI}{L^3} \begin{bmatrix} AL^2/I & 0 & 0 & -AL^2/I & 0 & 0 \\ 0 & 12 & 6L & 0 & -12 & 6L \\ 0 & 6L & 4L^2 & 0 & -6L & 2L^2 \\ -AL^2/I & 0 & 0 & AL^2/I & 0 & 0 \\ 0 & -12 & -6L & 0 & 12 & -6L \\ 0 & 6L & 2L^2 & 0 & -6L & 4L^2 \end{bmatrix} \begin{bmatrix} L\beta^2 \\ -L\beta \\ 2\beta \\ -L\beta^2 \\ L\beta \\ 2\beta \end{bmatrix} = \begin{bmatrix} 2AE\beta^2 \\ 0 \\ 0 \\ -2AE\beta^2 \\ 0 \\ 0 \end{bmatrix} \quad (9)$$

From (8) and (9), when the more exact rigid body rotation vector is used, neither [Ke] nor [Kg] possesses rigid body rotation capabilities, although from (8), $2AE\beta^2$ approaches 0 as half the angle of rotation gets very small. A similar procedure shows that both possess rigid body translation capability in two directions.

DEVELOPMENT OF MODIFIED [Kg]

Using rigid body translation relationships, and the expanded rigid body rotation vector, I can solve for additional terms in the [Kg] matrix which enforces the rigid body capabilities.

Using rigid body translation constraints, [Kg] has the form

$$[Kg]=P_o\begin{bmatrix} A & B & C & -A & -B & C \\ B & 6/5L & 1/10 & -B & -6/5L & 1/10 \\ C & 1/10 & 2L/15 & -C & -1/10 & -L/30 \\ -A & -B & -C & A & B & -C \\ -B & -6/5L & -1/10 & B & 6/5L & -1/10 \\ C & 1/10 & -L/30 & -C & -1/10 & 2L/15 \end{bmatrix} \text{----------(10)}$$

Multiplying (10) by (7) and setting the product equal to the zero vector yields

$$P_o\begin{bmatrix} A & B & C & -A & -B & C \\ B & 6/5L & 1/10 & -B & -6/5L & 1/10 \\ C & 1/10 & 2L/15 & -C & -1/10 & -L/30 \\ -A & -B & -C & A & B & -C \\ -B & -6/5L & -1/10 & B & 6/5L & -1/10 \\ C & 1/10 & -L/30 & -C & -1/10 & 2L/15 \end{bmatrix}\begin{bmatrix} L\beta^2 \\ -P_o \\ 2\beta \\ -L\beta^2 \\ \beta L \\ 2\beta \end{bmatrix}=\begin{bmatrix} 0 \\ 0 \\ 0 \\ 0 \\ 0 \\ 0 \end{bmatrix} \text{-----(11)}$$

Expanding row 3 yields

$$P_o\,[2CL\beta^2 - \beta L/5 + 4\beta L/15 - 2\beta L/30] = 0$$

$$P_o 2CL\beta^2 = 0$$

$$C = 0 \quad \text{------(12)}$$

Expanding row 2 yields

$$P_o\,[2BL\beta^2 - 12\beta L/5 + 4\beta/10] = 0$$

$$2BL\beta - 2 = 0$$

$$B = 1/L\beta \quad \text{----------(13)}$$

Expanding row 1 yields

$$P_o\,[2AL\beta^2 - 2] = 0$$

$$AL\beta^2 - 1 = 0$$

$$A = 1/L\beta^2 \quad \text{----------(14)}$$

Thus, substituting (12), (13), and (14) into (10) yields

$$[\underline{Kg}]=P_o\begin{bmatrix} 1/L\beta^2 & 1/L\beta & 0 & -1/L\beta^2 & -1/L\beta & 0 \\ 1/L\beta & 6/5L & 1/10 & -1/L\beta & -6/5L & 1/10 \\ 0 & 1/10 & 2L/15 & 0 & -1/10 & -L/30 \\ -1/L\beta^2 & -1/L\beta & 0 & 1/L\beta^2 & 1/L\beta & 0 \\ -1/L\beta & -6/5L & -1/10 & 1/L\beta & 6/5L & -1/10 \\ 0 & 1/10 & -L/30 & 0 & -1/10 & 2L/15 \end{bmatrix} \quad \text{----(15)}$$

The strain energy U should equal zero. It can be calculated from the equation

$$P_o\beta^2/2\ [L\beta,-L,2,-L\beta,L,2]\ [\underline{Kg}]\begin{bmatrix} L\beta \\ -L \\ 2 \\ -L\beta \\ L \\ 0 \\ 2 \end{bmatrix} \qquad \text{----------(16)}$$

Performing the matrix multiplication in (16) yields $[0,\ 0,\ 0,\ 0,\ 0,\ 0]^T$. Therefore, no strain energy occurs during rigid body rotation using $[\underline{Kg}]$.

INABILITY TO APPLY MODIFICATION PROCEDURES TO [Ke]

$[\underline{Ke}]$ has the form

$$[\underline{kE}]=\frac{EI}{L^3}\begin{bmatrix} AL^2/I & K_{12} & K_{13} & -AL^2/I & -K_{12} & K_{16} \\ K_{12} & 12 & 6L & -K_{12} & -12 & 6L \\ K_{13} & 6L & 4L^2 & -K_{13} & -6L & 2L^2 \\ -AL^2/I & -K_{12} & -K_{13} & AL^2/I & K_{12} & -K_{16} \\ -K_{12} & -12 & -6L & K_{12} & 12 & -6L \\ K_{16} & 6L & 2L^2 & -K_{16} & -6L & 4L^2 \end{bmatrix} \qquad \text{----------(17)}$$

Multiplying (17) by (7) and setting the product equal to the zero vector yields

$$\frac{EI}{L^3}\begin{bmatrix} AL^2/I & K_{12} & K_{13} & -AL^2/I & -K_{12} & K_{16} \\ K_{12} & 12 & 6L & -K_{12} & -12 & 6L \\ K_{13} & 6L & 4L^2 & -K_{13} & -6L & 2L^2 \\ -AL^2/I & -K_{12} & -K_{13} & AL^2/I & K_{12} & -K_{16} \\ -K_{12} & -12 & -6L & K_{12} & 12 & -6L \\ K_{16} & 6L & 2L^2 & -K_{16} & -6L & 4L^2 \end{bmatrix} = \begin{bmatrix} 0 \\ 0 \\ 0 \\ 0 \\ 0 \\ 0 \end{bmatrix} \quad \text{------(18)}$$

Expanding row 2 yields

$$2K_{12}L\beta^2 - 24L\beta + 24L\beta = 0$$

$$2K_{12}L\beta^2 = 0 \quad \text{----------(19)}$$

Therefore, K_{12} must equal 0.

Expanding row 3 yields

$$-2K_{13}L\beta^2 - 12L^2\beta + 8L^2\beta + 4L^2\beta = 0$$

$$-2K_{13}L\beta^2 = 0 \quad \text{----------(20)}$$

Therefore, K_{13} must equal zero.

If K_{12} and K_{13} equal zero, no additional coefficients appear in line 1 of the [Ke] matrix. Suppose I add a correction term to K_{11}.

$$(AL^2/I+C)L\beta^2-(AL^2/I+C)(-L\beta^2) = 2(AL^2/I+C)(L\beta^2) \quad \text{--------(21)}$$

From (21) it can be seen that adding a correction term to K_{11} will not eliminate the error.

Thus, [Ke] can not be modified to obtain rigid body rotation capabilities for large rotations utilizing the procedure used to modify [Kg]. The only possibility for improving [Ke] must include corrections to existing terms.

VERIFICATION OF MODIFIED [Kg]

Several tests of the modified stiffness matrix were undertaken. Summary of the tests follow.

a. RFORCE Check

One and two element beam stiffness matrices were multiplied with the expanded rigid body matrix. In all cases, no pseudo-forces were produced from rigid body translation. The expanded rigid body rotation vector yielded the following pseudo-forces.

Matrix		Pseudo-forces
[Ke]	one element	$[2A\beta^2E,0,0,-2A\beta^2E,0,0]$
	two elements	$[2A\beta^2E,0,0,0,0,0,0,-2A\beta^2E,0,0]$
[Kg]	one element	$[0,-2\beta P_o,0,0,2\beta P_o,0]$
	two elements	$[0,-2\beta P_o,0,0,0,0,0,2\beta P_o,0]$
[$\underline{Kg}$]	one element	[0,0,0,0,0,0]
[$\underline{Kg}$]	two elements	[0,0,0,0,0,0,0,0,0]
[Ke+Kg]	one element	$[2A\beta^2E,-2\beta P_0,0,-2A\beta^2E,2\beta P_o,0]$
[Ke+Kg]	two elements	$[2A\beta^2E,-2\beta P_0,0,0,0,0,-2A\beta^2E,2\beta P_o,0]$
[Ke+$\underline{Kg}$]	one element	$[2A\beta^2E,0,0,-2A\beta^2E,0,0]$
[Ke+$\underline{Kg}$]	two elements	$[2A\beta^2E,0,0,0,0,0,-2A\beta^2E,0,0]$

Based on the above, the modified [$\underline{Kg}$] matrix eliminates the β error terms generated using [Kg] standard. The β^2 terms generated from [Ke] remain. Thus, when β (half

the angle of rotation) is less than one radian, the total error is reduced. The error is associated with a pseudo-axial force only.

b. Eigenvalues

Using [Ke] and [Kg] standard, it was found that only two zero eigenvalues exist. [Kg] has three zero eigenvalues, plus one eigenvalues which is very close to zero. The eigenvalues are close to zero even when only one or two elements are used.

c. Stability Analysis

[Kg] was used in the solution of a simply supported beam subjected to an axial load. The critical buckling load was calculated, and compared with the traditional solution using Martin's [Kg], as well as the exact solution.

When the boundary condition, β_1 equals $-\beta_2$ (as occurs during buckling) was applied, the solution using [Kg] was identical with the solution using Martin's [Kg].

CONCLUSIONS

Continuing effort is being made on improving the capabilities of the element stiffness matrices used in the solar array dynamic analysis. The modified [Kg] developed reduces the pseudo-forces produced in the beam-column stiffening problem, provided that the angle of

rotation is less than two radians. Modifications must be developed, however, to eliminate the pseudo-force contributions from [Ke] which result from utilizing the expanded rigid body rotation vector. This would permit the tangential stiffness matrix [K_T] to possess the three zero eigenvalues associated with rigid body movement of any magnitude.

It was disappointing that the [Kg] developed did not approve upon the relatively slow convergence rate of the stability problem. Further investigation is needed to determine whether a modified [Ke] + [Kg] would improve upon this convergence rate.

Extension of the modifications to the stiffness matrices of other elements, particularly plate elements, will also be developed.

Finally, testing of the performance of the modified matrices in the actual solar array model, and comparison with the continuum mechanics approach, will be performed.

REFERENCES

1 Shaker, Frank, and Carney, Kelly,: Free-vibration Characteristics and Correlation of a Space Station Split-Blanket Solar Array.

2 Shaker, F.J.: Free-Vibration Characteristics of a Large Split-Blanket Solar Array in a 1 G Field, NASA TN D-8376, 1976

3 Joseph, J.A. Ed.: MSC/Nastran Applications Manual, the MacNeal-Schwendler Corp., 1984

4 Martin, H.C.: On the Derivation of Stiffness Matrices for the Analysis of Large Deflection and Stability Problems, AFFDL-TR-66-80

APPENDIX B

Matrix Methods (Dr. Bellini, Cleveland State University)

Finite Element Approach

$$\pi = U - V$$

$$U = \int_0^L \left[\frac{EA}{2} \left[\frac{du_o}{dx} + \frac{1}{2} \left[\frac{dW}{dx} \right]^2 \right]^2 + \frac{EI}{2} \left[\frac{d^2W}{dx^2} \right]^2 \right] dx$$

$$U = \int_0^L \left[\frac{EA}{2} \left[\underset{\{1\}}{\left[\frac{du_o}{dx} \right]^2} + \underset{\{2\}}{\frac{du_o}{dx} \left[\frac{dW}{dx} \right]^2} \underset{\{3\}}{\frac{1}{4} \left[\frac{dW}{dx} \right]^4} \right]^2 + \frac{EI}{2} \left[\frac{d^2W}{dx^2} \right]^2 \right] dx$$

Assumption: $$u_o(x) = \begin{bmatrix} H_1 & H_4 \end{bmatrix} \begin{bmatrix} u_1 \\ u_4 \end{bmatrix}$$

$$W(x) = \begin{bmatrix} H_2 & H_3 & H_5 & H_6 \end{bmatrix} \begin{bmatrix} u_2 \\ u_3 \\ u_5 \\ u_6 \end{bmatrix}$$

Which are the shape functions for the static beam.

Therefore, [Kg] is only approximate.

$$H_1 = 1 - x/L \qquad H_4 = x/L$$

$$H_2 = (1-3(x/L)^2 + 2(x/L)^3) \qquad H_5 = (3(x/L)^2 - 2(x/L)^3)$$

$$H_3 = (x - 2x^2/L + x^3/L^2) \qquad H_6 = (-x^2/L + x^3/L^2)$$

Shape functions for the static beam (Figure 22).

$$u = H_1 u_1 + H_4 u_4$$

$$\frac{du}{dx} = H_1' u_1 + H_4' u_4$$

$$W = H_2 u_2 + H_3 u_3 + H_5 u_5 + H_6 u_6$$

$$\frac{dW}{dx} = H_2'u_2 + H_3'u_3 + H_5'u_5 + H_6'u_6$$

$$\frac{d^2W}{dx^2} = H_2"u_2 + H_3"u_3 + H_5"u_5 + H_6"u_6$$

Term {1}

$$\int_0^L \left[\frac{EA}{2} \left[\left[\frac{du_o}{dx} \right]^2 = \int_0^L \frac{EA}{2} \left[\frac{du_o}{dx} \right]^T \left[\frac{du_o}{dx} \right] dx \right.$$

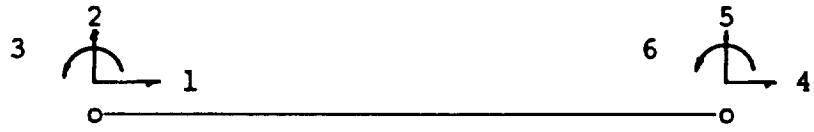

Figure 22 2-Node Element Degrees of Freedom

$$= \frac{1}{2}\begin{bmatrix} u_1 & u_4 \end{bmatrix}^T \int_0^L EA \begin{bmatrix} -\frac{1}{L} \\ \frac{1}{L} \end{bmatrix} \begin{bmatrix} -\frac{1}{L} & \frac{1}{L} \end{bmatrix} dx \begin{bmatrix} u_1 \\ u_4 \end{bmatrix}$$

For constant EA

$$= \frac{1}{2}\begin{bmatrix} u_1 & u_4 \end{bmatrix}^T \frac{EA}{L} \begin{bmatrix} 1 & -1 \\ -1 & 1 \end{bmatrix} \begin{bmatrix} u_1 \\ u_4 \end{bmatrix}$$

For <u>term {3}</u>

$$U = \int_0^L \frac{EI}{2} \left[\frac{d^2W}{dx^2} \right]^2 dx = \int_0^L \frac{EI}{2} \left[\frac{d^2W}{dx^2} \right]^T \left[\frac{d^2W}{dx^2} \right] dx$$

$$= \frac{1}{2}\begin{bmatrix} u_2 & u_3 & u_5 & u_6 \end{bmatrix} \int_0^L EI \begin{bmatrix} H_2'' \\ H_3'' \\ H_5'' \\ H_6'' \end{bmatrix} \begin{bmatrix} H_2'' & H_3'' & H_5'' & H_6'' \end{bmatrix} dx \begin{bmatrix} u_2 \\ u_3 \\ u_5 \\ u_6 \end{bmatrix}$$

$H_2'' = -6/L^2 + 12x/L^3$

$H_3'' = -4/L + 6x/L^2$

$H_5'' = 6/L^2 - 12x/L^3$

$$H_6'' = -2/L + 6x/L^2$$

For EI = constant

$$\frac{1}{2}\begin{bmatrix} u_2 & u_3 & u_5 & u_6 \end{bmatrix}\frac{EI}{L^3}\begin{bmatrix} 12 & 6L & -12 & 6L \\ 6L & 4L^2 & -6L & 2L^2 \\ -12 & -6L & 12 & -6L \\ 6L & 2L^2 & -6L & 4L^2 \end{bmatrix}\begin{bmatrix} u_2 \\ u_3 \\ u_5 \\ u_6 \end{bmatrix}$$

For <u>term {2}</u>

$$\int_0^L \frac{EA}{2}\left[\frac{du_o}{dx}\right]\left[\frac{dW}{dx}\right]^2 dx = \int_0^L \frac{EA}{2}\frac{du_0}{dx}\left[\frac{dW}{dx}\right]^T \frac{dW}{dx}\, dx$$

$$= \frac{1}{2}\begin{bmatrix} u_2 & u_3 & u_5 & u_6 \end{bmatrix}\int_0^L EA\frac{du_0}{dx}\begin{bmatrix} H_2' \\ H_3' \\ H_5' \\ H_6' \end{bmatrix}\begin{bmatrix} H_2' & H_3' & H_5' & H_6' \end{bmatrix} dx \begin{bmatrix} u_2 \\ u_3 \\ u_5 \\ u_6 \end{bmatrix}$$

$$H_2' = -6x/L^2 + 6x^2/L^3$$

$$H_3' = 1 - 4(x/L) + 3(x/L)^2$$

$$H_5' = 6x/L^2 - 6x^2/L^3$$

$$H_6' = -2(x/L) + 3(x/L)^2$$

Setting $EA \frac{du_0}{dx} = P$ Axial force in member, and assuming

P = constant + tension

- compression

$$\frac{1}{2}\begin{bmatrix} u_2 & u_3 & u_5 & u_6 \end{bmatrix} \frac{P}{30L}\begin{bmatrix} 36 & 3L & -36 & 3L \\ 3L & 4L^2 & -3L & -L^2 \\ -36 & -3L & 36 & -3L \\ 3L & -L^2 & -3L & 4L^2 \end{bmatrix} \begin{bmatrix} u_2 \\ u_3 \\ u_5 \\ u_6 \end{bmatrix}$$

[Kg]

APPENDIX C

NLFINITE.FOR Computer Program and Output

```
C  NLFINITE.FOR   (GEOMETRIC NONLINEAR PROBS)
C  REVISED 10-24-90 (IF STATEMENT IN JCBI REVISED
C  MODIFICATION OF PROGRAM FINITEL.FOR VIBRATION
C  ANALYSIS OF BEAMS, RODS, AND PLANE FRAMES USING BEAM
C  ELEMENTS WITH AN AXIAL PRETENSION LOAD. SUBROUTINES
C  JCBI, DECOMP, MATINV, MATMPY, AND SEARCH.
C  DEVICE * IN READ AND WRITE STATEMENTS IS THE CONSOLE.
C  DEVICE 2 IN WRITE STATEMENTS IS THE PRINTER.
C  * IN THE PLACE OF A FORMAT STATEMENT NUMBER MEANS FREE FORMAT.
      IMPLICIT REAL*8 (A-H,O-Z)
      REAL*8 L,IA,KEL,MEL,KEG,MEG
      INTEGER SUB,ROWSUB,COLSUB,B,Z,EN,CFIX
      DIMENSION KEL(6,6,8),MEL(6,6,8),KEG(6,6,8),MEG(6,6,8),
     $RT(6,6),
     $R(6,6),TK(6,6),TM(6,6),SK(27,27),SM(27,27),RSK(27,27),
     $RSM(27,27),E(8),A(8),X(9),Y(9),GAMMA(8),IA(8)
      DIMENSION JNM(8,2),CFIX(27),SUB(6)
      OPEN(UNIT=2,FILE='PRN')
C  READ IN PROBLEM DATA AS INDICATED BY MESSAGES ON CONSOLE.  DATA
C  READ IN IS PRINTED OUT.  (PROGRAM STATEMENTS 2 THROUGH 40)
      WRITE(2,1)
    1 FORMAT('NLFINITE.FOR; FULL KE+KG MATRICES,REVISED 10-24-90')
      WRITE(*,2)
    2 FORMAT(/,' ENTER THE NUMBER OF BEAM ELEMENTS (I1)',/)
      READ(*,3)NUMEL
    3 FORMAT(I1)
      DO 4 I=1,NUMEL
      WRITE(*,5)I
    4 READ(*,6)A(I)
    5 FORMAT(/,' ENTER A(',I1,') (F20.0)',/)
    6 FORMAT(F20.0)
      WRITE(2,7)
    7 FORMAT(6X,'THE AREA ARRAY A IS:',/)
      DO 8 I=1,NUMEL
    8 WRITE(2,9)I,A(I)
    9 FORMAT(6X,'A(',I1,') = ',E14.7)
      DO 10 I=1,NUMEL
      WRITE(*,11)I
   10 READ(*,12)E(I)
   11 FORMAT(/,' ENTER E(',I1,') (F20.0)',/)
   12 FORMAT(F20.0)
      WRITE(2,13)
   13 FORMAT(/6X,'THE ELASTICITY ARRAY E IS;',/)
      DO 14 I=1,NUMEL
   14 WRITE(2,15)I,E(I)
   15 FORMAT(6X,'E(',I1,') = ',E14.7)
      DO 16 I=1,NUMEL
      WRITE(*,17)I
```

```
16 READ(*,18)IA(I)
17 FORMAT(/,'ENTER IA(',I1,') (F20.0)',/)
18 FORMAT(F20.0)
   WRITE(2,19)
19 FORMAT(/,6X,'THE MOMENT OF INERTIA ARRAY IA IS;',/)
   DO 20 I=1,NUMEL
20 WRITE(2,21)I,IA(I)
21 FORMAT(6X,'IA(',I1,') = ',E14.7)
   DO 82 I=1,NUMEL
   WRITE(*,83)I
82 READ(*,84)GAMMA(I)
83 FORMAT(/,' ENTER GAMMA(',I1,')  (F20.0)',/)
84 FORMAT(F20.0)
   WRITE(2,85)
85 FORMAT(/,6X, 'THE GAMMA ARRAY IS;',/)
   DO 86 I=1,NUMEL
86 WRITE(2,87)I,GAMMA(I)
87 FORMAT(6X,'GAMMA(',I1,') = ',E14.7)
   WRITE(*,88)
88 FORMAT(' ','ENTER THE AXIAL TENSION PRELOAD (PLOAD)',/)
   READ(*,89)PLOAD
89 FORMAT(F20.0)
   WRITE(2,90)
90 FORMAT(/,6X,'THE AXIAL PRETENSION LOAD IS;',/)
   WRITE(2,91)PLOAD
91 FORMAT(F20.0)
   WRITE(*,22)
22 FORMAT(/,'ENTER THE NUMBER OF JOINTS, NJTS (I1)',/)
   READ(*,23)NJTS
23 FORMAT(I1)
   DO 24 I=1,NUMEL
   DO 24 J=1,2
   WRITE(*,25)I,J
24 READ(*,26)JNM(I,J)
25 FORMAT(/,' ENTER JNM(',I1,',',I1,')  (I1)',/)
26 FORMAT(I1)
   WRITE(2,27)
27 FORMAT(/,6X,'THE JOINT-NUMBER MATRIX IS;',/)
   DO 28, I=1,NUMEL
28 WRITE(2,29)JNM(I,1),JNM(I,2)
29 FORMAT(10X,I5,I4)
   DO 30 I=1,NJTS
   WRITE(*,31)I,I
30 READ(*,*)X(I),Y(I)
31 FORMAT(/' ENTER JOINT COORD. X(',I1,'),Y(',I1,')(2F20.0)',/)
   WRITE(2,33)
33 FORMAT(/,6X,'THE JOINT COORDINATES ARE;',/)
   DO 34 I=1,NJTS
34 WRITE(2,35)I,X(I),I,Y(I)
35 FORMAT(6X,'X(',I1,')=',E14.7,5X,'Y(',I1,')=',E14.7)
   WRITE(*,36)
36 FORMAT(/,' ENTER THE NUMBER OF FIXED COORDINATES(12)',/)
   READ(*,37)NB
37 FORMAT(I2)
   IF(NB.EQ.0)GO TO 94
   DO 38 I=1,NB
   WRITE(*,39)I
```

```
      38 READ(*,40)CFIX(I)
      39 FORMAT(/,' ENTER CFIX(',I2,') (I2)',/)
      40 FORMAT(I2)
         WRITE(2,41)
      41 FORMAT(/,6X,'ARRAY CFIX IS;',/)
         DO 42 I=1,NB
      42 WRITE(2,43)I,CFIX(I)
      43 FORMAT(6X,'CFIX(',I2,')=',I2)
C     GENERATE NULL 3-DIMENSIONAL ARRAYS KEL AND MEL.  PLANES OF KEL
C     AND MEL WILL LATER CONTAIN THE LOCAL ELEMENT STIFFNESS AND MASS
C     MATRICES, RESPECTIVELY.
      94 DO 44 I=1,6
         DO 44 J=1,6
         DO 44 M=1,NUMEL
         KEL(I,J,M)=0.
      44 MEL(I,J,M)=0.
C     GENERATE NULL MATRICES  R  AND  RT  WHICH WILL LATER BECOME THE
C     TRANSFORMATION MATRIX AND ITS TRANSPOSE, RESPECTIVELY.
         DO 45 I=1,6
         DO 45 J=1,6
         R(I,J)=0.0
      45 RT(I,J)=0.0
C     GENERATE THE LOCAL ELEMENT STIFFNESS MATRICES AND STORE IN THE 3
C     3-DIMENSIONAL STIFFNESS ARRAY KEL (SEE FIG. 8-11 FOR THE
C     EQUATION USED).  EACH PLANE IN THE 3-DIM. ARRAY IS ONE ELEMENT
C     STIFFNESS MATRIX.
         DO 100 EN=1,NUMEL
      IC=JNM(EN,1)
      ID=JNM(EN,2)
      L=DSQRT((X(ID)-X(IC))**2+(Y(ID)-Y(IC))**2)
      QUOT=IA(EN)/A(EN)
      R1=DSQRT(QUOT)
      F=E(EN)*IA(EN)/L
      P=F/R1**2
      Q=4.*P*R1**2
      S=3.*Q/(2.*L)
      T=S*2./L
      SINA=(Y(ID)-Y(IC))/L
      COSA=(X(ID)-X(IC))/L
      KEL(1,1,EN)=P
      KEL(1,4,EN)=-P
      KEL(2,2,EN)=T+(6.*PLOAD/(5.*L))
      KEL(2,3,EN)=S+.1*PLOAD
      KEL(2,5,EN)=-T-(6.*PLOAD/(5.*L))
      KEL(2,6,EN)=S+.1*PLOAD
      KEL(3,3,EN)=Q+(2.*PLOAD*L/15.)
      KEL(3,5,EN)=-S-.1*PLOAD
      KEL(3,6,EN)=Q/2.-(PLOAD*L/30.)
      KEL(4,4,EN)=P
      KEL(5,5,EN)=T+(6.*PLOAD/(5.*L))
      KEL(5,6,EN)=-S-.1*PLOAD
      KEL(6,6,EN)=Q+(2.*PLOAD*L/15.)
      DO 46 I=2,6
      IM1=I-1
      DO 46 J=1,IM1
   46 KEL(I,J,EN)=KEL(J,I,EN),
  GENERATE THE LOCAL ELEMENT MASS MATRICES AND STORE THEM IN THE
```

```
C  3-DIMENSIONAL MASS ARRAY MEL (SEE FIG. 8-11 FOR THE EQUATION
C  USED).  EACH PLANE OF THE 3-DIM. ARRAY MEL CONTAINS ONE LOCAL
C  ELEMENT MASS MATRIX.
      F=GAMMA(EN)*L/420.
      P=70.*F
      P2=2.*P
      Q=156.*F
      S=22.*L*F
      T=54.*F
      U=4.*L*L*F
      V=13.*L*F
      W=3.*L*L*F
      MEL(1,1,EN)=P2
      MEL(1,4,EN)=P
      MEL(2,2,EN)=Q
      MEL(2,3,EN)=S
      MEL(2,5,EN)=T
      MEL(2,6,EN)=-V
      MEL(3,3,EN)=U
      MEL(3,5,EN)=V
      MEL(3,6,EN)=-W
      MEL(4,4,EN)=P2
      MEL(5,5,EN)=Q
      MEL(5,6,EN)=-S
      MEL(6,6,EN)=U
      DO 47 I=2,6
      IM1=I-1
      DO 47 J=1,IM1
   47 MEL(I,J,EN)=MEL(J,I,EN)
C  GENERATE THE TRANSFORMATION MATRIX  R  AND ITS TRANSPOSE RT.
      R(1,1)=COSA
      R(1,2)=SINA
      R(2,1)=-SINA
      R(2,2)=COSA
      R(3,3)=1.
      R(4.4)=COSA
      R(4,5)=SINA
      R(5,4)=-SINA
      R(5,5)=COSA
      R(6,6)=1.
      DO 48 I=1,3
      DO 48 J=1,3
      RT(I,J)=R(J,I)
   48 RT(I+3,J+3)=R(J+3,I+3)
C  DETERMINE THE ELEMENT STIFFNESS MATRICES IN THE GLOBAL
C  COORDINATE SYSTEM (EQ. 8-93B) AND STORE THEM IN THE 3-DIM.
C  STIFFNESS ARRAY KEG.  EACH PLANE OF THE 3-DIM. ARRAY CONTAINS
C  ONE GLOBAL ELEMENT STIFFNESS MATRIX.
      DO 95 I=1,6
      DO 95 J=1,6
      TK(I,J)=0.0
      DO 95 K=1,6
   95 TK(I,J)=TK(I,J)+KEL(I,K,EN)*R(K,J)
      DO 96 I=1,6
      DO 96 J=1,6
      KEG(I,J,EN)=0.0
      DO 96 K=1,6
```

```
   96 KEG(I,J,EN)=KEG(I,J,EN)+RT(I,K)*TK(K,J)
C  DETERMINE THE ELEMENT MASS MATRICES IN THE GLOBAL SYSTEM (EQ.
C  8-93A) AND STORE THEM IN THE 3-DIM. MASS ARRAY MEG.  EACH PLANE
C  OF THE 3-DIM. ARRAY CONTAINS ONE GLOBAL ELEMENT MASS MATRIX.
      DO 97 I=1,6
      DO 97 J=1,6
      TM(I,J)=0.0
      DO 97 K=1,6
   97 TM(I,J)=TM(I,J)+MEL(I,K,EN)*R(K,J)
      DO 98 I=1,6
      DO 98 J=1,6
      MEG(I,J,EN)=0.0
      DO 98 K=1,6
   98 MEG(I,J,EN)=MEG(I,J,EN)+RT(I,K)*TM(K,J)
  100 CONTINUE
C  GENERATE NULL MATRICES SK AND SM WHICH WILL BECOME THE
C  SYSTEM STIFFNESS AND MASS MATRICES, RESPECTIVELY.
      N=NJTS*3
      DO 49 I=1,N
      DO 49 J=1,N
      SK(I,J)=0.
   49 SM(I,J)=0.
C  ASSEMBLE THE STIFFNESS AND MASS MATRICES.
      DO 51 I=1,NUMEL
      DO 50 J=1,2
      DO 50 M=1,3
      J1=J*3-M+1
   50 SUB(J1)=3*JNM(I,J)-M+1
      DO 51 B=1,6
      DO 51 Z=1,6
      ROWSUB=SUB(B)
      COLSUB=SUB(Z)
      SK(ROWSUB,COLSUB)=SK(ROWSUB,COLSUB)+KEG(B,Z,I)
   51 SM(ROWSUB,COLSUB)=SM(ROWSUB,COLSUB)+MEG(B,Z,I)
C  CALCULATE THE NUMBER OF DEGREES OF FREEDOM AND REMOVE ROWS AND
C  COLUMNS FROM THE SYSTEM STIFFNESS AND MASS MATRICES.
      NF=N-NB
      IF(NB .EQ. 0)GO TO 69
      NA=1
      KL=N-1
   62 JC=1
   63 IF(JC .EQ. CFIX(NA))GO TO 64
      JC=JC+1
      IF(JC .EQ. N)GO TO 68
      GO TO 63
   64 DO 65 I=1,N
      DO 65 J=JC,KL
      SK(I,J)=SK(I,J+1)
      SM(I,J)=SM(I,J+1)
   65 CONTINUE
      DO 66 J=1,N
      DO 66 I=JC,KL
      SK(I,J)=SK(I+1,J)
      SM(I,J)=SM(I+1,J)
   66 CONTINUE
      IF(NA .EQ. NB)GO TO 68
      NA=NA+1
```

```
      DO 67 I=NA,NB
   67 CFIX(I)=CFIX(I)-1
      GO TO 62
   68 CONTINUE
C  ASSIGN REDUCED STIFFNESS AND MASS MATRIX ELEMENTS TO ARRAY
C  NAMES RSK AND RSM, RESPECTIVELY.
   69 DO 70 I=1,NF
      DO 70 J=1,NF
      RSK(I,J)=SK(I,J)
   70 RSM(I,J)=SM(I,J)
C  WRITE OUT THE REDUCED STIFFNESS AND MASS MATRICES OBTAINED
C  FROM THE BOUNDARY CONDITIONS.
      WRITE(2,71)
   71 FORMAT(/,' THE REDUCED SYSTEM STIFFNESS MATRIX IS:',/)
      WRITE(2,72) ((RSK(I,J),J=1,NF),I=1,NF)
   72 FORMAT(' ',6E11.4/)
      WRITE(2,73)
   73 FORMAT(/,' THE REDUCED SYSTEM MASS MATRIX IS:',/)
      WRITE(2,74) ((RSM(I,J),J=1,NF),I=1,NF)
   74 FORMAT(' ',6E11.4/)
      WRITE(2,200)
  200 FORMAT(//,' ')
C  CALL SUBPROGRAM JCBI TO CALCULATE FREQUENCIES AND MODE SHAPES
      CALL JCBI(NF,RSK,RSM)
      STOP
      END
C  LIBRARY.FOR
C  SUBROUTINES JCBI, DECOMP, MATINV, MATMPY, AND SEARCH AS REQUI
C  BY FINITEL.FOR AND TRUSS.FOR
      SUBROUTINE JCBI(N,K,M)
      IMPLICIT REAL*8 (A-H,O-Z)
      REAL*8 K,M,L,LT,LINV,LINVTR,RT,A,OMEGA,PROD,AV,DIFF,RAD
      REAL*8 COSINE,SINE,Q,PROD1
      DIMENSION K(27,27),RT(27,27),A(27,27)
      DIMENSION OMEGA(27),M(27,27),L(27,27),LT(27,27)
      DIMENSION LINV(27,27),LINVTR(27,27),PROD(27,27)
      CALL DECOMP(M,N,L,LT)
      CALL MATINV(L,LINV,N)
      DO 204 I=1,N
      DO 204 J=1,N
  204 LINVTR(I,J)=LINV(J,I)
      CALL MATMPY(N,K,LINVTR,PROD)
      CALL MATMPY(N,LINV,PROD,A)
      DO 14 I=1,N
      DO 13 J=1,N
      RT(I,J)=0.0
   13 CONTINUE
      RT(I,I)=1.0
   14 CONTINUE
      NSWEEP=0
   15 NRSKIP=0
      NMIN1=N-1
      DO 25 I=1,NMIN1
      IP1=I+1
      DO 24 J=IP1,N
      AV=0.5*(A(I,J)+A(J,I))
      DIFF=A(I,I)-A(J,J)
```

```
      RAD=DSQRT(DIFF*DIFF+4.*AV*AV)
      IF(RAD.EQ.0.0)GO TO 20
      IF(DIFF.LT.0.0)GO TO 18
      IF(DABS(A(I,I)).EQ.DABS(A(I,I))+100.*DABS(AV))GO TO 16
      GO TO 17
   16 IF(DABS(A(J,J)).EQ.DABS(A(J,J))+100.0*DABS(AV))GO TO 20
   17 COSINE=DSQRT((RAD+DIFF)/(2.0*RAD))
      SINE=AV/(RAD*COSINE)
      GO TO 19
   18 SINE=DSQRT((RAD-DIFF)/(2.0*RAD))
      IF(AV.LT.0.0)SINE=-SINE
      COSINE=AV/(RAD*SINE)
C     REVISION OF IF STATEMENT FROM ORIGINAL PROGRAM
   19 DBS=DABS(SINE)
      IF(DBS.GT.1.0E-16)GO TO 21
   20 NRSKIP=NRSKIP+1
      GO TO 24
   21 DO 22 L1=1,N
      Q=A(I,L1)
      A(I,L1)=COSINE*Q+SINE*A(J,L1)
      A(J,L1)=-SINE*Q+COSINE*A(J,L1)
   22 CONTINUE
      DO 23 L1=1,N
      Q=A(L1,I)
      A(L1,I)=COSINE*Q+SINE*A(L1,J)
      A(L1,J)=-SINE*Q+COSINE*A(L1,J)
      Q=RT(L1,I)
      RT(L1,I)=COSINE*Q+SINE*RT(L1,J)
      RT(L1,J)=-SINE*Q+COSINE*RT(L1,J)
   23 CONTINUE
   24 CONTINUE
   25 CONTINUE
C  KEEP A TALLY OF THE NUMBER OF SWEEPS.
      NSWEEP=NSWEEP+1
      IF(NSWEEP.GT.100)GO TO 33
      WRITE(2,26)NRSKIP,NSWEEP
   26 FORMAT(' ',5X,'THERE WERE ',I2,
     $' ROTATIONS SKIPPED ON SWEEP NUMBER ',I2)
      IF(NRSKIP.LT.N*(N-1)/2)GO TO 15
      PROD1=0.0
      DO 27 J=1,N
      PROD1=PROD1+RT(J,1)*RT(J,N)
   27 CONTINUE
      WRITE(2,28)
   28 FORMAT(/,' ',5X,'THE SCALAR PRODUCT OF THE FIRST AND LAST')
      WRITE(2,29)PROD1
   29 FORMAT(' ',5X,'EIGENVECTORS OF THE TRANSFORMED MATRIX IS ',
     $F19.17/)
      CALL MATMPY(N,LINVTR,RT,PROD)
      DO 30 I=1,N
      DO 30 J=1,N
   30 RT(I,J)=PROD(I,J)
      DO 42 J=1,N
      SUM=0.0
      DO 31 I=1,N
   31 SUM=SUM+DABS(RT(I,J))
      AV=SUM/N
```

```
      QUOT=DABS(RT(1,J))/AV
      IF(QUOT.LT.0.000001)GO TO 40
      DO 32 I=2,N
   32 RT(I,J)=RT(I,J)/RT(1,J)
      RT(1,J)=1.0D0
      GO TO 42
   40 CALL SEARCH(RT,J,II,N)
      BIG=RT(II,J)
      DO 41 I=1,N
   41 RT(I,J)=RT(I,J)/BIG
   42 CONTINUE
      DO 110 I=1,N
      IF(A(I,I).LE.0.0)GO TO 43
      OMEGA(I)=DSQRT(A(I,I))
      GO TO 110
   43 OMEGA(I)=0.0
  110 CONTINUE
   33 WRITE(2,34)NSWEEP
   34 FORMAT(/,' ',5X,'THERE WERE ',I3,' SWEEPS PERFORMED.',
     $/,5X,' THE EIGENVALUES AND EIGENVECTORS FOLLOW:')
      DO 39 JJ=1,N
      J=N-JJ+1
      WRITE(2,35)JJ,A(J,J)
   35 FORMAT(/,' ',5X,'LAMBDA (',I2,') = ',F20.4)
      WRITE(2,111)JJ,OMEGA(J)
  111 FORMAT(' ',5X,'OMEGA(',I2,') = ',F20.4,' RAD/S')
      WRITE(2,36)
   36 FORMAT(/,' ',5X,'THE ASSOCIATED EIGENVECTOR IS:')
      DO 37 I=1,N
   37 WRITE(2,38)RT(I,J)
   38 FORMAT(' ',5X,D17.10)
   39 CONTINUE
      RETURN
      END
C
C
C
      SUBROUTINE DECOMP(A,N,L,LT)
      IMPLICIT REAL*8(A-H,O-Z)
      DIMENSION A(27,27)
      REAL*8 L(27,27),LT(27,27)
      DO 9 J=1,N
      IF(J.EQ.1)GO TO 7
      JM1=J-1
      DO 6 I=J,N
      IF(I.NE.J)GO TO 4
      SUM=0.0
      DO 3 K=1,JM1
    3 SUM=SUM+L(I,K)*L(J,K)
      L(J,J)=DSQRT(A(J,J)-SUM)
      GO TO 6
    4 SUM=0.0
      DO 5 K=1,JM1
    5 SUM=SUM+L(I,K)*L(J,K)
      L(I,J)=(A(I,J)-SUM)/L(J,J)
    6 CONTINUE
      GO TO 9
```

```
      7 L(1,1)=DSQRT(A(1,1))
        DO 8 I=2,N
      8 L(I,1)=A(I,1)/L(1,1)
      9 CONTINUE
C   FILL IN ZERO VALUES OF MATRIX L
        DO 11 J=2,N
        JM1=J-1
        DO 11 I=1,JM1
     11 L(I,J)=0.0
C   ASSIGN VALUES TO THE UPPER TRIANGULAR MATRIX LT
        DO 12 I=1,N
        DO 12 J=1,N
     12 LT(I,J)=L(J,I)
        RETURN
        END



C
C
C
        SUBROUTINE MATINV(B,A,N)
C   MATRIX INVERSION USING GAUSS-JORDAN REDUCTION AND PARTIAL
C   PIVOTING.  MATRIX B IS THE MATRIX TO BE INVERTED AND A IS
C   THE INVERTED MATRIX.
        IMPLICIT REAL*8(A-H,O-Z)
        DIMENSION B(27,27),A(27,27),INTER(27,2)
        DO 2 I=1,N
        DO 2 J=1,N
      2 A(I,J)=B(I,J)
C   CYCLE PIVOT ROW NUMBER FROM 1 TO N
        DO 12 K=1,N
        JJ=K
        IF(K.EQ.N)GO TO 6
        KP1=K+1
        BIG=DABS(A(K,K))
C   SEARCH FOR LARGEST PIVOT ELEMENT
        DO 5 I=KP1,N
        AB=DABS(A(I,K))
        IF(BIG-AB)4,5,5
      4 BIG=AB
        JJ=I
```

```
    5 CONTINUE
C   MAKE DECISION ON NECESSITY OF ROW INTERCHANGE AND
C   STORE THE NUMBER OF THE TWO ROWS INTERCHANGED DURING KTH
C   REDUCTION.  IF NO INTERCHANGE, BOTH NUMBERS STORED EQUAL K
    6 INTER(K,1)=K
      INTER(K,2)=JJ
      IF(JJ-K)7,9,7
    7 DO 8 J=1,N
      TEMP=A(JJ,J)
      A(JJ,J)=A(K,J)
    8 A(K,J)=TEMP
C   CALCULATE ELEMENTS OF REDUCED MATRIX
C   FIRST CALCULATE NEW ELEMENTS OF PIVOT ROW
    9 DO 10 J=1,N
      IF(J.EQ.K)GO TO 10
      A(K,J)=A(K,J)/A(K,K)
   10 CONTINUE
C   CALCULATE ELEMENT REPLACING PIVOT ELEMENT
      A(K,K)=1./A(K,K)
C   CALCULATE NEW ELEMENTS NOT IN PIVOT ROW OR COLUMN
      DO 11 I=1,N
      IF(I.EQ.K)GO TO 11
      DO 110 J=1,N
      IF(J.EQ.K)GO TO 110
      A(I,J)=A(I,J)-A(K,J)*A(I,K)
  110 CONTINUE
   11 CONTINUE
C   CALCULATE NEW ELEMENTS FOR PIVOT COLUMN--EXCEPT PIVOT ELEMENT
      DO 120 I=1,N
      IF(I.EQ.K)GO TO 120
      A(I,K)=-A(I,K)*A(K,K)
  120 CONTINUE
   12 CONTINUE
C   REARRANGE COLUMNS OF FINAL MATRIX OBTAINED
      DO 13 L=1,N
      K=N-L+1
      KROW=INTER(K,1)
      IROW=INTER(K,2)
      IF(KROW.EQ.IROW)GO TO 13
      DO 130 I=1,N
      TEMP=A(I,IROW)
      A(I,IROW)=A(I.KROW)
      A(I,KROW)=TEMP
  130 CONTINUE
   13 CONTINUE
      RETURN
      END
C
      SUBROUTINE MATMPY(N,A,B,C)
      IMPLICIT REAL*8(A-H,O-Z)
C   C IS THE PRODUCT MATRIX OF A AND B
      DIMENSION A(27,27),B(27,27),C(27,27)
      DO 2 I=1,N
      DO 2 J=1,N
      C(I,J)=0.0
      DO 2 K=1,N
    2 C(I,J)=C(I,J)+A(I,K)*B(K,J)
      RETURN
      END
```

```
C
C
      SUBROUTINE SEARCH(RT,J,II,N)
C  THIS SUBROUTINE SEARCHES THE JTH COLUMN OF THE MATRIX RT
C  FOR THE LARGEST EIGENVECTOR COMPONENT.  ITS ROW NUMBER IS
C  ASSIGNED TO THE NAME II.
      IMPLICIT REAL*8(A-H,O-Z)
      DIMENSION RT(27,27)
      II=1
      BIG=DABS(RT(1,J))
      DO 3 I=2,N
      AB=DABS(RT(I,J))
      IF(BIG-AB)2,3,3
    2 BIG=AB
      II=I
    3 CONTINUE
      RETURN
      END
```

```
NLFINITE.FOR; FULL KE+KG MATRICES,REVISED 10-24-90
      THE AREA ARRAY A IS:

      A(1) =  0.4800000E+02

      THE ELASTICITY ARRAY E IS;

      E(1) =  0.3000000E+08

      THE MOMENT OF INERTIA ARRAY IA IS;

      IA(1) =  0.1000000E+04

      THE GAMMA ARRAY IS;

      GAMMA(1) =  0.3525000E-01

      THE AXIAL PRETENSION LOAD IS;

                0.

      THE JOINT-NUMBER MATRIX IS;

              1   2

      THE JOINT COORDINATES ARE;

      X(1)= 0.0000000E+00     Y(1)= 0.0000000E+00
      X(2)= 0.1000000E+03     Y(2)= 0.0000000E+00

 THE REDUCED SYSTEM STIFFNESS MATRIX IS:

 0.1440E+08 0.0000E+00 0.0000E+00-0.1440E+08 0.0000E+00 0.0000E+00

 0.0000E+00 0.3600E+06 0.1800E+08 0.0000E+00-0.3600E+06 0.1800E+08

 0.0000E+00 0.1800E+08 0.1200E+10 0.0000E+00-0.1800E+08 0.6000E+09

-0.1440E+08 0.0000E+00 0.0000E+00 0.1440E+08 0.0000E+00 0.0000E+00

 0.0000E+00-0.3600E+06-0.1800E+08 0.0000E+00 0.3600E+06-0.1800E+08

 0.0000E+00 0.1800E+08 0.6000E+09 0.0000E+00-0.1800E+08 0.1200E+10
```

```
 THE REDUCED SYSTEM MASS MATRIX IS:

  0.1175E+01 0.0000E+00 0.0000E+00 0.5875E+00 0.0000E+00 0.0000E+00

  0.0000E+00 0.1309E+01 0.1846E+02 0.0000E+00 0.4532E+00-0.1091E+02

  0.0000E+00 0.1846E+02 0.3357E+03 0.0000E+00 0.1091E+02-0.2518E+03

  0.5875E+00 0.0000E+00 0.0000E+00 0.1175E+01 0.0000E+00 0.0000E+00

  0.0000E+00 0.4532E+00 0.1091E+02 0.0000E+00 0.1309E+01-0.1846E+02

  0.0000E+00-0.1091E+02-0.2518E+03 0.0000E+00-0.1846E+02 0.3357E+03



      THERE WERE  5 ROTATIONS SKIPPED ON SWEEP NUMBER  1
      THERE WERE  9 ROTATIONS SKIPPED ON SWEEP NUMBER  2
      THERE WERE  9 ROTATIONS SKIPPED ON SWEEP NUMBER  3
      THERE WERE 14 ROTATIONS SKIPPED ON SWEEP NUMBER  4


THERE WERE 15 ROTATIONS SKIPPED ON SWEEP NUMBER  5

THE SCALAR PRODUCT OF THE FIRST AND LAST
EIGENVECTORS OF THE TRANSFORMED MATRIX IS 0.00000000000000000


THERE WERE   5 SWEEPS PERFORMED.
THE EIGENVALUES AND EIGENVECTORS FOLLOW:

LAMBDA ( 1) =                0.0000
OMEGA( 1) =                0.0000 RAD/S

THE ASSOCIATED EIGENVECTOR IS:
 0.1000000000D+01
 0.0000000000D+00
 0.0000000000D+00
 0.1000000000D+01
 0.0000000000D+00
 0.0000000000D+00

LAMBDA ( 2) =                0.0000
OMEGA( 2) =                0.0000 RAD/S

THE ASSOCIATED EIGENVECTOR IS:
 0.0000000000D+00
 0.9334669755D+00
 0.6653302446D-03
 0.0000000000D+00
 0.1000000000D+01
 0.6653302446D-03
```

```
LAMBDA ( 3) =                0.0000
OMEGA( 3) =                0.0000 RAD/S

THE ASSOCIATED EIGENVECTOR IS:
 0.00000000000D+00
 0.10000000000D+01
-0.19773193200D-01
 0.00000000000D+00
-0.97731932040D+00
-0.19773193200D-01

LAMBDA ( 4) =          6127659.5745
OMEGA( 4) =             2475.4110 RAD/S

THE ASSOCIATED EIGENVECTOR IS:
 0.00000000000D+00
 0.10000000000D+01
-0.60000000000D-01
 0.00000000000D+00
 0.10000000000D+01
 0.60000000000D-01

LAMBDA ( 5) =         49021276.5957
OMEGA( 5) =             7001.5196 RAD/S

THE ASSOCIATED EIGENVECTOR IS:
 0.10000000000D+01
 0.00000000000D+00
 0.00000000000D+00
-0.10000000000D+01
 0.00000000000D+00
 0.00000000000D+00

LAMBDA ( 6) =         71489361.7021
OMEGA( 6) =             8455.1382 RAD/S


THE ASSOCIATED EIGENVECTOR IS:
 0.00000000000D+00
 0.10000000000D+01
-0.12000000000D+00
 0.00000000000D+00
-0.10000000000D+01
-0.12000000000D+00
```

APPENDIX D

3-Node Beam Derivation of [Kg]

Consider the 3-node beam shown in Figure 23.

$$u(x) = a_0 + a_1x + a_2x^2$$

$$u' = a_1 + 2a_2x$$

$$u'' = 2a_2$$

$$(u')^2 = a_1^2 + 4a_1a_2x + 4a_2^2x^2$$

$$v(x) = b_0 + b_1x + b_2x^2 + b_3x^3 + b_4x^4$$

$$v' = b_1 + 2b_2x + 3b_3x^2 + 4b_4x^3$$

$$v'' = 2b_2 + 6b_3x + 12b_4x^2$$

$$(v')^2 = 16x^6b_4^2 + 24x^5b_3b_4 + 16x^4b_2b_4 + 9x^4b_3^2 + 8x^3b_1b_4 + 12x^3b_2b_3 + 6x^2b_1b_3 + 4x^2b_2^2 + 4xb_1b_2 + b_1^2$$

$$u_1 = u(-L/2) = a_0 - a_1L/2 + a_2L^2/4$$

$$u_2 = u(0) = a_0$$

$$u_3 = uL/2) = a_0 + a_1L/2 + a_2L^2/4$$

$$v_1 = v(-L/2) = b_0 - b_1L/2 + b_2L^2/4 - b_3L^3/8 + b_4L^4/16$$

$$v_2 = v(0) = b_0$$

$$v_3 = v(L/2) = b_0 + b_1L/2 + b_2L^2/4 + b_3L^3/8 + b_4L^4/16$$

$$\theta_1 = v'(-L/2) = b_1 - b_2L + 3b_3L^2/4 - b_4L^3/2$$

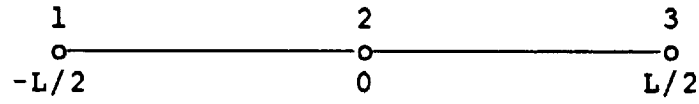

Figure 23 3-Node Beam Element

$$\theta_2 = v'(0) = b_1$$

$$\theta_3 = v'(L/2) = b_1 + b_2L + 3b_3L^2/4 + b_4L^3/2$$

Solve for a_i and b_i

$$\boxed{\begin{aligned} a_0 &= u_2 \\ b_0 &= v_2 \\ b_1 &= \theta_2 \end{aligned}}$$

$$u_1 - u_2 = -a_1L/2 + a_2L^2/4$$

$$u_3 - u_2 = a_1L/2 + a_2L^2/4$$

$$u_1 - 2u_2 + u_3 = a_2L^2/2$$

$$\boxed{a_2 = \frac{2u_1 - 4u_2 + 2u_3}{L^2}}$$

$$u_1 - u_3 = -a_1L$$

$$\boxed{a_1 = \frac{u_3 - u_1}{L}}$$

$$v_3 - v_1 - \theta_2L = b_3L^3/4$$

$$\boxed{b_3 = \frac{4v_3}{L^3} - \frac{4v_1}{L^3} - \frac{4\theta_2}{L^2}}$$

$$v_3 - v_1 = b_1L + b_3L^3/4$$

$$v_1 + v_3 - 2v_2 = 2b_0 + b_2L^2/2 + b_4L^4/8 - 2b_0$$

$$\theta_3 - \theta_1 = 2b_2L + b_4L^3$$

$$4v_1/L + 4v_3/L - 8v_2/L = 2b_2L + b_4L^3/2$$

$$4v_1/L + 4v_3/L - 8v_2/L - \theta_3 + \theta_1 = -b_4L^3/2$$

$$\boxed{b_4 = -\frac{8v_1}{L^4} - \frac{8v_3}{L^4} + \frac{16v_2}{L^4} + \frac{2\theta_3}{L^3} - \frac{2\theta_1}{L^3}}$$

$$b_2 = \frac{\theta_3}{2L} - \frac{\theta_1}{2L} - \frac{L^2}{2}\left[-\frac{8v_1}{L^4} - \frac{8v_3}{L^4} + \frac{16v_2}{L^4} + \frac{2\theta_3}{L^3} - \frac{2\theta_1}{L^3}\right]$$

$$b_2 = \frac{\theta_3}{2L} - \frac{\theta_1}{2L} + \frac{4v_1}{L^2} + \frac{4v_3}{L^2} - \frac{8v_2}{L^2} - \frac{\theta_3}{L} + \frac{\theta_1}{L}$$

$$\boxed{b_2 = -\frac{\theta_3}{2L} + \frac{\theta_1}{2L} + \frac{4v_1}{L^2} + \frac{4v_3}{L^2} - \frac{8v_2}{L^2}}$$

$$u_1 = \frac{1}{2} P_0 \int_0^L \frac{u'}{\sqrt{2a_1 + 4a_2x}} + \sqrt{(a1^2 + 4a_1a_2x + 4a_2{}^2x^2)} \sqrt{+ (16x^6b_4{}^2 + 24x^5b_3b_4 + 16x^4b_2b_4 + 9x^4b_3{}^2 + 8x^3b_1b_4 + 12x^3b_2b_3)} \, dx$$

$$U_1=\frac{1}{2}P_0\int_0^L\begin{bmatrix}a_1 & a_2 & b_1 & b_2 & b_3 & b_4\end{bmatrix}\begin{bmatrix}1 & 2x & 0 & 0 & 0 & 0\\ 2x & 4x^2 & 0 & 0 & 0 & 0\\ 0 & 0 & 1 & 2x & 3x^2 & 4x^3\\ 0 & 0 & 2x & 4x^2 & 6x^3 & 8x^4\\ 0 & 0 & 3x^2 & 6x^3 & 9x^4 & 12x^5\\ 0 & 0 & 4x^3 & 8x^4 & 12x^5 & 16x^6\end{bmatrix}\begin{bmatrix}a_1\\ a_2\\ b_1\\ b_2\\ b_3\\ b_4\end{bmatrix}dx$$

Integration yields

$$\int_0^L[X]\,dx=\begin{bmatrix}L & L^2 & 0 & 0 & 0 & 0\\ L^2 & 4L^3/3 & 0 & 0 & 0 & 0\\ 0 & 0 & L & L^2 & L^3 & L^4\\ 0 & 0 & L^2 & 4L^3/3 & 3L^4/2 & 8L^5/5\\ 0 & 0 & L^3 & 3L^4/2 & 9L^5/5 & 2L^6\\ 0 & 0 & L^4 & 8L^5/5 & 2L^6 & 16L^7/7\end{bmatrix}$$

$$\begin{bmatrix} a_1 & a_2 & b_1 & b_2 & b_3 & b_4 \end{bmatrix} =$$

$$\begin{bmatrix} u_1 & v_1 & \theta_1 & u_2 & v_2 & \theta_2 & u_3 & v_3 & \theta_3 \end{bmatrix} \underset{[L_1]^T}{\begin{bmatrix} -1/L & 2/L^2 & 0 & 0 & 0 & 0 \\ 0 & 0 & 0 & 4/L^2 & -4/L^3 & -8/L^4 \\ 0 & 0 & 0 & 1/2L & 0 & -2/L^3 \\ 0 & -4/L^2 & 0 & 0 & 0 & 0 \\ 0 & 0 & 0 & -8/L^2 & 0 & 16/L^4 \\ 0 & 0 & 1 & 0 & -4/L^2 & 0 \\ 1/L & 2/L^2 & 0 & 0 & 0 & 0 \\ 0 & 0 & 0 & 4/L^2 & 4/L^3 & -8/L^4 \\ 0 & 0 & 0 & -1/2L & 0 & 2/L^3 \end{bmatrix}}$$

$$P_0 \begin{bmatrix}
\frac{7}{3L} & 0 & 0 & \frac{-20}{3L} & 0 & 0 & \frac{13}{3L} & 0 & 0 \\
0 & \frac{18272}{105L} & \frac{3469}{105} & 0 & \frac{-22096}{105L} & \frac{304}{5} & 0 & \frac{3824}{105L} & \frac{-3469}{105} \\
0 & \frac{3469}{105} & \frac{659L}{105} & 0 & \frac{-4208}{105} & \frac{23L}{2} & 0 & \frac{739}{105} & \frac{-659L}{105} \\
\frac{-20}{3L} & 0 & 0 & \frac{64}{3L} & 0 & 0 & \frac{-44}{3L} & 0 & 0 \\
0 & \frac{-22096}{105L} & \frac{-4208}{105} & 0 & \frac{27392}{105L} & -72 & 0 & \frac{-5296}{105L} & \frac{4208}{105} \\
0 & \frac{304}{5} & \frac{23L}{2} & 0 & -72 & \frac{109L}{5} & 0 & \frac{56}{5} & \frac{-23L}{2} \\
\frac{13}{3L} & 0 & 0 & \frac{-44}{3L} & 0 & 0 & \frac{31}{3L} & 0 & 0 \\
0 & \frac{3824}{105L} & \frac{739}{105} & 0 & \frac{-5296}{105L} & \frac{56}{5} & 0 & \frac{147}{105} & \frac{-739}{105} \\
0 & \frac{-3469}{105} & \frac{-659L}{105} & 0 & \frac{4208}{105} & \frac{-23L}{2} & 0 & \frac{-739}{105} & \frac{659L}{105}
\end{bmatrix}$$

$[Kg]_{3\text{-NODE ELEMENT}}$

3 NODE RIGID BODY ROTATION VECTOR

Exact	Expanded to 2 Terms	Factor out ßL
$\begin{bmatrix} L/2\ (1-\cos 2ß) \\ -L/2 \sin 2ß \\ 2ß \\ 0 \\ 0 \\ 2ß \\ -L/2\ (1-\cos 2ß) \\ L/2 \sin 2ß \\ 2ß \end{bmatrix}$	$\begin{bmatrix} L(ß^2-ß^4/3) \\ -L(ß-2ß^3/3) \\ 2ß \\ 0 \\ 0 \\ 2ß \\ -L(ß^2-ß^4/3) \\ L(ß-2ß^3/3) \\ 2ß \end{bmatrix}$	$\begin{bmatrix} ß-ß^3/3 \\ -1 + 2ß^2/3 \\ 2/L \\ 0 \\ 0 \\ 2/L \\ -ß + ß^3/3 \\ 1 - 2ß^2/3 \\ 2ß \end{bmatrix}$

$$\begin{bmatrix} -2\ ß^2 \\ 91.733\ ß^3 - 16\ ß \\ L(17.333\ ß^3 - 3\ ß \\ 8\ ß^2 \\ 16\ ß - 106.666\ ß^3 \\ L(33.0666\ ß^3 - 6\ ß \\ -6\ ß^2 \\ 14.9333\ ß^3 \\ L(3\ ß - 17.3333\ ß^3) \end{bmatrix}$$

RFORCES using expanded rigid body rotation vector

$$
\begin{bmatrix}
\cos 2\beta - 1 \\
121.6\,\beta - 68.6 \sin 2\beta \\
23\,L\beta - 13L \sin 2\beta \\
4 - 4 \cos 2\beta \\
80 \sin 2\beta - 144\,\beta \\
43.6\,L\beta - 24.8\,L \sin 2\beta \\
3 \cos 2\beta - 3 \\
22.4\,\beta - 11.2 \sin 2\beta \\
13\,L \sin 2\beta - 23\,L\,\beta
\end{bmatrix}
$$

RFORCES using exact rigid body rotation vector

APPENDIX E

Dynamic Analysis of Space-Related Linear and Non-Linear Structures

Bosela[1], Paul A., MS, PE, Shaker[2], Francis J., PH.D., and Fertis[3], Demeter G., PH.D.

[1] Professor of Engineering Technology, Cleveland State University, Cleveland, Ohio, 44115 (Research Grant NAG 3-1008, with NASA Lewis Research Center)

[2] Branch Deputy, NASA Lewis Research Center, Structural Systems, Dynamics Branch, Cleveland, Ohio 44135

[3] Professor of Civil Engineering, University of Akron, Akron, Ohio 44325

Presented at the Southeast Conference of Theoretical and Applied Mechanics, XV
Atlanta, Georgia
APRIL, 1990

Abstract

In order to be cost-effective, space structures must be extremely light-weight, and subsequently, very flexible structures. The power system for Space Station Freedom is such a structure. Each array consists of a deployable truss mast and a split "blanket" of photo-voltaic solar collectors. The solar arrays are deployed in orbit, and the blanket is stretched into position as the mast is extended. Geometric stiffness due to the preload make this an interesting non-linear problem.

The space station will be subjected to various dynamic loads, during shuttle docking, solar tracking, attitude adjustment, etc. Accurate prediction of the natural frequencies and mode shapes of the space station components, including the solar arrays, is critical for determining the structural adequacy of the components, and for designing a dynamic controls system.

This paper chronicles the process used in developing and verifying the finite element dynamic model of the photo-voltaic arrays. Various problems were identified in the investigation, such as grounding effects due to geometric stiffness, large displacement effects, and pseudo-stiffness (grounding) due to lack of required rigid body modes. Various analysis techniques, such as development of rigorous

solutions using continuum mechanics, finite element solution sequence altering, equivalent systems using a curvature basis, Craig-Bampton superelement approach, and modal ordering schemes were utilized. This paper emphasizes the grounding problems associated with the geometric stiffness.

Nomenclature

a	factor defined by Eq.(13)
D_i	arbitrary constants in Eq. (10)
d/dx, or '	differential operator with respect to position
d/dt, or ·	differential operator with respect to time
E	modulus of elasticity
e_a	axial strain
{F}	input force vector at the beginning of a step
F(x,t)	applied transverse force
g	factor defined by Eq.(14)
I	moment of inertia
[K]	stiffness matrix
$[K_e]$	elastic stiffness matrix
$[K_g]$	geometric stiffness matrix
L	length
M	moment
dM	change in moment
m	mass per unit length
P	axial force
P'	pseudo-force necessary for equilibrium

{R}	force vector, output force vector at the end of a step
T	kinetic energy
{u}	displacements at the node points
u	longitudinal displacement
U_A	strain energy due to axial load
U_B	strain energy due to bending
v	transverse displacement
V	shear
dV	change in shear
$\underline{V}$	potential of the external loads
dVol	change in volume
x	axis defined by Figure 25
y	axis defined by Figure 25
ß	1/2 the angle of rotation
δ	factor defined by Eq.(11)
ε	factor defined by Eq.(12)
θ	angle of rotation
σ	stress

Introduction

NASA's Space Station Freedom consists of various modules supported by a space truss. Power for the space station will be provided by a deployable system of split blanket photo-voltaic arrays, which will have two degree of freedom rotational capabilities in order to track the sun during its orbit. The arrays are designed to be operated in

during its orbit. The arrays are designed to be operated in a zero-gravity environment.

NASA Lewis Research Center, along with its contractors, have the responsibility for developing a verified finite element dynamics model of the solar arrays, which could be combined with the other space station substructures for both structural and dynamic control studies. The development of the model necessitated the use of unique procedures, and rigorous analytical checks.

The procedure included the following:

1. Development of an idealized model of the solar arrays, and derivation of a unique solution for the response frequencies for the idealized array cantilevered from the space truss, using equations developed from continuum mechanics.[1]

2. Comparison of the frequencies from the MSC/NASTRAN finite element dynamic model of the idealized array with the rigorous solution from continuum mechanics.[2]

3. Refinement of the finite element mesh.

4. Rigid body mode checks of the finite element models.

5. Various parameter studies involving the amount of tension in the blanket, rigidity of the blanket tip beam, type of elements used, etc..

6. Craig-Bampton approach for appending rigid body modes to substructures (superelements) [3].
7. Modal ordering schemes for identifying "important" modes.
8. Study of grounding effects due to lack of rigid body mode capabilities.[4]

A detailed summary of the project was presented [5]. It should be noted that this study is ongoing at the present time. This paper will be restricted to the grounding problems associated with the geometric stiffness due to blanket pre-load.

Grounding

The space station solar arrays were modeled utilizing MSC/NASTRAN. As a routine check, the stiffness matrices generated by the model were multiplied by a matrix of rigid body modes, and large pseudo-forces were developed (grounding). The cause of this "grounding" phenomenum was examined.

Finite element solves non-linear problems of the form

$$[[Ke] + [Kg]] * \{u\} = \{R\} - \{F\}$$

where [Ke] is the elastic stiffness matrix, and [Kg] is the geometric, or initial stress stiffness matrix.

[Kg] is a function of the pre-load. Thus, it equals zero for a linear problem. [Ke] possesses the required rigid body modes. However, [Kg] lacks the capacity for rigid body rotation. Hence, an erroneous stiffening, or "grounding", occurs when a pre-loaded beam deforms.

The traditional, or consistent geometric stiffness matrix, developed by Martin [6] and others, is

$$K_g = P \begin{bmatrix} 6/5L & 1/10 & -6/5L & 1/10 \\ 1/10 & 2L/15 & -1/10 & -L/30 \\ -6/5L & -1/10 & 6/5L & -1/10 \\ 1/10 & -L/30 & -1/10 & 2L/15 \end{bmatrix}$$

This matrix does not possess rigid body rotation capabilities. Various refinements to the geometric stiffness have been developed which contain higher order terms [6,7,8] . However, none of these possess all the rigid body modes. Bosela [4] developed a modified [Kg] with complete rigid body modes when used with an exact rigid body rotation matrix, but [Kg] lost some of its rigid body capabilities.

Closer examination of the traditional formulation of [Kg] indicated that there is a load imbalance in the representation, and that pseudo-forces occur to maintain equilibrium (Figure 24).

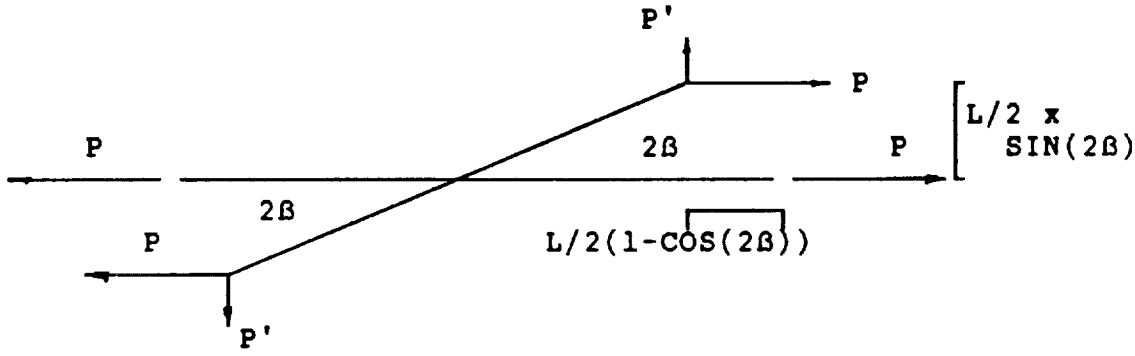

Figure 24 P' Represents Pseudo-forces Required for Equilibrium

the lack of rigid body rotation capabilities for [Kg] is not a problem, because the energy representation is correct. It can be shown that it is correct to β^2 terms, but error does occur, as a function of β^4. For large rigid body rotation, as will occur with the solar arrays, this is significant.

It should be noted that as long as the pre-load P is assumed to remain horizontal during rotation, work will be done by the force. Thus, true rigid body rotation cannot occur. In order for the strain energy to equal zero, the force P must change its orientation as the beam rotates (ie. a follower force).

Rigorous Solution Of Pre-Loaded Beam

Suppose we have an axially loaded beam in space subjected to a time varying transverse loading (Figure 25).

The kinetic energy is

$$T = \int_0^L \frac{m\,(v')^2}{2}\,dx \quad . \qquad (1)$$

The strain energy due to bending is

$$U_B = \int \frac{E\,I}{2}\,(v'')^2\,dx \quad . \qquad (2)$$

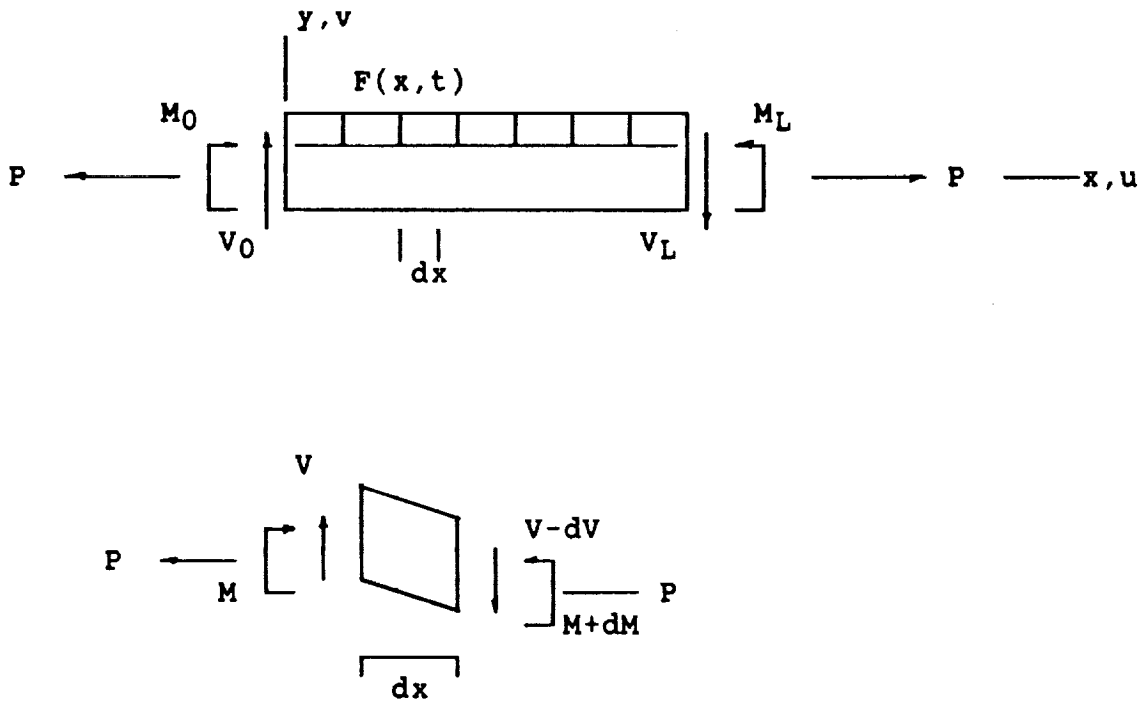

Figure 25 Beam in Tension and Differential Element

The strain energy due to axial load is

$$U_A = \frac{1}{2} \int \sigma \, e_a \, dVol \qquad (3)$$

Letting dVol = dA dx and applying non-linear elasticity yields

$$U_A = \int \frac{EA}{2} \left[(du/dx)^2 + du/dx(dv/dx)^2 + 1/4(dv/dx)^4 \right] dx \qquad (4)$$

Neglecting axial displacement and higher order terms yields

$$U_A = \int_0^L \frac{P}{2} \left[(v')^2 \right] dx \qquad (5)$$

The potential of the external loads is

$$\underline{V} = - \int F(x,t) \, v \, dx + V_o \, v(0,t) + M_o \, v'(0,t) - V_L \, v(L,t) - M_L \, v'(L,t) \qquad (6)$$

Applying Hamilton's principle, and performing the variation, yields

$$\int_{t_1}^{t_2}\left[\int_{0}^{L}\left[EIv''\delta(v'')+Pv'\delta(v')-m\dot{v}\delta(\dot{v})-F(x,t)\delta(v)\right]dx + V_o\delta v(0,t)+M_o\delta v'(0,t)-V_L\delta v(L,t)-M_L\delta v'(L,t)\right]dt = 0. \quad (7)$$

Integrating by parts yields the differential equation

$$d^2/dx^2(EId^2v/dx^2) - P\, d^2v/dx^2 + m\, d^2v/dt^2 = F(x,t) \quad , \quad (8)$$

which agrees with Clough in reference [10], after a sign change required to express the axial force in tension instead of compression. This is also in agreement with Shaker in Reference [11].

For a beam in space, the moment and shear at the end points must equal zero. Thus, the boundary conditions are

$$EIv''(0,t)=EIv''(L,t)=v'''(0,t)-\frac{P}{EI}v'(0,t)=v'''(L,t)-\frac{P}{EI}v'(L,t)=0 \quad (9)$$

Choose a solution of the form

$$v(x) = D_1\sin(\delta x) + D_2\cos(\delta x) + D_3\sinh(\varepsilon x) + D_4\cosh(\varepsilon x). \quad (10)$$

where $$\delta = \left[(a^4+g^4/4)^{1/2}-g^2/2\right] \quad (11)$$

$$\varepsilon = \left[(a^4+g^4/4)^{1/2}+g^2/2\right] \tag{12}$$

$$a^4 = mw^2/EI \tag{13}$$

$$g^2 = P/EI \quad . \tag{14}$$

Applying the boundary conditions at x=0, and after much mathematical manipulation, yields

$$v(x) = D_3\left[\frac{\delta\sin\delta x + \sinh\varepsilon x}{\varepsilon}\right] + D_4\left[\frac{\varepsilon^2\cos\delta x + \cosh\varepsilon x}{\delta^2}\right] \tag{15}$$

Applying the boundary conditions at x=L, and after more mathematical manipulations, yields

$$D_3\left[\delta^3\cosh\varepsilon L - \delta^3\cos\delta L\right] + D_4\left[\varepsilon^3\sin\delta L + \delta^3\sinh\varepsilon L\right] \quad . \tag{16}$$

Expressing Eq.(15) and Eq.(16) into matrix form, setting the determinant equal to zero, and after more mathematical manipulations, the following characteristic equation is obtained

$$\pm 2a^6(\cosh\varepsilon L\cos\delta L-1) + (\varepsilon^6-\delta^6)\sinh\varepsilon L\sin\delta L = 0 \quad . \tag{17}$$

Using Eq.(13), this can be expressed as

$$\pm w^3(m/EI)^{3/2}(\cosh\varepsilon L\cos\delta L-1) + (\varepsilon^6-\delta^6)\sinh\varepsilon L\sin\delta L = 0 \quad . \tag{18}$$

By observation, when w=0, a=0, and δ=0. Letting sin(0)=0 yields

$$w^3(m/EI)^{3/2}(\cosh\varepsilon L\cos\delta L-1) = 0 \quad . \qquad (19)$$

The w^3 term indicates that there must be three zero roots of "w", which suggests the three required rigid body modes.

Conclusion

Lack of complete rigid body mode capabilities is inherent in the physical representation of the pre-tensioned beam problem currently used to formulate the geometric stiffness matrix. This lack of complete rigid body mode capabilities invalidates the rigid body mode check for non-linear problems, and adversely impacts the use of traditional finite element techniques to predict dynamic response of pre-loaded structures unless the missing rigid body modes are somehow apppended on to the structure, such as by the Craig-Bampton technique.

The rigorous solution of the axially-loaded beam with free/free boundary conditions developed in this paper may lend itself to the development of a new geometric stiffness matrix for a beam element with full rigid body capabilities.

References

[1] Shaker, Francis J., "Free-Vibration Characteristics of a Large Split-Blanket Solar Array in a 1 G Field", NASA TN D-8376,1976.

[2] Carney, Kelly S., and Shaker, Francis J., "Free-Vibration Characteristics and Correlation of a Space Station Split-Blanket Solar Array", NASA TM 101452, 1989.

[3] Craig, R.R., Jr., and Bampton, M.C.C., "Coupling of Substructures for Dynamic Analysis", AIAA Journal, Vol. 6, N.7, July, 1968, pages 1313-1319.

[4] Bosela, Paul A., "Limitations of Current Nonlinear Finite Element Methods in Dynamic Analysis of Solar Arrays", MSC Users Conference, Los Angeles, CA, March, 1989.

[5] Carney, K., Chien, J., Ludwiczak, D., Bosela, P., and Nekoogar, F., Photovoltaic Array Modeling and Normal Modes Analysis, NASA Lewis Research Center, Structural Dynamics Branch, Space Station Freedom WP04, Response Simulation and Structural Analysis, September 1989.

[6] Martin, H.C., and Carey, G.F., Introduction to Finite Element Analysis, McGraw-Hill, Inc., 1973.

[7] Marcal, P.V., "The Effect of Initial Displacements on Problems of Large Deflection and Stability", Division of Engineering, Brown University, 1967, Department of Defense Contract SD-86, ARPA E54.

[8] Purdy, D.M., and Przemieniecki, J.S., "Influence of Higher-Order Terms in the Large Deflection Analysis of Frameworks", Air Force Institute of Technology, Wright-Patterson Air Force Base, Ohio

[9] Collar, A.r., and Simpson, A., Matrices and Engineering Dynamics, Halsted Press, New York, 1987.

[10] Clough, Ray W., and Penzien, Joseph, Dynamics of Structures, McGraw-Hill, Inc., 1975.

[11] Shaker, Francis J., "Effect of Axial Load on Mode Shapes and Frequencies of Beams", NASA TN D-8109, 1975.

APPENDIX F

Diagonalization/Partitioning Methodology

Example 1 (Structural Analysis, Third Edition, Ghali and Neville, Chapman and Hall Publishing Company, page 750.)

Consider the beam in Figure 26.

$$[K] = \frac{EI}{L^3} \begin{bmatrix} 1.6154 & -3.6923 & 2.7692 \\ -3.6923 & 10.1538 & -10.6154 \\ 2.7692 & -10.6154 & 18.4615 \end{bmatrix}$$

$$[M] = \frac{W}{g} \begin{bmatrix} 4 & 0 & 0 \\ 0 & 1 & 0 \\ 0 & 0 & 1 \end{bmatrix}$$

$$\{P\} = P_0 \, [\, 2, \, 1, \, 1 \,]^T \sin \Omega t$$

$$[M] \{ \ddot{X} \} + [K] \{X\} = \{0\}$$

$$| \, [K] - \Omega^2 \, [M] \, | = \{0\}$$

yields

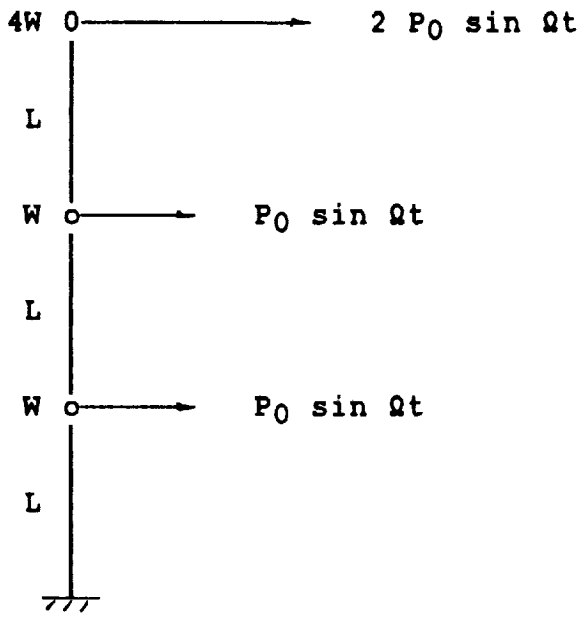

Figure 26 Example 1

$$\Omega_1^2 = 0.02588 \frac{gEI}{wL^3} \qquad D(1) = \begin{bmatrix} 1.0 \\ 0.5225 \\ 0.1506 \end{bmatrix}$$

$$\Omega_2^2 = 3.09908 \frac{gEI}{wL^3} \qquad D(2) = \begin{bmatrix} 1.0 \\ -6.3414 \\ -4.5622 \end{bmatrix}$$

$$\Omega_3^2 = 25.89415 \frac{gEI}{wL^3} \qquad D(3) = \begin{bmatrix} 1.0 \\ -13.1981 \\ 19.2222 \end{bmatrix}$$

In matrix form, the Eigenvectors are

$$[\phi] = \begin{bmatrix} 1.0 & 1.0 & 1.0 \\ 0.5224 & -6.3414 & -13.1981 \\ 0.1506 & -4.5622 & 19.2222 \end{bmatrix}$$

We can use this transformation matrix to create diagonal $\hat{[K]}$ and $\hat{[M]}$ matrices.

$$\hat{[K]} = \{\phi\}^T [K] \{\phi\}$$

$$\hat{[M]} = \{\phi\}^T [M] \{\phi\}$$

But, since $[K]\{\phi\} = \Omega^2 [M]\{\phi\}$,

Then, $[\hat{K}] = \Omega^2 [\hat{M}]$

$$[\hat{M}] = \begin{bmatrix} 4.296 & 0 & 0 \\ 0 & 65.027 & 0 \\ 0 & 0 & 547.68 \end{bmatrix}$$

$$[\hat{K}] = \Omega^2 \begin{bmatrix} 4.296 & 0 & 0 \\ 0 & 65.027 & 0 \\ 0 & 0 & 547.68 \end{bmatrix}$$

In normal coordinates, the equation of motion becomes

$$[\hat{M}]\{\ddot{n}\} + [\Omega][\hat{M}]\{n\} = \{f\}$$

Where

$$[\Omega] = \begin{bmatrix} \Omega_1^2 & 0 & 0 \\ 0 & \Omega_2^2 & 0 \\ 0 & 0 & \Omega_3^2 \end{bmatrix}$$

and

$$\{f\} = \{\phi\}^T \{P\}$$
$$= P_0 [\ 2.673, -8.9036, 8.02412]^T$$

$$\{\ddot{n}\} + [\Omega]\{n\} = [M]^{-1}\{f\}$$

or

$$\begin{bmatrix} \ddot{n}_1 \\ \ddot{n}_2 \\ \ddot{n}_3 \end{bmatrix} + \frac{gEI}{WL^3} \begin{bmatrix} 0.02588 & 0 & 0 \\ 0 & 3.09908 & 0 \\ 0 & 0 & 5.0886 \end{bmatrix} \begin{bmatrix} n_1 \\ n_2 \\ n_3 \end{bmatrix} = \frac{P_0 g}{W} \begin{bmatrix} 0.62206 \\ -0.136921 \\ 0.0146511 \end{bmatrix}$$

Note that the equations are now un-coupled.

Example 2

Consider the beam in Figure 27.

Let

$A = 48\ in^2$

$E = 30 \times 10^6\ psi$

$I = 1000\ in^4$

$L = 100\ in$

$m = 0.03525\ lb\text{-}sec^2/in^2$

$$[Ke] = \begin{bmatrix} 0.144x10^8 & & & & & \\ 0 & 0.36x10^6 & & & \text{SYMMETRIC} & \\ 0 & 0.18x10^8 & 0.12x10^{10} & & & \\ -0.144x10^8 & 0 & 0 & 0.144x10^8 & & \\ 0 & -0.36x10^6 & -0.18x10^8 & 0 & 0.36x10^6 & \\ 0 & 0.18x10^8 & 0.6x10^9 & 0 & -0.18x10^8 & .12x10^{10} \end{bmatrix}$$

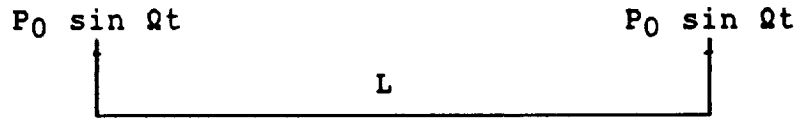

Figure 27 Example 2

$$[M] = \begin{bmatrix} 1.175 & & & & & \\ 0 & 1.309 & & \text{SYMMETRIC} & & \\ 0 & 18.46 & 335.7 & & & \\ 0.5875 & 0 & 0 & 1.175 & & \\ 0 & 0.4532 & 10.91 & 0 & 1.309 & \\ 0 & -10.91 & -251.8 & 0 & -18.46 & 335.7 \end{bmatrix}$$

$$\{P\} = P_0 \, [\, 0,\ 1,\ 0,\ 0,\ 1,\ 0 \,] \sin \Omega t$$

$$\Omega_1^2 = 0$$

$$\Omega_2^2 = 0$$

$$\Omega_3^2 = 0$$

$$\Omega_4^2 = 6{,}127{,}660$$

$$\Omega_5^2 = 49{,}021{,}277$$

$$\Omega_6^2 = 71{,}489{,}362$$

$$[\phi] = \begin{bmatrix} 1 & 0 & 0 & 0 & 1 & 0 \\ 0 & 1 & -50 & 1 & 0 & 1 \\ 0 & 0 & 1 & -0.6 & 0 & -0.12 \\ 1 & 0 & 0 & 0 & -1 & 0 \\ 0 & 1 & 50 & 1 & 0 & -1 \\ 0 & 0 & 1 & 0.06 & 0 & -0.12 \end{bmatrix}$$

$$\hat{[K]} = [\phi]^T [K] [\phi] =$$

$$\begin{bmatrix} 0 & 0 & 0 & 0 & 0 & 0 \\ 0 & 0 & 0 & 0 & 0 & 0 \\ 0 & 0 & 0 & 0 & 0 & 0 \\ 0 & 0 & 0 & 4.32 \times 10^6 & 0 & 0 \\ 0 & 0 & 0 & 0 & 5.76 \times 10^7 & 0 \\ 0 & 0 & 0 & 0 & 0 & 3.6 \times 10^7 \end{bmatrix}$$

$\hat{[K]}$ is a diagonal matrix.

Example 3

Now consider the beam with an axial load as shown in Figure 28.

Let

$A = 48 \text{ in}^2$

$E = 30 \times 10^6 \text{ psi}$

$I = 1000 \text{ in}^4$

$L = 100 \text{ in}$

$m = 0.03525 \text{ lb-sec}^2/\text{in}^2$

$T = 10{,}000{,}000 \text{ lbs}$

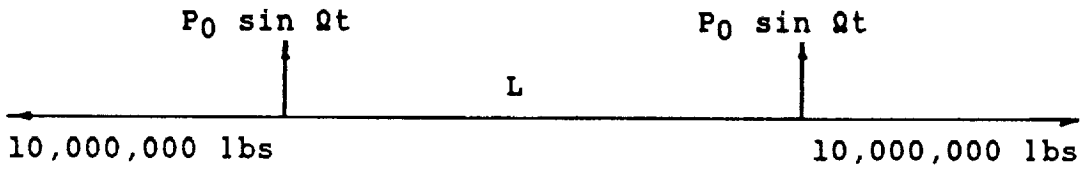

Figure 28 Example 3

$$[K_{TAN}]=\begin{bmatrix} 0.144x10^{8} & & & & & \\ 0 & 0.48x10^{6} & & \text{SYMMETRIC} & & \\ 0 & 0.19x10^{8} & 0.1333x10^{10} & & & \\ -0.144x10^{8} & 0 & 0 & 0.144x10^{8} & & \\ 0 & -0.48x10^{6} & -0.19x10^{8} & 0 & 0.48x10^{6} & \\ 0 & 0.19x10^{8} & 0.5667x10^{9} & 0 & -0.19x10^{8} & .1333x10^{10} \end{bmatrix}$$

$$\{P\} = P_0 [\ 0,\ 1,\ 0,\ 0,\ 1,\ 0\ ] \sin \Omega t$$

$$[\phi] = \begin{bmatrix} 1 & 0 & 0 & 0 & 1 & 0 \\ 0 & 1 & -1 & 1 & 0 & 1 \\ 0 & 0 & 0.018943 & -0.06 & 0 & -0.119554 \\ 1 & 0 & 0 & 0 & -1 & 0 \\ 0 & 1 & 1 & 1 & 0 & -1 \\ 0 & 0 & 0.018943 & 0.06 & 0 & -0.119554 \end{bmatrix}$$

$$[\hat{K}] = \{\phi\}^T [K] \{\phi\}$$

$$[\hat{K}]=\begin{bmatrix} 0 & 0 & 0 & 0 & 0 & 0 \\ 0 & 0 & 0 & 0 & 0 & 0 \\ 0 & 0 & 4.0403 \times 10^{5} & 0 & 0 & 1226 \\ 0 & 0 & 0 & 5.5174 \times 10^{6} & 0 & 0 \\ 0 & 0 & 0 & 0 & 5.76 \times 10^{7} & 0 \\ 0 & 0 & 1228 & 0 & 0 & 3.8053 \times 10^{7} \end{bmatrix}$$

$\hat{[K]}_{TAN}$ contains a large erroneous term (4.0403×10^5) in the 3,3 position.

Thus,

$\hat{[K]}_{Tan}$ is not the correct diagonal matrix.

The lack of rigid body rotation capability of the [Kg] matrix ultimately results in a large erroneous term in the $\hat{[K]}$ matrix.